INFORMATION TO USERS

This manuscript has been reproduced from the microfilm master. UMI films the text directly from the original or copy submitted. Thus, some thesis and dissertation copies are in typewriter face, while others may be from any type of computer printer.

The quality of this reproduction is dependent upon the quality of the copy submitted. Broken or indistinct print, colored or poor quality illustrations and photographs, print bleedthrough, substandard margins, and improper alignment can adversely affect reproduction.

In the unlikely event that the author did not send UMI a complete manuscript and there are missing pages, these will be noted. Also, if unauthorized copyright material had to be removed, a note will indicate the deletion.

Oversize materials (e.g., maps, drawings, charts) are reproduced by sectioning the original, beginning at the upper left-hand corner and continuing from left to right in equal sections with small overlaps.

ProQuest Information and Learning
300 North Zeeb Road, Ann Arbor, MI 48106-1346 USA
800-521-0600

Stochastic Mechanics and Reliability of Composite Laminates based on Experimental Investigation and Stochastic FEM

Shashank M Venugopal

A thesis

in

The Department

of

Mechanical and Industrial Engineering

Presented in Partial Fulfillment of the requirements

for the

Degree of Master of Applied Science

at

Concordia University

Montreal, Quebec, Canada

ABSTRACT

Stochastic Mechanics and Reliability of Composite Laminates based on Experimental Investigation and Stochastic FEM

Shashank M Venugopal

This work concerns the stochastic mechanics and reliability of composite laminates. The reliability of notched composite laminates is evaluated based on the average stress over a certain characteristic distance from the notch edge and the strength of the corresponding un-notched laminate. Laminates exhibit stochastic variations in mechanical and material properties. In practice, it is very difficult to achieve a perfect circular profile during the drilling operation on a composite laminate and also there is a possibility that the driven hole is offset from the desired coordinates. These imperfections affect the reliability of the laminate. In the present work the perturbation in the radius of the hole is modeled using a hypotrochoid variation and further, the location of the hole centre is modeled using a Gaussian random variable. Tests on laminate coupons show that the un-notched strength also has a stochastic distribution. Accordingly, the characteristic length to be used in design follows a stochastic distribution. Therefore, in order to achieve a design with a required reliability and safety, (i) the stress analysis of the notched laminate has to be conducted based on a stochastic approach, (ii) the strength distribution and its probabilistic parameters have to be determined based on a number of tests, and (iii) the reliability analysis has to be conducted. Two-dimensional stochastic finite element analyses of notched symmetric cross-ply $[0/90]_{4s}$ and angle-ply $[0_2/\pm 45]_{2s}$ composite laminates are conducted. A comprehensive experimental investigation is carried out to determine the strength values of the laminates subjected to tensile load. Average stress criterion is used to predict the characteristic length values of the laminates. The distributions of the strength and characteristic length of laminates with symmetric cross-ply $[0/90]_{4s}$ configuration are determined by testing 25 samples of notched and 25 samples of un-notched laminates. In a similar manner, tests on angle-ply laminate $[0_2/\pm 45]_{2s}$ are conducted. Stochastic simulation is performed on the laminates by subjecting them to uniaxial, biaxial, shear and bending loads. Probabilistic moments of

the stress parameters that are of interest are found out for the so-called controlled hole and uncontrolled hole laminates. The reliability indices for the two laminate configurations are calculated by combining the stochastic finite element analysis and the test results.

ACKNOWLEDGEMENTS

I would like to express my gratitude to all those who gave me the possibility to complete this thesis. I am deeply indebted to my enthusiastic supervisor Dr. Rajamohan Ganesan whose help, stimulating suggestions and encouragement helped me in all the time of research for and writing of this thesis. His broad and profound knowledge, and his patient instruction have given me a great help. He manages to strike the perfect balance between providing direction and encouraging independence.

I am grateful to many people in the department who have assisted me in the course of this work. Among them, Ming Xie, Paul Ouellette, Robert Oliver, John Elliott, Brian Cooper, Qi Zhao have been particularly helpful and generous with their time and expertise.

I would like to acknowledge the financial support provided by NSERC for the research project.

I am indebted to my many student colleagues for providing a stimulating and fun environment in which to learn and grow. In particular, I wish to thank Srikanth Marti and Ravi, for their understanding and cooperation.

I am grateful to my friends Amit Nigam and Vijay Kowda, for being the surrogate family and for their continued moral support through out the duration of my Master's program. They have shared my love of the mountains.

I would like to give my special thanks to my entire extended family for providing a loving environment, which enabled me to complete this work. My grand parents, uncles, aunties, and cousins were extremely supportive.

Lastly, and most importantly, I wish to thank my parents, M.R.Venugopal, Usha Venugopal and my brother Sameer Venugopal. My family have always encouraged me and guided me to independence, never trying to limit my aspirations. I am grateful to them and amazed at their generosity. I thank them for providing an untiring patience and support, reminding me of my priorities and keeping things in perspective. To them I dedicate this thesis.

TABLE OF CONTENTS

List of Tables

LIST OF FIGURES

Nomenclature

?, ?	Local co-ordinates for an element
N_i	Shape functions
$\{\varepsilon\}$	Strain vector
E	Young's Modulus
ν	Poisson's ratio
μ	Shear modulus
$\{u\ v\}^T, \{d\}$	Displacement vector
[B]	Strain-nodal displacement matrix
[J]	Jacobian matrix
$\{\sigma\}$	Stress vector
[E]	Elasticity matrix
$K^{(e)}$	Elemental stiffness matrix
h	Thickness of the element; thickness of the plate
W_p, W_q	Weight factors
q	Uniformly distributed load
σ_i^*	Stress component as a result of the circular opening stress field
σ_i^o	Stress component as a result of the uniform stress field
μ_1, μ_2	Principal complex roots of a characteristic equation
ϕ_1, ϕ_2	Complex potentials
$[a]$	Compliance matrix

$\bar{\sigma}_y$	Stress applied at infinity
a	Major axis dimension
b	Minor axis dimension
$E_x, E_y, G_{xy}, \nu_{xy}$	Effective laminate normal moduli, shear modulus and Poisson's ratio respectively in the x and y co-ordinate system
K_T, K_T^{∞}	Stress concentration factors for finite and infinite plate respectively
σ_y^{∞}	y-component of normal stress for an infinite-width plate
M	Magnification factor
[A]	Extensional stiffness matrix
[B]	Axial-bending coupling stiffness matrix
[D]	Bending stiffness matrix
[T]	Transformation matrix
t	Ply thickness
u,v,w	Displacement components
x,y,z	Global co-ordinate system
C_{aa}	Covariance matrix
R_{aa}	Auto-correlation function
$[L]$	Lower triangular matrix
d	Correlation length
$a(X)$	Fluctuating component
θ_x, θ_y	Rotations of the transverse normal about the y and x axes
$[D_M]$	Bending stiffness matrix

U	Strain energy
A	Area of the plate
N	Number of nodes
$\{\kappa\}$	Curvature matrix
$\{f\}$	Global load vector
$\overline{w}$	Non-dimensional form of the maximum displacement
a_o	Characteristic length
σ_N^∞	Notched strength of the laminate
σ_o	Un-notched strength of the laminate
$\sigma_y(x,0)$	Approximate solution for the stress distribution in orthotropic notched plate
r	Radius of the hole
μ_{equ}	Mean value of equivalent stress
$\mu_{\max}$	Mean value of maximum stress
μ	Mean value
σ	Standard deviation
z_R	Standardized variable
R	Reliability
R_{equ}	Reliability corresponding to equivalent stress

Chapter 1

Introduction

1.1 Composite materials and structures

Carbon Fibre Reinforced Plastics (CFRP) are used extensively in aircraft structures as they give high stiffness and strength with lower weight. Typical composite components of aircraft are wings and parts of fuselage. Wing ribs and intermediate spars are typical sub-structures, which can be built of CFRP. Cutouts are introduced in these structures for lightening the component. Introduction of holes leads to stress concentrations in addition to lowering the buckling load and load carrying capability.

Improvement in flight performance is one of the most important criteria in the design of aerospace structures. Weight reduction measures, coupled with compliance to strength, stiffness and stability requirements are important. Investigators have long been in search of materials that have less weight as well as sufficient strength and stiffness to withstand aerodynamic loads experienced by a structure in various flight conditions. Fibre reinforced composite materials have been found to have promising properties in this regard. These materials are being used extensively in the production of various aircraft components and their use is increasing day-by-day. This is due to the fact that they have a

very high strength-to-weight ratio, higher damage tolerance, better manufacturability and lesser number of joints compared to conventional materials.

Composites have also found many applications as advanced engineering materials, and they are effectively employed in various structural systems such as automobiles and power plants. In recent years, composite materials have become widely recognized as a viable construction material too. The safety and reliability of these systems are dependent on the design of the constituent components. These components are often subjected to complex service loading conditions, in which two or three dynamic or static principal stresses may exist.

The composite laminate design process typically involves optimization of the following four parameters:

1. Ply (or lamina) material
2. Ply thickness,
3. Ply orientation, and
4. Stacking (or lay-up) sequence.

The true optimization of a composite laminate, simultaneously considering the coupling effects of the four design parameters mentioned above, is a mathematical challenge in structural optimization. Characterization of deformation of composite laminates is not trivial and simulations need to be accompanied by experimental verification before various laminate theories can be used with confidence.

Carbon fibre composite materials are sensitive to open holes, defects, and low-velocity impact damage that can significantly reduce their stiffness and strength properties. To develop structures, which are more damage-tolerant, it is necessary to understand how the damage is caused and how it can affect residual performance. Many investigations of open holes and impact damage in carbon fibre composites are based on testing of small laminates rather than structural elements or full-scale structures.

To utilize these advanced materials to their full potential, the establishment of the strength criterion is important. Considerable efforts have been devoted to recent developments of strength/failure criteria for anisotropic materials [1]. Some of the currently existing anisotropic strength criteria are only extensions of isotropic yield criteria.

1.2 Cutouts in composites

Stress concentrations exist in all structures. It is an extremely important issue in both homogeneous isotropic and heterogeneous composite materials, because the point at, or near, the maximum stress concentration is normally the location of initial failure. Because of the importance of stress concentration problems, engineers must know how to analyze it, to predict failure and strength, and develop methods to reduce the effects of stress concentration. Stress concentration in a structure can be caused by many factors and they are listed below:

1) Openings
2) Discontinuous linear and smooth geometry

3) Joints which include bolted joints, bonded joints and other mechanical joints

4) Voids and damage due to material fabrication

Solutions to many issues related to stress concentration in laminated composites are still in the early stages of development. For instance, there are no criteria capable of predicting failure under a broad range of general stress states. A good design methodology in the presence of stress concentration in composite structures is also deficient.

It is a known fact that composite materials are widely used in structural components that withstand important mechanical loads. The design of these components requires the precise knowledge of the mechanical behavior of the material used. This is generally obtained from mechanical tests performed on composite coupons (tension, compression, shear, etc.). However, the preparation of these coupons very often requires some cutting operations (cutting coupons from a panel, machining notches, drilling holes, etc.). These tend to create damage on the cut surfaces. Since the failure of most of these coupons tends to initiate at the free surfaces, the cutting conditions are a possible source of strength reduction at the coupon level. Also, standards tend to contain limited information in terms of specimen cutting.

1.3 Literature review

In stress concentration analysis, it is significant to consider the open edge stress field. Analytical solutions are available in the literature with different degrees of mathematical complexity. Many of them considered only certain shapes of holes and few cases of loading. Muskhelishvili [2] principally developed a complex variable method for solving

boundary value problems in two-dimensional elasticity for an isotropic elastic solid. Lekhnitskii [3] gave solutions for stresses around different shapes of holes using the series method. These shapes are more approximate. Savin's [4] approach by conformal mapping is much simpler. Green [5] has given solutions for stress concentration problems in isotropic and aelotropic plates. The first analytical solution for multi-layered composite laminates with a circular hole has been given by Greszczuk [6]. Greszczuk obtained the failure strength and location of failure based on Hencky-Von Mises theory using the equations given by Fischer [7]. Hayashi [8] considered an arbitrary shape of hole in CFRP laminate. This solution is based on a series approach. Jong [9] adopted a variant of Lekhnitskii's [3] series method and the stress functions are determined by Cauchy integrals. Elaborate results are given for square, rectangular and circular holes in CFRP laminates of various geometry considering uniaxial, biaxial and shear stresses. Hwu [10] gave a solution to consider circular, elliptical, oval, square and pentagonal shaped holes in anisotropic plates. These shapes are approximate since Hwu [10] employed the same mapping function as that of Lekhnitskii [3]. Hufenbach *et al.* [11] gave a solution for the case of an elliptical hole in an anisotropic plate under uniaxial tension at different angles. The effects of hole geometry, fibre orientation and angle of loading on stresses around the hole are studied. Daoust and Hoa [12] gave the solution for a triangular hole in an anisotropic plate. This solution considers any ratio of base length and height of the triangle. Ukadgaonker and Rao [13] have extended Daoust and Hoa's [12] solution for multi-layered plates and considered several cases of in-plane loading.

Theocaris and Petrou [14,15] considered triangular, and rectangular holes in isotropic plates. The stress distribution around these holes is determined considering singular

points at the rounded corners and the results were verified by the method of caustics. Ukadgaonker and Awasare [16-18] gave solutions for elliptical hole in anisotropic plate and also for triangular, and rectangular holes in isotropic plate. Simha and Mahapatra [19] studied the perturbation of mean boundary stress and its root mean square value due to evolution of shape.

Many of the solutions cited for non-circular holes involve tedious algebra and in many cases, the results are given without detailed procedure. The series method employed in different solutions is more involved. It is felt that a solution based on simple mathematical approach is needed to consider any shape of hole in multi-layered plates and several cases of in-plane loading. Such a solution will be useful to study the effect of hole geometry, type of loading and laminate geometry on stress distribution around the hole.

A cutout may provide a passage for hydraulic lines, avionic harnesses, and on a larger scale, an access door in an aircraft fuselage. The presence of multiple layers as well as the anisotropy of the material system establishes a new challenge in terms of optimizing the cutout geometry. Many other researchers have conducted work on single and elliptical cutouts and to name a few: Cheng [20], Shastry and Rao [21], Tan [22-23], Lin and Ueng [24], Fan and Wu [25].

By definition, a Finite-Width Correction (FWC) factor is a scale factor, which is applied to multiply the notched infinite-plate solution to obtain the solution for the notched finite-

plate. FWC for anisotropic and orthotropic laminates containing a central elliptical opening has been derived and is presented in reference [26].

Very few experiments have been conducted for the residual strength of fibre-reinforced, resin-matrix-laminated composites containing elliptical openings. In an article written by Rowlands *et al.* [27] a boron epoxy laminate containing a large elliptical opening with major and minor diameters was tested. There is no indication that the opening size effect was investigated and no prediction has been reported. In another review by Awerbuch and Madhukar [28], the entire issue has been to discuss the residual strength of orthotropic laminates containing a circular hole or a straight crack under uniaxial normal load.

Several experimental techniques are available in the literature [29-32] for studying the shear response of composite laminates such as cross-sandwich beam test, off-axis coupon, splitting test, solid-rod torsion, rail shear tests, etc. Both the analytical investigation conducted by Whitney *et al.* [31] and the numerical analysis by Herakovich *et al.* [32] have shown that a state of uniform shear stress is obtained at a short distance away from the free edges of the two-rail shear specimen.

A lot of literature is available for in-plane loading problems and very few solutions are found for the bending case. Some of the important solutions known for the isotropic case involve, the solutions of Goodier [33] and Reissner [34] for thin plates and the solutions of Naghdi [35], Lee and Conlee [36] and Chen and Archer [37] for thick plates. Based on thin plate theory, Lekhnitskii [3] and Savin [4] gave the formulation of stress

concentration (due to hole) problems for the anisotropic case. Lekhnitskii [3] gave the results for a circular hole in plywood plate. In addition to the results for various shapes of holes in isotropic plate, Savin [4] gave detailed equations for an elliptical hole problem. Based on Stroh formalism, Hwu [10] gave the solution for in-plane loading and in-plane bending of anisotropic plates with holes. No other solutions are found for the anisotropic case except those of Lekhnitskii and Savin [4] for circular or elliptical hole problems.

1.4 Failure criteria for composite materials

The main objective of stress analysis is strength prediction. Stress analysis can be pursued with many different methods. They all require physical boundary conditions in the form of traction, displacement or both to solve for unknowns. For most failure criteria, a few basic strength parameters are defined and evaluated experimentally first, then they are used to predict the failure of a material in general stress or strain state.

Thus, after the stress distribution calculation, the point of interest should be examined with a failure criterion to determine whether the composite material will fail or not. Considerable efforts have been devoted to the formulation of composite material failure criteria and to their correlation with experimental data, but no criterion has been fully adequate. The analyses of the Hoffman [38], Fischer [7], and Cowin [39] theories show that they are valid only for special cases. This limits their direct application to general materials.

Composites have inherent scatter in elastic and strength properties. The analysis of structures, whether subjected to random or deterministic external loads, has been

developed mainly under the assumption that the structure's parameters are deterministic quantities. In a significant number of circumstances, this assumption is not valid, and the probabilistic aspects of the structure need to be taken into account.

In the last twenty years the powerful finite element method has undergone various new developments to incorporate these random effects, and is now termed as Stochastic Finite Element Method (SFEM). The developments in this field are reviewed by Contreras [40], Vanmarcke and Griguriu [41] and Yamazaki, Shinozuka and Dasgupta [42]. The stochastic finite element method is capable of dealing with random structural properties described by random fields very efficiently. Ganesan [43] developed a new finite element formulation to analyse the self-adjoint and non-self-adjoint structures with more than one parameter behaving in a stochastic manner using the virtual work method. Ganesan and Pondugala [44] have developed an effective finite element analysis methodology for evaluating the stochastic J-integral of laminated composites.

1.4.1 Average stress criterion

Average stress criterion was developed to generalize failure criterion and is applied to fibre-reinforced composites with a circular cutout. The purpose of a material failure criterion is to establish a theoretical margin of safety that has been validated by experiments. Obtaining the open edge stress field is necessary before a failure criterion of composite material is applied. However, the open edge stress field is complicated because numerous factors influence open edge stress distribution. Understanding the factors that contribute to open edge stress fields is of critical importance in analyzing composite laminates.

In the cases where stress gradients exist, very few failure criteria have been developed for composite materials. Strictly speaking, the criterion of Waddoups-Eisenmann-Kaminski [45], the Whitney-Nuismer's [46] point stress criterion, the average stress criterion, the point strain criterion and the average strain criterion are valid only for unidirectional composites. These criteria have been widely used to predict the notched strength of laminated composites with very good results. They should be considered as models rather than failure criteria because they do not take into account the details of the complex failure mechanisms.

1.5 Scope and objective of the thesis

In reality, it is difficult to achieve a perfect circular profile in notched laminates. Also there is a high probability that the driven hole is offset from the desired coordinates. These facts would eventually lead to a non-uniform stress distribution near the hole edge. This variation in the stress distribution caused as a result of hole eccentricity and imperfection in the notch geometry is due to a single hole. It is a fact that a typical F-16XL aircraft has millions of tiny holes (2,500 holes over an area of 10 sq. feet) and there exists a possibility that a series of holes drilled over an area, might generate a multiple effect of the variation in the stress distribution over the region. This calls for a study of stress state on the boundary and at a distance away from a nearly circular, eccentric hole in an orthotropic laminate, subjected to uniform loading condition. Thus a better understanding of the behaviour of stress parameters of composite laminates leads to a reliable design and safer operation of mechanical components. As the spatial properties of a composite laminate are random in nature, it is inevitable to quantify the

stress concentration in the composite laminates based on a stochastic approach. Further the stochastic variation in material properties of the laminate is incorporated in the finite element analysis to determine the nodal displacements and hence the nodal stresses.

The primary objectives of the present thesis are:

(1) To develop a combined experimental and stochastic finite element analysis methodology for the stress concentration analysis of composite laminates which incorporates the probability distributions of material and geometric parameters;

(2) To develop a corresponding MATLAB® code which is easy to use and more flexible,

(3) To calculate the stochastic characteristics of the stress parameters of composite laminates for both the so-called controlled hole and uncontrolled hole laminates; (A controlled hole laminate exhibits the stochastic variation in the material properties over the laminate but does not exhibit the geometric variation around the circumference of the hole and hole eccentricity. An uncontrolled hole laminate takes into account the stochastic variation in material properties over the laminate, the geometric variation around the circumference of the hole, and hole eccentricity.)

(4) To determine an effective design parameter that can be used to determine the best laminate configuration for a particular load application;

(5) To compute the reliability of composite laminates based on Gaussian distribution using equivalent stress and the stress experienced by the un-notched laminate.

1.6 Organization of thesis

The present chapter gives an over-view of composite laminates, includes a brief literature survey covering also the topic of probabilistic stress concentration effects studied using finite element method. It also highlights the criteria, which have been employed in the present thesis work. The last section provides the scope and objectives of the thesis.

Chapter 2 briefly describes the theory and formulation involved in the calculation of stress distribution due to a circular opening in isotropic plates and orthotropic laminates using the finite element method. Orthotropic laminates are analyzed using the stochastic finite element analysis. A two-dimensional, 8-node isoparametric element is used to model the laminates considering the stochastic variation in material properties. The MATLAB® software is made use of, which performs the stress concentration analysis of the mechanical component.

Chapter 3 applies the concepts of First order shear deformation theory (FSDT) or equivalently the Mindlin plate bending theory to analyze the laminates under out-of-plane loading. Finite element analysis is first developed for isotropic plates, which involves the aspect of transverse shear deformation. Theory is then extended to orthotropic laminates and accordingly the computer program is also modified. Nodal displacements and stresses are calculated and a thorough program validation is carried out.

Chapter 4 highlights the need for calculating the value of characteristic length in composite laminates and a description of the Average stress criterion. A detailed procedure of the manufacturing technique and testing of composite laminates is provided.

Explanation of the micro structural study using optical microscope is provided and a check for delamination in the laminate is made. Analysis results for $[0/90]_{4s}$ and $[0_2/\pm 45]_{2s}$ laminates subjected to tensile loads are presented. Testing is performed on 25 samples of notched and 25 samples of un-notched laminates considering both the configurations. Finally the value of characteristic length a_o is calculated.

Chapter 5 is completely devoted to simulation of the behaviour of controlled hole and uncontrolled hole laminates using the stochastic finite element methodology. Both these cases are analyzed considering $[0/90]_{4s}$ and $[0_2/\pm 45]_{2s}$ laminate configurations. Simulation is performed on laminates by subjecting the same to uniaxial, biaxial, shear and bending loads. From the simulation process, probabilistic quantities of the stress parameters that are of interest are found out. Useful conclusions are drawn from the results, which reflect the behaviour of a laminate configuration.

Chapter 6 deals with the reliability of notched composite laminates. Probability distributions for the stress parameters are determined using Gaussian distribution method for both the laminate configurations. Reliability is calculated for laminates with controlled and uncontrolled circular opening. Finally the variation of the reliability with change in the applied load has been determined and presented.

The thesis culminates with chapter 7, providing the conclusion of present thesis work and some recommendations for future work.

Chapter 2

Stochastic Finite Element Analysis of Notched Plates

2.1 Introduction

Metals and fiber reinforced composite laminates find wide applications in mechanical, aerospace, underwater and automotive structures. Cutouts of different shapes will be made into the plates for practical reasons. In order to predict the structural behavior of these laminates with some degree of assurance, a detailed study of the effects of hole geometry, type of loading and laminate geometry on the stress distribution around the hole is necessary. The present chapter deals with problems related to the determination of stresses in plates weakened by an opening and deformed by forces applied to the middle plane. Mechanical components are bound to have some irregularities such as holes, grooves, and notches or other kinds of discontinuities. Any such discontinuity alters the stress distribution and causes an increase of stresses in places near the opening. These discontinuities are called stress raisers and the regions in which they occur are called areas of stress concentration.

Study of stress concentration effect in anisotropic laminates is much more complicated than that for isotropic plates, because of the directional anisotropy. As the closed form solutions exist only for very few cases it becomes difficult to analyze the stress

concentration in all practical situations. Thus in this chapter, stress concentration factors for isotropic and anisotropic materials are found out using a numerical method which results in an approximate solution.

A detailed description of the finite element formulation is provided in this chapter. A study on the minimum number of elements to be used in the finite element mesh to achieve results, that will be close enough to the exact solution, is made. A MATLAB® code is developed which inherits the concept of finite element method to determine the stress concentration in a notched laminate. In order to validate the correctness of the program, few examples are considered and the results are compared with exact and ANSYS® solutions.

2.2 Finite element formulation for isotropic plates

An eight-noded two-dimensional isoparametric element is employed to analyze the stress concentration effect in the plates subjected to in-plane loadings. Elements of this type are termed as serendipity elements and is shown in Figure 2.1. The interpolation or shape functions for this element with local co-ordinates, ? and ? are [47]

$$N_i = \begin{cases} \frac{1}{4}(1+\xi\xi_i)(1+\eta\eta_i)(\xi\xi_i+\eta\eta_i-1) & ;\quad i=1,2,3,4 \\ \frac{\xi_i^2}{2}(1+\xi\xi_i)(1-\eta^2)+\frac{\eta_i^2}{2}(1+\eta\eta_i)(1-\xi^2) & ;\quad i=5,6,7,8 \end{cases} \tag{2.1}$$

The node numbering and local co-ordinate system used for the present element are represented in Figure 2.1.

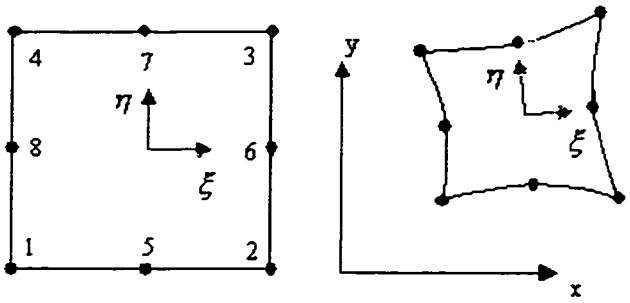

Figure 2.1 (a) Parent Element (b) Global Element

In the plane stress case a two-dimensional stress state exists in the x-y plane when the stresses σ_{zz}, τ_{xz} and τ_{yz} are equal to zero. The stresses along the direction of the thickness (z-direction) can be ignored. Considering only the x and y directions, the matrices of displacements and strains can be expressed as

$$\{u\} = \begin{Bmatrix} u \\ v \end{Bmatrix} \quad and \quad \{\varepsilon\} = \begin{Bmatrix} \varepsilon_x \\ \varepsilon_y \\ \gamma_{xy} \end{Bmatrix} \tag{2.2}$$

respectively, in which

$$\varepsilon_x = \frac{\partial u}{\partial x} \quad ; \quad \varepsilon_y = \frac{\partial v}{\partial y} \quad ; \quad \gamma_{xy} = \frac{\partial u}{\partial y} + \frac{\partial v}{\partial x} \tag{2.3}$$

The stresses and strains are related by

$$\{\sigma\} = [E]\{\varepsilon\} \tag{2.4}$$

in which the matrix representing the stresses is given by

$$\{\sigma\} = \begin{Bmatrix} \sigma_x \\ \sigma_y \\ \tau_{xy} \end{Bmatrix} \tag{2.5}$$

For linear elastic plane-stress conditions, the elasticity matrix also known as the constitutive matrix or the stress-strain matrix, relating the strains to the stresses is given by

$$[E] = \frac{E}{(1-\nu^2)} \begin{bmatrix} 1 & \nu & 0 \\ \nu & 1 & 0 \\ 0 & 0 & \frac{(1-\nu)}{2} \end{bmatrix} \tag{2.6}$$

in which E and ν are the Young's modulus and the Poisson's ratio respectively.

The element displacements can be expressed as

$$\{u\}^{(e)} = [N]^{(e)}\{d\}^{(e)} \tag{2.7}$$

in which the matrix of the shape functions is given by

$$[N]^{(e)} = \begin{bmatrix} N_1 & 0 & N_2 & 0 & \dots & \dots & N_8 & 0 \\ 0 & N_1 & 0 & N_2 & \dots & \dots & 0 & N_8 \end{bmatrix} \tag{2.8}$$

and the displacement vector is given by

$$\{d\}^{(e)} = \{u_1 \quad v_1 \quad u_2 \quad v_2 \quad \dots\dots \quad \dots\dots \quad u_8 \quad v_8\}^T \tag{2.9}$$

The details about the strain-displacement matrix and Jacobian matrix are presented in Appendix-A.

The element stiffness matrix can be written as

$$K^{(e)} = \int_{V_{(e)}} \left[B^{(e)}\right]^T [E] \left[B^{(e)}\right] dV_{(e)} \tag{2.10}$$

in which

$$dV_{(e)} = h|J|\, d\xi\, d\eta \tag{2.11}$$

where h is the thickness of the element.

The stiffness matrix coefficient linking nodes i and j in any element *(e)* is given by

$$K_{ij}^{(e)} = \sum_{r=1}^{NGAUS} \sum_{s=1}^{NGAUS} \left[B_{ir}^{(e)}\right]^T \left[E_{rs}^{(e)}\right] \left[B_{sj}^{(e)}\right] \mathrm{h}\, \left|\mathrm{J}^{(e)}\right| \mathrm{d}\xi\, \mathrm{d}\eta \tag{2.12}$$

in which *NGAUS* represents the order of Gauss quadrature for numerical integration. The elements of the stiffness matrix of each element can be numerically evaluated as

$$K_{ij}^{(e)} = \sum_{q=1}^{NGAUS} \sum_{p=1}^{NGAUS} T\left(\xi_p, \eta_q\right)_{ij}^{(e)} W_p W_q \tag{2.13}$$

in which

$$T_{ij}^{(e)} = \sum_{r=1}^{NGAUS} \sum_{s=1}^{NGAUS} \left[B_{ir}^{(e)}\right]^T \left[E_{rs}^{(e)}\right] \left[B_{sj}^{(e)}\right] h \left|\mathrm{J}^{(e)}\right| \tag{2.14}$$

In the above, $(?_p, ?_q)$ represents a sampling position and W_p and W_q are the weighting factors. If 'q' is the uniformly acting load along the edge of length L of an element (e), the nodal loads can be expressed as

$$\begin{Bmatrix} \textit{Equivalent load at the left node} \\ \textit{Equivalent load at the central node} \\ \textit{Equivalent load at the right node} \end{Bmatrix} = \frac{qL}{6} \begin{Bmatrix} 1 \\ 4 \\ 1 \end{Bmatrix} \tag{2.15}$$

The flowchart for the computation of the element stiffness matrix, nodal loads and nodal displacements is given in Figure 2.2. The main MATLAB® program is given in Appendix-B.

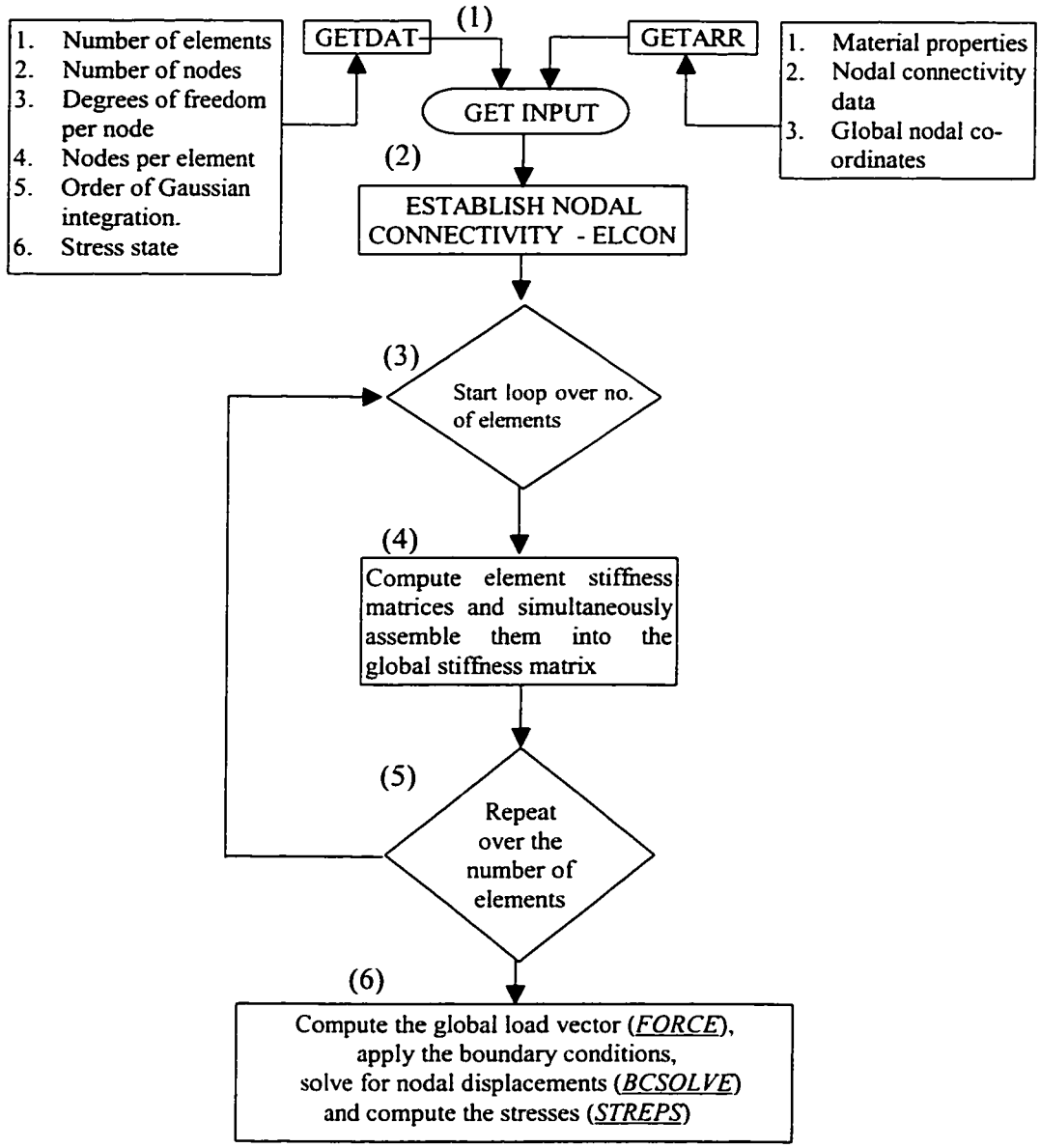

Figure 2.2 Flowchart for 2-D FEA and computation of displacements and stresses

2.2.1 Application 1: Isotropic quarter-plate analysis

For validating the program an isotropic plate with a hole diameter of 5.1 mm, length of 75.8 mm, width of 18.95 mm and thickness of 2 mm is used. It is to be noted, that the dimensions of the plate used in the present analysis, are based on the dimensions employed in the composite laminate analysis. These dimensions are used in testing the composite laminate under uniaxial tensile mode which has been discussed in chapter 4. Again, the dimensions used for composite laminate testing is based on the previous work [1]. Thus care has been taken to maintain a uniformity in dimension. Because the plate is symmetric about its axes analysis is carried out for a quarter-plate that is shown in Figure 2.3.

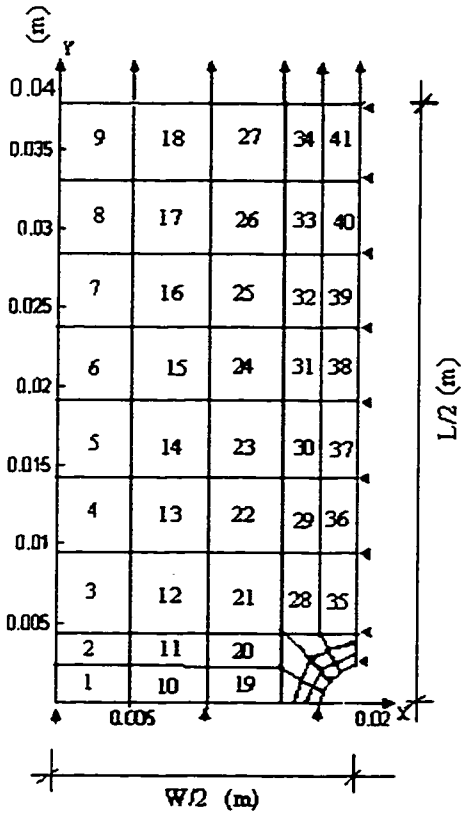

Figure 2.3 Finite element mesh, boundary conditions and loading for a quarter isotropic plate

A total of 53 elements are used to mesh the plate. Material properties assumed are as follows: Young's Modulus E is 210 *GPa* and Poisson's ratio μ is 0.3. Uniformly distributed load of 1.5 x 10^6 N/m is applied on the top edge of the plate and appropriate boundary conditions are imposed as depicted in Figure 2.3. Accordingly, in the ANSYS® package an attempt has been made to generate approximately the same number of elements, so that, the results of ANSYS® and MATLAB® program results can be compared.

Tables 2.1 and 2.2 give the nodal displacements and stresses respectively near the hole and at the boundary of the plate. It is clear that the MATLAB® program results are in close comparison with the ANSYS® results.

GLOBAL NODE	MATLAB® RESULTS		ANSYS® RESULTS	
Boundary	u (mm)	v (mm)	u (mm)	v (mm)
131	0.0203	0	0.0232	0
15	0.0202	0.1346	0.0197	0.137
45	0.0101	0.1349	0.0117	0.137
82	0	0.0711	0	0.073
90	0	0.1376	0	0.137
Near the hole				
162	0.0080	0	0.00921	0
166	0	0.0281	0	0.0221
157	0.0005	0.0305	0.00488	0.0235

Table 2.1 Displacement values for an isotropic quarter-plate

GLOBAL NODE	MATLAB® RESULTS		ANSYS® RESULTS	
Near hole and boundary	sigma x (GPa)	sigma y (GPa)	sigma x (GPa)	sigma y (GPa)
154	0	1.96	0	1.80
82	0.00852	0.743	0.00852	0.727
15	0.000224	0.749	0.000224	0.750
90	0.000224	0.749	0.000224	0.750
45	0.00371	0.750	0.00361	0.750

Table 2.2 Stress values for an isotropic quarter-plate

The above values are also compared with the closed form solution. As per the references [48] and [49], taking any point at a distance 'r' from the centre of the hole, the normal stress at that point from the exact theory is given as follows :

$$\sigma_y = \frac{\sigma}{2}\left(2 + \frac{a^2}{r^2} + \frac{3a^4}{r^4}\right) \tag{2.16}$$

and in the polar co-ordinate form it can be expressed as,

$$\sigma_{rr} = \frac{\sigma}{2}\left(1 - \frac{a^2}{r^2}\right) + \frac{\sigma}{2}\left(1 - \frac{a^2}{r^2}\right)\left(1 - \frac{3a^2}{r^2}\right)\cos 2\theta \tag{2.17}$$

$$\sigma_{\theta\theta} = \frac{\sigma}{2}\left(1 + \frac{a^2}{r^2}\right) - \frac{\sigma}{2}\left(1 + 3\frac{a^4}{r^4}\right)\cos 2\theta \tag{2.18}$$

where σ is the applied stress, 'a' is the distance measured along x-axis and 'r' is the radius of the hole. It is seen that the maximum stress occurs at $\theta = \pi/2$. Thus

$$\sigma_\theta = \sigma(1 - 2\cos 2\theta) = 3\sigma = 2.25 \text{ x } 10^9 N/m^2$$

It is seen from the Table 2.1, that, the displacement values obtained from MATLAB® and ANSYS® results have a close comparison. On comparing the stress values between MATLAB® and ANSYS® results from Table 2.2, it is observed that there is a variation of 8.1% relative to MATLAB® results. Again on comparing the MATLAB® results with exact results, there is a variation of 14.7%. This variation in the value can be reduced by suitably increasing the number of elements in the finite element mesh.

2.2.2 Stress concentration effects in complete isotropic plate

As an exercise a complete plate analysis is also performed. Similar dimensions and material properties are considered for the analysis. It can be observed from Tables 2.3 and 2.4, that, although the displacements are higher in the complete plate analysis when compared to a quarter-plate results, the stresses generated near the hole edge remains the same.

GLOBAL NODE	MATLAB® RESULTS		ANSYS® RESULTS	
At the boundary	u (mm)	v (mm)	u (mm)	v (mm)
9	0.0231	0.136	0.0234	0.129
17	0.0198	0.273	0.0197	0.274
75	0	0.276	0	0.274
140	-0.0198	0.275	-0.0197	0.276
132	-0.0231	0.137	-0.0234	0.131
Near the hole				
173	-0.0085	0.136	-0.0092	0.136
181	0	0.110	0	0.109
157	-0.0085	0.136	-0.0092	0.136
165	0	0.161	0	0.163

Table 2.3 Displacement values for a complete isotropic plate

GLOBAL NODE	MATLAB® RESULTS	ANSYS® RESULTS
At the boundary	sigma y (GPa)	sigma y (GPa)
9	0.755	0.751
22	0.753	0.761
35	0.755	0.765
75	0.747	0.749
141	0.749	0.737
Near the hole		
173	1.991	2.040
157	1.991	2.040
149	0.777	0.767
106	0.772	0.765
132	0.775	0.750

Table 2.4 Stress values for a complete isotropic plate

Nodal displacements and stresses calculated using the finite element formulation are compared with the closed form and ANSYS® solutions. From Table 2.3 it is clear that the nodal displacement values are varying within 1% of the ANSYS® result. Figure 2.4 shows a comparison of nodal stress values between MATLAB® program result and ANSYS® result.

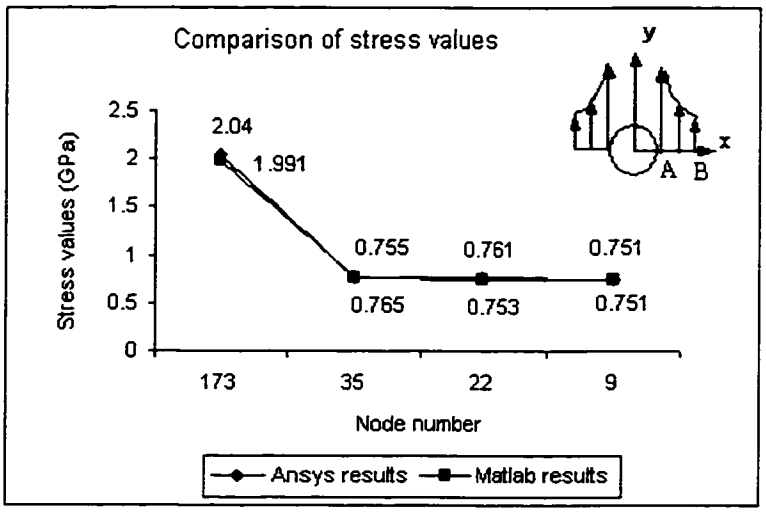

Figure 2.4 The distribution of σ_y along AB

It is clear from Figure 2.4 that σ_y is large near the hole edge along AB and decreases as we approache the plate side. On noticing the stress value at the plate sides which is 0.747 *GPa*, it is almost equal to the applied stress on the plate which is 0.75 *GPa*. Also from Table 2.4 and Figure 2.4, it can be observed that the stress concentration factor calculated using the MATLAB® program result is varying between 1-2% of that of the ANSYS® solution.

2.3 Stress concentration effects in composite laminate

The stress analysis of an infinite-width anisotropic laminate containing a central cutout is derived using a complex variable method [3] as given in the following. Closed-form solutions are obtained in the case of a laminate containing an elliptical or circular opening and subjected to in-plane loading. The derivation is pursued on the basis of a superposition method. The present section follows and summarizes the analysis presented in reference [3]. The total laminate stresses along 1-2 axes can be expressed as,

$$\sigma_i = \sigma_i^* + \sigma_i^o \qquad i = 1,2,6 \tag{2.19}$$

where

σ_i^* is the component as a result of the circular opening stress field

σ_i^o is the component as a result of the uniform stress field

The details of the derivation are given in an earlier work [50]. For clarity the procedure is presented in Appendix-C.

The total stress and displacement fields are the summation of circular opening stress field and uniform stress field. The uniform stress field is

$$\begin{aligned} \sigma_1^o &= \bar{\sigma}_y \cos^2 \varphi \\ \sigma_2^o &= \bar{\sigma}_y \sin^2 \varphi \\ \tau_{12}^o &= \bar{\sigma}_y \sin\varphi \cos\varphi \end{aligned} \tag{2.20}$$

where $\bar{\sigma}_y$ is the applied stress and the total stress and displacement fields are

$$\sigma_i = \sigma_i^* + \sigma_i^o \qquad i = 1,2,6$$

$$u_i = u_i^* + u_i^o \qquad i = 1,2 \tag{2.21}$$

where $u_1 = u$ and $u_2 = v$

The exact solution of the stress distribution in an infinite orthotropic composite laminate with an elliptic or circular opening [3] can also be found out using the following expression:

$$\sigma_y(x,0) = \bar{\sigma}_y \left\{ \mathrm{Re} \frac{1}{\mu_1 - \mu_2} \left[\begin{array}{l} \dfrac{-\mu_2(1 - i\mu_1\lambda)}{\sqrt{\gamma^2 - 1 - \mu_1^{\,2}\lambda^2}\left(\gamma + \sqrt{\gamma^2 - 1 - \mu_1^{\,2}\lambda^2}\right)} \\ + \dfrac{\mu_1(1 - i\mu_2\lambda)}{\sqrt{\gamma^2 - 1 - \mu_2^{\,2}\lambda^2}\left(\gamma + \sqrt{\gamma^2 - 1 - \mu_2^{\,2}\lambda^2}\right)} \end{array} \right] \right\} + \bar{\sigma}_y \tag{2.22}$$

where $\sigma_y(x,0)$ is the normal stress distribution along AB as shown in Figure 2.4. $\lambda = \dfrac{b}{a}$; $\gamma = \dfrac{x}{a}$; $\bar{\sigma}_y$ is the stress applied at infinity; 'a' is the major axis dimension; 'b' is the minor axis dimension. For a circular opening a = b. Also μ_1 and μ_2 in equation (2.22) are solutions of the characteristic equation:

$$a_{22}\mu^4 - 2a_{26}\mu^3 + (2a_{12} + a_{66})\mu^2 - 2a_{16}\mu + a_{11} = 0 \tag{2.23}$$

and

$$\mu_1 = \frac{i}{2}\left[\sqrt{\frac{E_x}{G_{xy}} - 2\nu_{xy} + 2\sqrt{\frac{E_x}{E_y}}} + \sqrt{\frac{E_x}{G_{xy}} - 2\nu_{xy} - 2\sqrt{\frac{E_x}{E_y}}}\right]$$
$$\mu_2 = \frac{i}{2}\left[\sqrt{\frac{E_x}{G_{xy}} - 2\nu_{xy} + 2\sqrt{\frac{E_x}{E_y}}} - \sqrt{\frac{E_x}{G_{xy}} - 2\nu_{xy} - 2\sqrt{\frac{E_x}{E_y}}}\right] \quad (2.24)$$

where E_x, E_y, G_{xy} and ν_{xy} are the effective laminate normal moduli, shear modulus and Poisson's ratio respectively. x and y are parallel and transverse to the loading direction.

2.3.1 Finite-width correction factor (FWC) for composite laminates

Finite-width correction factor is a scale factor which is applied to multiply the notched infinite-plate solution to obtain the solution for the notched finite plate. According to the definition of the FWC factor stated above, and an assumption that the normal stress profile for a finite plate is identical to that for an infinite plate except for an FWC factor, the following relation is obtained:

$$\frac{K_T}{K_T^\infty}\sigma_y^\infty(x,0) = \sigma_y(x,0) \quad (2.25)$$

where $\frac{K_T}{K_T^\infty}$ is the finite width correction factor; K_T denotes the stress concentration factor at point A (in Figure 2.4) along x-axis for a finite-width plate and K_T^∞ for an infinite-width plate. The parameter σ_y is the normal stress acting along y-axis for a finite-width plate and σ_y^∞ is the normal stress acting along y-axis for an infinite-width plate.

For orthotropic laminates containing a central circular hole, the derivation of the FWC factor is based on an approximate stress analysis. The solution for the inverse of the FWC factor is given by [1]:

$$\frac{K_T^{\infty}}{K_T}=\frac{3(1-2a/w)}{2+(1-2a/w)^3}+\frac{1}{2}\left(\frac{2a}{w}M\right)\left(K_T^{\infty}-3\right)\left[1-\left(\frac{2a}{w}M\right)^2\right] \tag{2.26}$$

where M is the Maginification factor, defined as:

$$M^2=\frac{\sqrt{1-8\left[\frac{3(1-2a/w)}{2+(1-2a/w)^3}-1\right]}-1}{2(2a/w)^2} \tag{2.27}$$

Also the SCF of an infinite orthotropic plate, K_T^{∞}, is defined by:

$$K_T^{\infty}=1+\sqrt{\frac{2}{A_{66}}\left(\sqrt{A_{11}A_{22}}-A_{12}+\frac{A_{11}A_{22}-A^2{}_{12}}{2A_{66}}\right)} \tag{2.28}$$

where A_{ij} ,i,j=1,2,6 denote the effective laminate stiffness values. Axes 1 and 2 are parallel and transverse to the loading direction respectively.

2.3.2 Equivalent elasticity matrix for composite laminates [58]

The laminate constitutive equation for a composite laminate is given by:

$$\begin{Bmatrix} N_x \\ N_y \\ N_{xy} \\ M_x \\ M_y \\ M_{xy} \end{Bmatrix} = \left[\begin{array}{ccc:ccc} A_{11} & A_{12} & A_{16} & B_{11} & B_{12} & B_{16} \\ & A_{22} & A_{26} & & B_{22} & B_{26} \\ symm & & A_{66} & symm & & B_{66} \\ \hdashline B_{11} & B_{12} & B_{16} & D_{11} & D_{12} & D_{16} \\ & B_{22} & B_{26} & & D_{22} & D_{26} \\ symm & & B_{66} & symm & & D_{66} \end{array}\right] \begin{Bmatrix} \varepsilon_x^0 \\ \varepsilon_y^0 \\ \gamma_{xy}^0 \\ k_x \\ k_y \\ k_{xy} \end{Bmatrix} \tag{2.29}$$

In a concise form we can represent the above equation as,

$$\begin{Bmatrix} N \\ M \end{Bmatrix} = \begin{bmatrix} A & B \\ B & D \end{bmatrix} \begin{Bmatrix} \varepsilon \\ \kappa \end{Bmatrix} \tag{2.30}$$

where

$$A_{ij} = \sum_{k=1}^{n} \bar{Q}_{ij}^{k} \left(h_k - h_{k-1}\right) \text{ (Axial stiffness)} \tag{2.31}$$

$$B_{ij} = \frac{1}{2} \sum_{k=1}^{n} \bar{Q}_{ij}^{k} \left(h_k^2 - h_{k-1}^2\right) \text{ (Axial-bending coupling stiffness)} \tag{2.32}$$

$$D_{ij} = \frac{1}{3} \sum_{k=1}^{n} \bar{Q}_{ij}^{k} \left(h_k^3 - h_{k-1}^3\right) \text{ (Bending stiffness)} \tag{2.33}$$

with $i,j = x, y, s = 1,2,6$. Further $\bar{Q}_{ij}^{k}$ denotes transformed reduced stiffness coefficient.

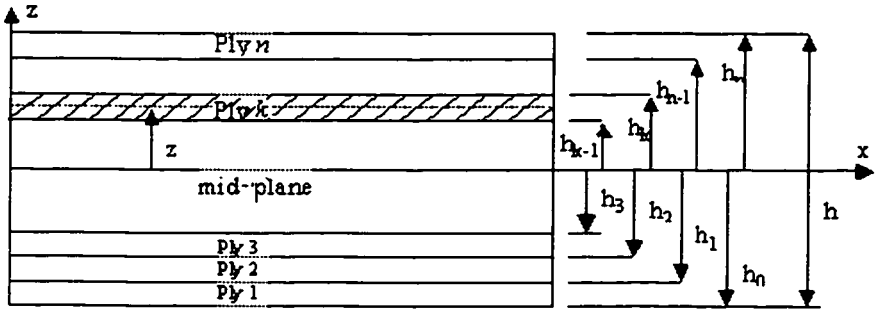

Figure 2.5 Multilayer laminate with co-ordinate notation for individual plies

In the case of a multilayer laminate the total force and moment resultants are obtained by summing the contributions from all layers. Thus for the laminate with n plies as shown in Figure 2.5, the force and moment resultants can be written as

$$\begin{Bmatrix} N_x \\ N_y \\ N_{xy} \end{Bmatrix} = \sum_{k=1}^{n} \int_{h_{k-1}}^{h_k} \begin{Bmatrix} \sigma_x \\ \sigma_y \\ \tau_{xy} \end{Bmatrix}_k dz \tag{2.34}$$

and

$$\begin{Bmatrix} M_x \\ M_y \\ M_{xy} \end{Bmatrix} = \sum_{k=1}^{n} \int_{h_{k-1}}^{h_k} \begin{Bmatrix} \sigma_x \\ \sigma_y \\ \tau_{xy} \end{Bmatrix}_k z dz \tag{2.35}$$

2.3.3 Equivalent elastic constants [58]

In-plane forces for symmetric laminates, for which the axial-bending coupling stiffness B_{ij} are zero, can be written as

$$\begin{Bmatrix} N_x \\ N_y \\ N_{xy} \end{Bmatrix} = \begin{bmatrix} A_{11} & A_{12} & A_{16} \\ A_{12} & A_{22} & A_{26} \\ A_{16} & A_{26} & A_{66} \end{bmatrix} \begin{Bmatrix} \varepsilon_x^0 \\ \varepsilon_y^0 \\ \gamma_{xy}^0 \end{Bmatrix} \tag{2.36}$$

Inversion of the equation (2.36) gives

$$\begin{Bmatrix} \varepsilon_x^0 \\ \varepsilon_y^0 \\ \gamma_{xy}^0 \end{Bmatrix} = \begin{bmatrix} a_{11} & a_{12} & a_{16} \\ a_{12} & a_{22} & a_{26} \\ a_{16} & a_{26} & a_{66} \end{bmatrix} \begin{Bmatrix} N_x \\ N_y \\ N_{xy} \end{Bmatrix} \tag{2.37}$$

in which $[a]$ is the extensional laminate compliance matrix, which is the inverse of the corresponding stiffness matrix, $[A]$, as given below:

$$[a]=[A]^{-1} \tag{2.38}$$

The average laminate stresses can be defined as

$$\bar{\sigma}_x = \frac{N_x}{h}, \qquad \bar{\sigma}_y = \frac{N_y}{h}, \text{ and } \quad \bar{\tau}_{xy} = \frac{N_{xy}}{h} \tag{2.39}$$

in which h is the laminate thickness.

So equation (2.37) can be rewritten in terms of average laminate stresses as

$$\begin{Bmatrix} \varepsilon_x^0 \\ \varepsilon_y^0 \\ \gamma_{xy}^0 \end{Bmatrix} = \begin{bmatrix} ha_{11} & ha_{12} & ha_{16} \\ ha_{12} & ha_{22} & ha_{26} \\ ha_{16} & ha_{26} & ha_{66} \end{bmatrix} \begin{Bmatrix} \frac{N_x}{h} = \bar{\sigma}_x \\ \frac{N_y}{h} = \bar{\sigma}_y \\ \frac{N_{xy}}{h} = \bar{\tau}_{xy} \end{Bmatrix} \tag{2.40}$$

By superposition of the three loadings $\bar{\sigma}_x$, $\bar{\sigma}_y$, and $\bar{\tau}_{xy}$ the following strain-stress relation can be obtained in terms of engineering constants.

$$\begin{Bmatrix} \varepsilon_x \\ \varepsilon_y \\ \gamma_{xy} \end{Bmatrix} = \begin{bmatrix} \frac{1}{E_x} & -\frac{\nu_{yx}}{E_y} & -\frac{1}{G_{xy} m_x} \\ -\frac{\nu_{xy}}{E_x} & \frac{1}{E_y} & -\frac{1}{G_{xy} m_y} \\ -\frac{m_x}{E_x} & -\frac{m_y}{E_y} & \frac{1}{G_{xy}} \end{bmatrix} \begin{Bmatrix} \sigma_x \\ \sigma_y \\ \tau_{xy} \end{Bmatrix} \tag{2.41}$$

The equivalent elasticity matrix [E] for a composite laminate can be calculated by inverting equation (2.37) as

$$\begin{Bmatrix} \bar{\sigma}_x \\ \bar{\sigma}_y \\ \bar{\tau}_{xy} \end{Bmatrix} = \begin{bmatrix} ha_{11} & ha_{12} & ha_{16} \\ ha_{12} & ha_{22} & ha_{26} \\ ha_{16} & ha_{26} & ha_{66} \end{bmatrix}^{-1} \begin{Bmatrix} \varepsilon_x^0 \\ \varepsilon_y^0 \\ \gamma_{xy}^0 \end{Bmatrix} \tag{2.42}$$

Now comparing equation (2.42) with equation (2.4) for calculating the elasticity matrix [E], one gets

$$[E] = \begin{bmatrix} ha_{11} & ha_{12} & ha_{16} \\ ha_{12} & ha_{22} & ha_{26} \\ ha_{16} & ha_{26} & ha_{66} \end{bmatrix}^{-1} \tag{2.43}$$

It is to be noted that, the elasticity matrix for the composite laminate thus obtained will be incorporated in the finite element formulation. Accordingly the equation (2.43) will be used in equation (2.12) for the finite element analysis.

2.4 Stochastic finite element analysis of composite laminates

Most modern mechanical systems possess a high degree of structural complexity. Therefore, when their behavior is to be predicted under various loading and environmental conditions, advanced analytical and numerical techniques are required. In the case of composite laminates, significant randomness in their material properties are present due to the variations in fiber volume fraction, void content, fiber orientation angles in various plies, thickness of the lamina, etc. introduced during the manufacturing processes. As a result, tests on a single material specimen provide a specific value for each material parameter and mechanical property. However, when a number of specimens are tested, randomly distributed values are obtained for the same material property. Therefore, the analysis of laminates has to be performed based on a probabilistic approach. When finite element analysis is performed based on a stochastic approach such that a stochastic description can be provided for both the material parameters and the response of the laminates, the resulting FEA is termed as *Stochastic Finite Element Analysis* (*SFEA*). The remainder of this chapter is devoted to the stress analysis of notched composite laminates based on a stochastic approach.

2.4.1 Stochastic field modeling of material parameters

The material properties are modeled in terms of two-dimensional stochastic processes that have zero mean. To this end, the procedure employed in the earlier works [51,52] is used here. Further, for the purpose of clarity, the procedure is presented in detail.

Material properties of NCT-301 as obtained from laboratory experiments are presented in Table 2.5. They are used to describe the stochastic processes that correspond to the Young's moduli, Poisson's ratio and shear modulus. Sample realizations are obtained at

each Gauss point in the finite element mesh. Using the generated sample realizations of material properties at each Gauss point, the stochastic elasticity matrix, $[E]$, is calculated for each Gauss point. The stochastic elasticity matrix thus generated is incorporated in the determination of the element stiffness matrix. The flow chart for computing the stochastic fields of the elastic constants is given in Figure 2.6.

Parameter	E_1 (GPa)	E_2 (GPa)	ν_{21}	ν_{12}	G_{12} (GPa)	Ave. exp. shear strength (GPa)
Mean value	113.9	7.985	0.020	0.29	3.130	0.0333
Standard dev.	0.019	0.041	0.086	0.031	0.040	0.0025

Table 2.5 Composite material properties [51]

Variations of the material properties such as the Young's modulus, Poisson's ratio and shear modulus are brought about using a fluctuating component $a(X)$ associated with a material property, which has a zero mean. For instance, the stochastic field of the Young's modulus in the fiber direction (E_1) is expressed as given in equation (2.68) and a similar procedure is applicable to E_2, G_{12}, ν_{12}, ν_{21}, ply orientation angle and ply thickness.

$$E_1 = \bar{E}_1[1 + a(X)] \quad ; \quad E[a(X)] = 0 \tag{2.44}$$

The auto-correlation function is given by [53]

$$R_{aa}(\xi) = E[a(X)a(X+\xi)] \tag{2.45}$$

where $X = [x, y]^T$ indicates the position vector and $\xi = [\xi_x, \xi_y]^T$ represents the separation vector between two points X and $(X + \xi)$. It is a fact that each material property is considered to vary at each Gauss point. Thus, if n represents the number of finite

elements present in the structure, and m represents the order of Gauss quadrature, then there are N (equal to n x m) material property values associated with the structure. Consider only the fluctuating component of the homogeneous stochastic field, which is used to model the material property variations around the expected value. These N values $a_i = a(X_i)$ $(i = 1,2,3,....,N)$ are correlated random variables with zero mean. Also X_i corresponds to the location of each Gauss point. Their correlation characteristics can be specified in terms of the covariance matrix C_{aa} of order N x N, whose ij^{th} component is given by

$$c_{ij} = Cov[a_i a_j] = E[a_i a_j] = R_{aa}(\xi_{ij}); \quad i,j = 1,....,N \tag{2.46}$$

in which $\xi_{ij} = (X_j - X_i)$ is the separation distance between the Gauss points i and j. Now a vector $\{a\} = [a_1 \quad a_2 \quad a_3 \quad ... \quad a_N]^T$ can be generated by

$$\{a\} = [L]\{Z\} \tag{2.47}$$

in which $\{Z\} = [Z_1 \quad Z_2 \quad Z_3 \quad ... \quad Z_N]^T$ is a vector consisting of N independent Gaussian random variables with zero mean and unit standard deviation, and $[L]$ is a lower triangular matrix obtained by the Cholesky decomposition of the covariance matrix $[C_{aa}]$. Thus,

$$[L][L]^T = [C_{aa}] \tag{2.48}$$

Once the Cholesky decomposition is accomplished, different sample vectors of $\{a\}$ are easily obtained by generating different samples for the Gaussian random vectors $\{Z\}$. The correlation properties of the stochastic field representing the fluctuating components of

material properties are expressed using the Markov correlation model, also known as the First-order autoregressive model. The choice of this model in this work is due to its wide use in the literature [54].

2.4.2 Markov model

The first- order autoregressive correlation model or the Markov model is given by

$$R_{aa}(\xi) = \sigma_o^2 \exp\left[-\left(\frac{|\xi|}{d}\right)\right] \tag{2.49}$$

in which σ_o is the standard deviation of the stochastic field $a(X)$ and further d is a parameter called the correlation length, which is defined such that the correlation is negligible when d is large. The stochastic field $a(X)$ represents the deviatoric components of the material property with autocorrelation function as given in equation (2.49). The stochastic field $a(X)$ for each Gauss point is represented by the value of a_g of $a(X)$ at the Gauss point X_g of the structure i.e., $a_g = a(X_g)$.

The Young's modulus along the fiber direction can now be assumed to have a distribution as given by the vector $\{a\}$ and can be represented by

$$E_{1g} = E_{1m}(1 + a_g) \tag{2.50}$$

where E_{1g} is the value of the Young's modulus in the fiber direction at a Gauss point. Moreover, E_{1m} is the mean value of the Young's modulus in the fiber direction and is taken from the Table 2.5. Similarly, the other material properties are represented by

Young's modulus in the transverse direction, $E_{2g} = E_{2m}(1 + b_g)$ (2.51)

1-2 directional Poisson's ratio, $\nu_{12g} = \nu_{12m}(1 + c_g)$ (2.52)

Shear modulus, $G_{12g} = G_{12m}(1 + d_g)$ (2.53)

in which E_{2m} is the mean value of the Young's modulus in the transverse direction and further, ν_{12m} and G_{12m} are the mean values of the 1-2 directional Poisson's ratio and the shear modulus respectively.

It should be noted here that the standard deviations of a_g, b_g, c_g and d_g represents the coefficients of variation of the material properties E_{1g}, E_{2g}, $?_{12g}$ and G_{12g}. Also the variation of the ply orientation angle, $?_g$ and the ply thickness t_g are evaluated in a manner similar to equations (2.50 – 2.53) as

$$\theta_g = \theta_m(1 + e_g) \tag{2.54}$$

$$t_g = t_m(1 + f_g) \tag{2.55}$$

in which $?_m$ and t_m are the mean values of the ply orientation angle and ply thickness respectively. The assumption of Gaussian distribution implies the possibility of generating negative values for the material properties. In order to avoid this difficulty, the values of the random variable, a_g, in the case of Monte-Carlo simulation are confined to the range

$$-1 + \varepsilon \le a_g \le 1 - \varepsilon \tag{2.56}$$

where e is a very small perturbation parameter.

2.4.3 Programming the stochastic finite element analysis

Using the test data of the material properties provided in Table 2.5, the stochastic processes that correspond to the Young's moduli, Poisson's ratio and shear modulus are determined according to equations (2.51 - 2.53) and further, sample realizations at each Gauss point in the finite element mesh are obtained. A similar procedure applies to θ and t. Using the generated sample realizations of material properties at each Gauss point the stochastic elasticity matrix, $[E]$, is calculated for each Gauss point. The stochastic elasticity matrix thus generated is incorporated into the equation (2.12) for the element stiffness matrix. The flow chart for computing the stochastic fields of the elastic constants is given below in Figure 2.6.

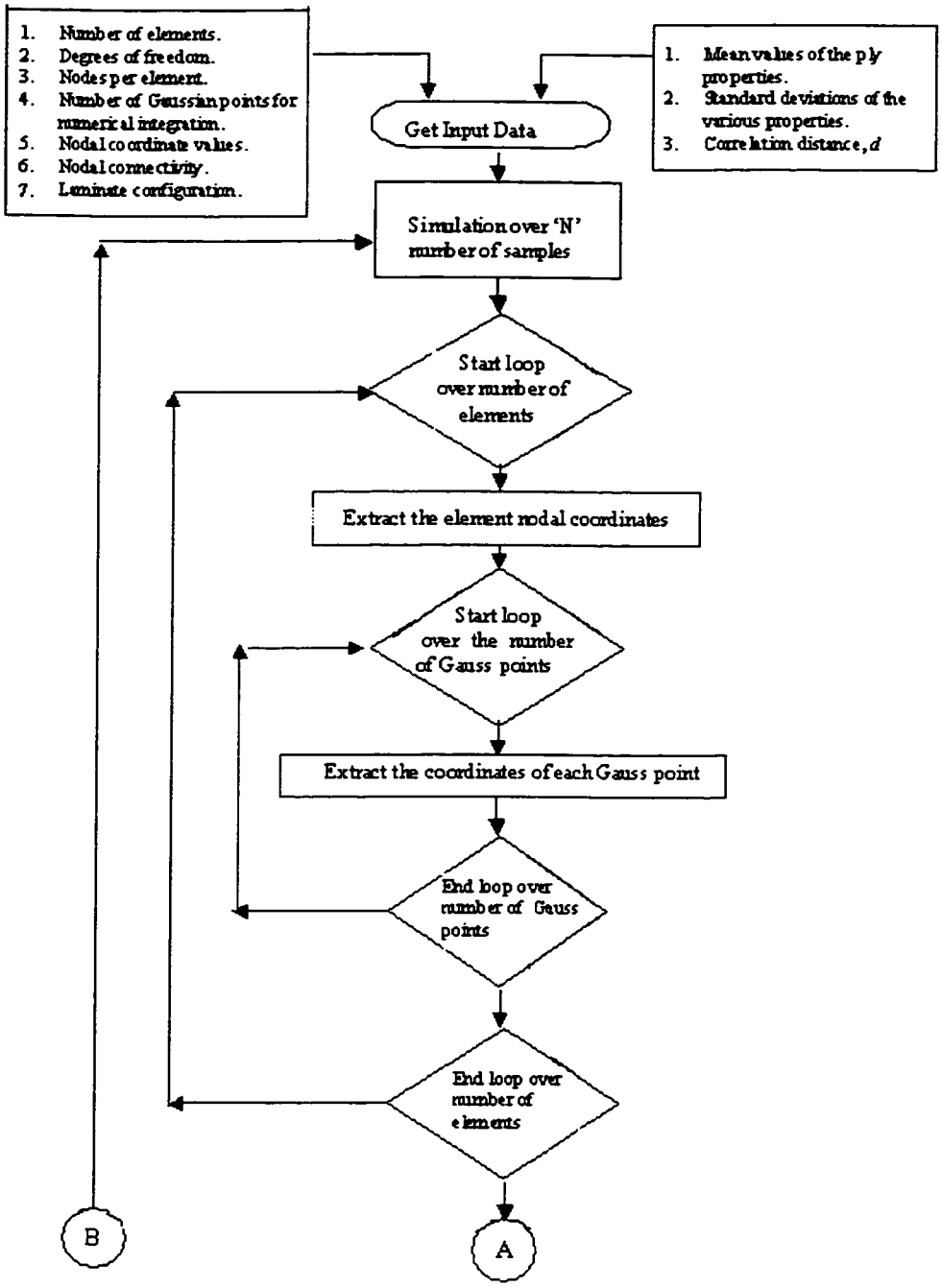
1. Number of elements.
2. Degrees of freedom.
3. Nodes per element.
4. Number of Gaussian points for numerical integration.
5. Nodal coordinate values.
6. Nodal connectivity.
7. Laminate configuration.
1. Mean values of the ply properties.
2. Standard deviations of the various properties.
3. Correlation distance, d
Get Input Data
Simulation over 'N' number of samples
Start loop over number of elements
Extract the element nodal coordinates
Start loop over the number of Gauss points
Extract the coordinates of each Gauss point
End loop over number of Gauss points
End loop over number of elements
B
A

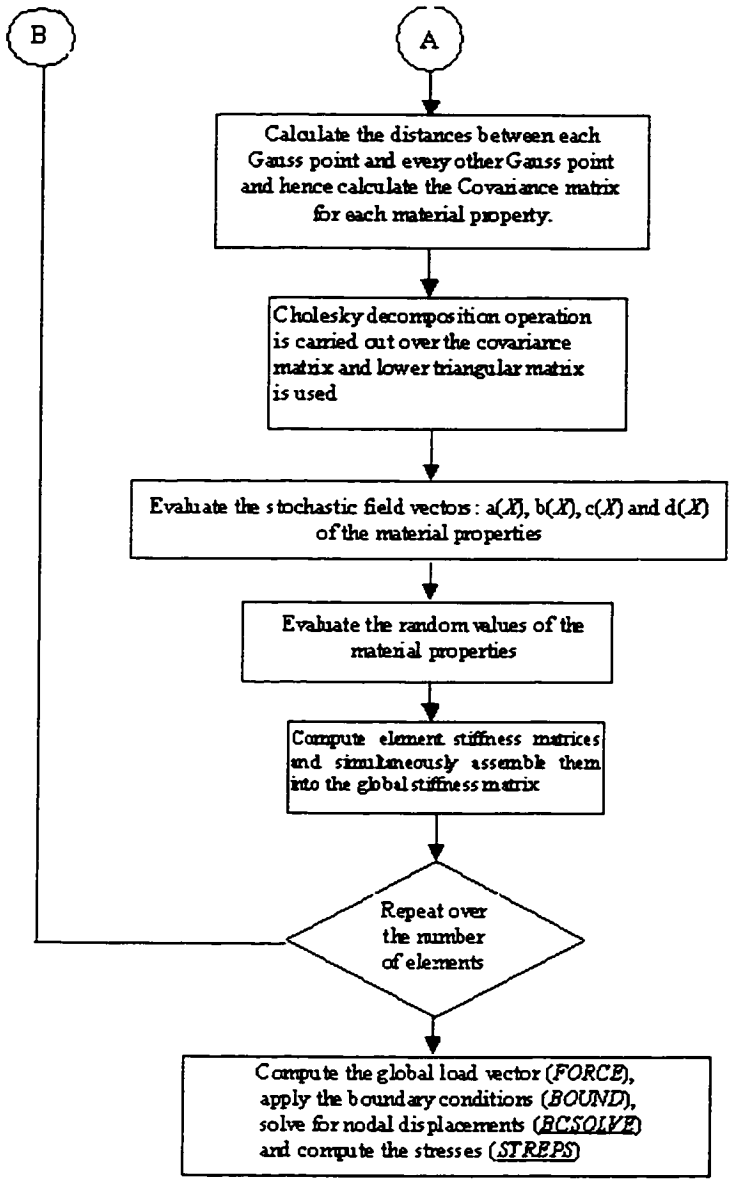

Figure 2.6 Flow chart used for the calculation of stochastic material properties based on stochastic field modeling, and stiffness matrix

2.4.3.1 Application 1

If we consider the irregularity in hole shape and offset of hole from the central coordinates, it is not possible to exploit the symmetry of a plate by modeling only half or quarter portion of the plate for the analysis, since the stress distribution will not be

uniform over the entire laminate. Thus it calls for the analysis of a complete plate. A laminate with $[\pm 45]_{4s}$ configuration having a width of 37.9 mm, length of 151.6 mm and a hole diameter of 5.1 mm at the center of the laminate is considered for the analysis. Ply thickness is assumed to be 0.125 mm. The material properties are taken from Table 2.5. A uniformly distributed load of 0.8 x 10^6 N/m is applied over an edge of the plate acting along the Y-axis. Choice of the load value is based on the experimental results obtained for $[0_2/\pm 45]_{2s}$ laminate. Since we lack information regarding the ultimate load a $[\pm 45]_{4s}$ laminate might take, a factor of safety on the ultimate load of $[0_2/\pm 45]_{2s}$ laminate is considered and thus a 0.8 x 10^6 N/m uniformly distributed load value is imposed on the lamiante. Finite element mesh used for the MATLAB® program is shown in Figure 2.9. Standard commercial ANSYS® package is used for comparing the results obatined from MATLAB® program. In the ANSYS® package, a similar model with nearly the same number of elements in the finite element mesh is generated using SOLID46 element and analyzed. SOLID46 is a layered version of the 8-node structural solid designed to model layered thick shells or solids. A set of sample nodal displacements realized using the stochastic approach is listed in Table 2.6. Corresponding nodal stress values developed near the boundary and hole edge of the plate based on MATLAB®, ANSYS® and exact solutions are listed in Table 2.7. Stress concentration factor for $[\pm 45]_{4s}$ ply configuration is shown in Figure 2.8c. Also Figure 2.8a represents a displacement value comparison made at random nodes and Figure 2.8b shows the stress distribution along x-axis in the region near hole edge.

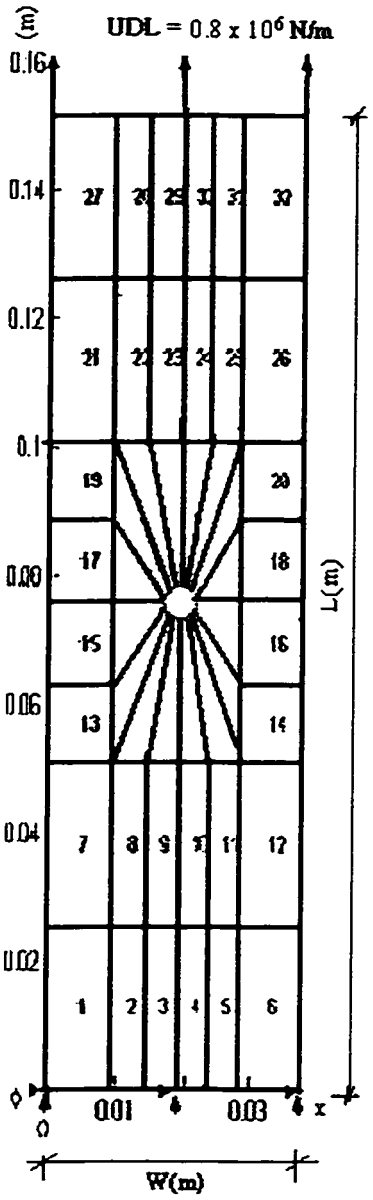

Figure 2.7 Finite element mesh, boundary conditions and loading for a complete laminate

GLOBAL NODE	MATLAB® RESULTS	ANSYS® RESULTS

At the Boundary	u (mm)	v (mm)	u (mm)	v (mm)
9	0.0449	0.240	0.0445	0.231
17	-0.0435	0.507	-0.0430	0.482
75	-0.0031	0.509	-0.0033	0.483
140	-0.0219	0.499	-0.0564	0.485
132	-0.0421	0.238	-0.0449	0.234
Near the hole edge along AB				
173	0.0198	0.236	0.0041	0.236
181	-0.0098	0.222	-0.0019	0.216
157	-0.0014	0.234	-0.0039	0.234
165	-0.0145	0.255	-0.0004	0.250

Table 2.6 Displacement values obtained using 300 simulations

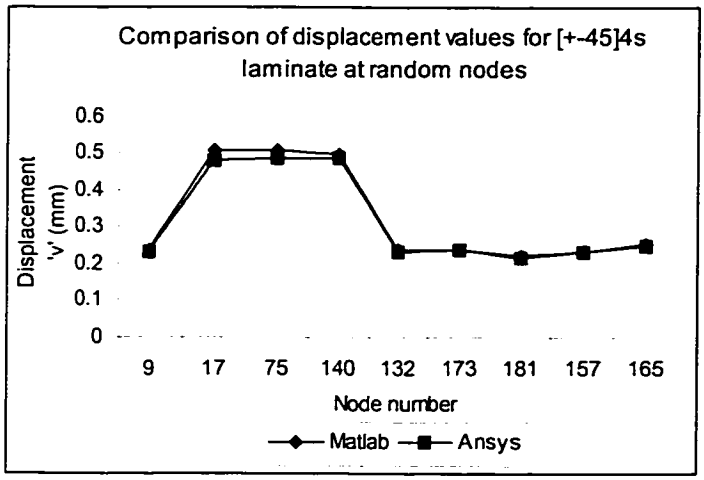

Figure 2.8-a The displacement values around the boundary and hole region

GLOBAL NODE	MATLAB®	ANSYS®	EXACT
Near hole edge along AB and boundary	sigma y (GPa)	sigma y (GPa)	sigma y (GPa)
173	0.778	0.784	0.761
157	0.775*	0.779	0.761
149	0.478	0.488	0.460
106	0.447	0.451	0.418
132	0.398	0.399	0.403

Table 2.7 Sample values of stress obtained in the simulation
* Mean value of maximum stress obtained using 300 simulations

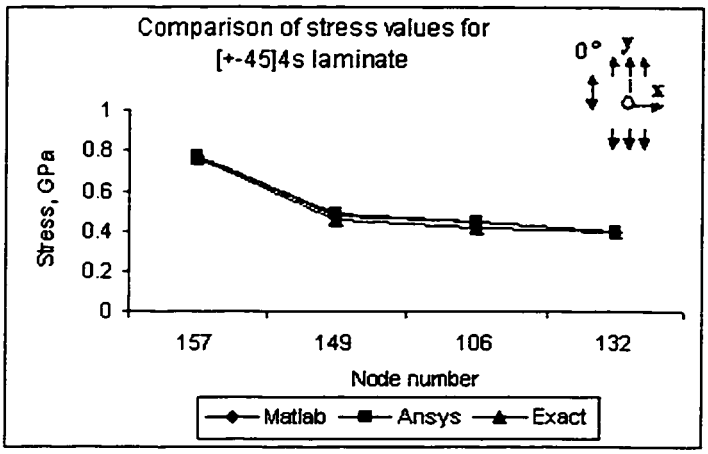

Figure 2.8-b The values of stress σ_y around the hole region

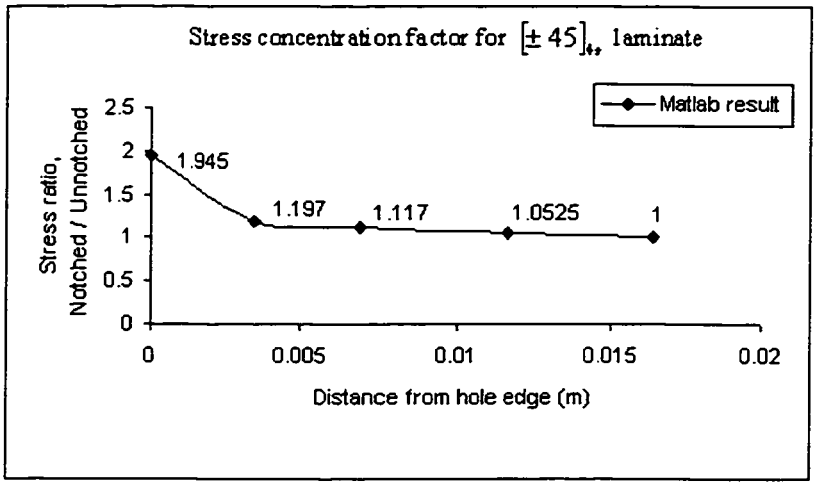

Figure.2.8c Ratio of values of σ_y corresponding to notched and unnotched laminates

Simulation is carried out over 300 laminates and the results are shown in Tables 2.6 and 2.7 and Figures 2.8a and 2.8b. Data corresponding to the maximum stress value of each and every laminate is acquired and further the mean, standard deviation and coefficent of variation values are calculated. Accordingly the mean value of maximum stress at node 157 is 0.775 GPa and the corresponding standard deviation value is 0.0229 GPa. The corresponding coefficient of variation is 0.02954. It can be seen that the stress value for node number 173 in Table 2.7 is almost the same as that for node 157 as this node is

placed symmetric to the node 157 which in turn is exactly placed on the hole edge. On comparing the results from Tables 2.6 and 2.7 and Figures 2.8a and 2.8b, the present results are in good correlation with the closed form and ANSYS® results.

2.4.3.2 Application 2

As another example [55] we consider a laminate of configuration $[0/\pm 45]_s$ made of a graphite-epoxy material having the material properties as follows:

$$E_1 = 141\,GPa; E_2 = 9.44\,GPa; G_{12} = 5.18\,GPa; \nu_{12} = 0.31$$

The boundary conditions and a uniformly distributed load of 1.5 x 10^6 N/m as expressed in section 2.4.3.1 for application 1 are borrowed for the current analysis. Table 2.8 gives details about the stress values obtained at 300th simulation. For node number 157 the mean value of maximum stress obtained using 300 simulations is shown in the table with an asterix. It is clear from Figure 2.9a, that the stress values obtained from MATLAB® nearly matches with exact and reference solutions. Stress concentration factor for $[0/\pm 45]_s$ ply configuration is shown in Figure 2.9b.

GLOBAL NODE	MATLAB®	EXACT	REF. [55]
Near Hole and Boundary	sigma y (GPa)	sigma y (GPa)	sigma y (GPa)
157	5.62*	5.78	5.94
149	2.36	2.30	2.33
106	2.18	2.09	2.11
119	2.07	2.037	2.06
132	2.02	2.019	2.01

Table 2.8 Sample values of stress obtained in the simulation
* Mean value of maximum stress obtained using 300 simulation

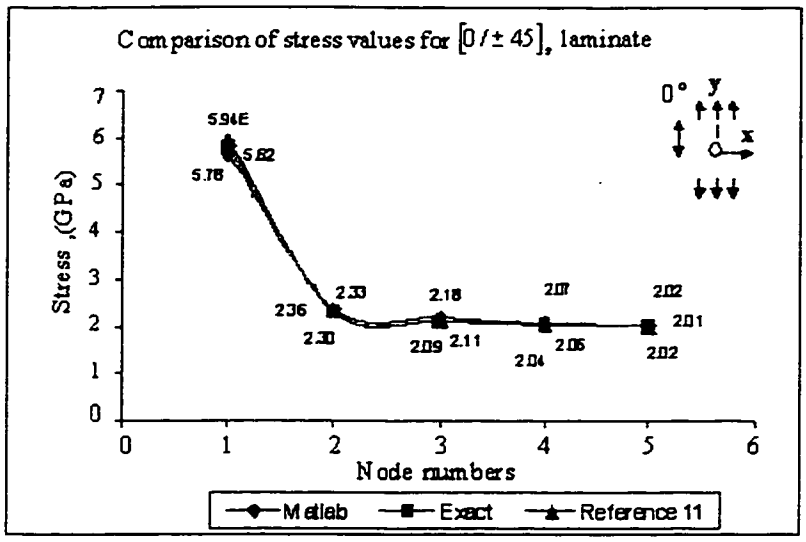

Figure 2.9-a The values of stress σ_y around the hole region

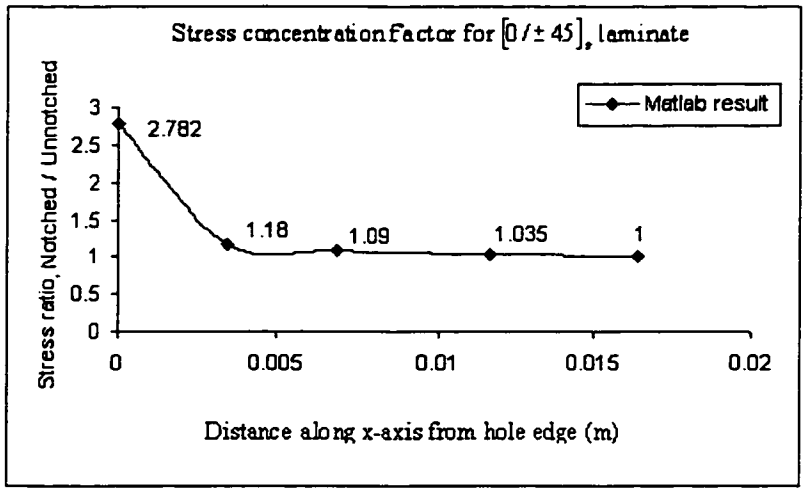

Figure 2.9-b Ratio of values of σ_y corresponding to notched and unnotched laminates

Results are compared with exact and reference results [55] and found to have a good match. Mean, standard deviation and coefficent of variation values are calculated for the maximum stress value based on the data collected over 300 simulations. Accordingly the mean value of maximum stress is 5.628 *GPa* as denoted for node 157 and the standard deviation value is 0.2043 *GPa.* Coefficient of variation attained for the laminate is

0.0363. Comparing the stress concentration factor values from Figures 2.8c and 2.9b, it can be observed that laminate $[\pm 45]_{4s}$ has a lower SCF value as opposed to $[0/\pm 45]_s$ laminate. Considering the coefficient of variation value for the laminates, $[0/\pm 45]_s$ laminate exhibits more variation when compared with $[\pm 45]_{4s}$ laminate.

2.5 Conclusions and discussions

A detailed analysis of stress concentration effects in isotropic plates under plane stress condition subjected to uniaxial tensile load is conducted using a MATLAB® program. Utilizing the symmetry of the plate, a quarter plate analysis is carried out. Results are presented in the Tables 2.1 and 2.2 and the finite element mesh adopted is shown in Figure 2.3. A complete plate analysis is also performed.

Finite element formulation for composite laminates is given in sections 2.3 and 2.4 and is implemented. Necessary modifications are made in the MATLAB® program written for isotropic case. Normal stress distribution around the circumference of a hole in an infinite orthotropic sheet under the in-plane loading is presented. The output includes the stress distribution along the axis perpendicular to the loading direction.

The fundamental solution is derived from the consideration of resultant force equilibrium in the loading condition. The present approach assumes that the normal stress, $\sigma_y(x,0)$ across the net section of a finite-width plate is proportional to that of an infinite-width plate by a factor called Finite Width Correction factor (FWC). Thus FWC is used to multiply the infinite-plate solution to obtain the stress distribution of a finite-plate. The basic theory is improved significantly by multiplying the opening-to-width ratio, 2a/W,

by a magnification factor 'M'. Stochastic variations in material properties over the laminate are established using Markov model and sample realizations of the material properties at every Gauss point are obtained. Now the entire analysis is performed for a number of plates and the mean and standard deviation values of maximum stress near the hole edge are computed.

Application problems involving laminates of different ply configurations are analyzed and stress concentration factor for each case is calculated.

It is to be noted that in the case of composites, SCF is not only the parameter of consideration for prediction of failure of notched laminates. Thus, the measure of strength for a composite laminate with a circular cutout needs a more complete description of the stresses near the hole. This is discussed in detail in chapters 4 and 5.

Chapter 3

Stochastic Finite Element Analysis of Plate Bending

3.1 Introduction

Isotropic and composite materials find wide applications in transportation and other construction industries because of their superior properties. Generally plates of large size will be used in these applications and holes will be made into these plates for practical reasons. Often, the stress concentration is a serious concern to the designer and the stress distribution around holes must be known to predict the failure strength. Structurally efficient designs of these structures have to be developed based on a thorough understanding of the response to fundamental loading conditions. Efforts have been made to analyze the lateral deformations of isotropic and symmetric composite laminates subjected to different types of uniformly distributed static loadings based on Mindlin theory.

Of all the shear deformation theories available, first-order shear deformation theory (FSDT) is the one most commonly used in modeling of thick plates. When normality assumption is not used i.e. plane sections remain plane but not necessarily normal to the

longitudinal axis after deformation, then transverse shear strain is not zero. Therefore rotation of a transverse normal plane about the y-axis is not equal to $-\frac{\partial w}{\partial x}$. This theory is commonly known as "Mindlin plate theory or First-order shear deformation theory".

In the thin plate problem transverse shear deformation is neglected, and deformation is completely described by a function $w = w(x, y)$, where lateral displacement w and coordinate z are perpendicular to the plate [55]. In particular, the assumption that u and v displacements are linear functions of the z co-ordinate proves to be completely inadequate for predicting the gross laminate response. Thus a higher order theory was developed based on the work given in reference [57] and the result is the First-order shear deformation theory (FSDT). The FSDT considers the aspect of transverse shear deformation in the laminate and thus can be implemented when thick components are encountered. For composites having a high ratio of E_{11} / G_{12} and a width to thickness ratio less than 10, radical departure from classical or Kirchhoff's theory has been demonstrated [58]. A pictorial description, illustrated in Figures 3.1 and 3.2 highlights the differences between Kirchhoff's theory and First-order shear deformation theory.

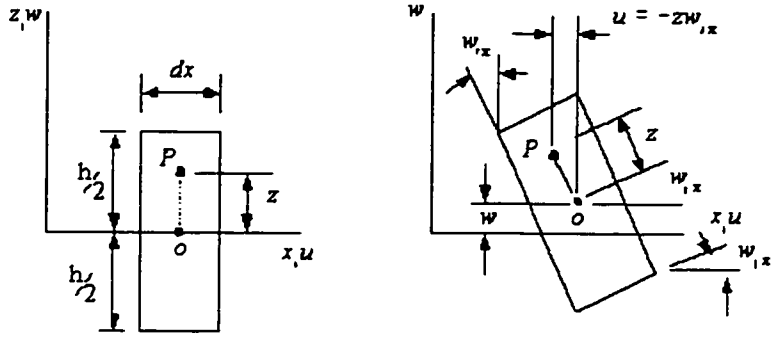

Figure 3.1 Thin plate theory (Kirchhoff Plate Theory)

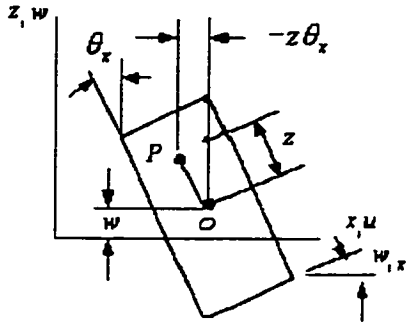

Figure 3.2 Mindlin Plate Theory

3.2 Formulation of plate bending analysis for isotropic plates

The formulation used in the present work has been described in reference [47] and for a better understanding details are given in the following.

From the Figure 3.2, displacements of any point 'P' in the plate can be described as,

$$u = u_o - z\theta_x(x,y),\ v = v_o - z\theta_y(x,y),\ w = w_o(x,y) \tag{3.1}$$

where

(u,v,w) are the displacements of a point 'P', θ_x and θ_y are the rotations of the transverse normal about the 'y' and 'x' axes respectively. It is to be noted that the displacements 'u' and 'v' that result from bending due to the transverse load have been considered to be negligible in the case of isotropic plates (that are not subjected to any in-plane loadings) and thus will not participate in the formulations to come. The sign convention, geometry, moment and shear force resultants for a plate element are given in the Figure 3.3.

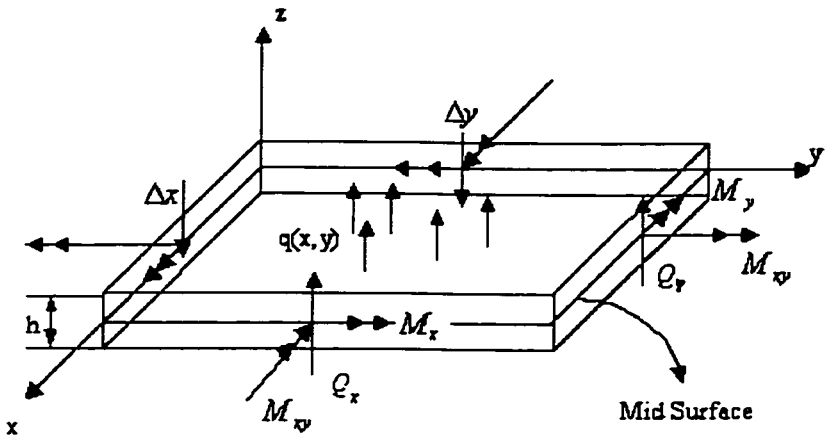

Figure 3.3 Moment and shear force resultants for a homogeneous linearly elastic plate element

In the following analysis a three-degree of freedom (d.o.f) system is considered which accounts for each and every node, one translation, 'w' in the direction of z-axis and two rotations θ_x and θ_y about 'y' and 'x' axes respectively as shown in Figure 3.4. If represented as rotation vectors by the right-hand rule, θ_x and θ_y point in the -y and +x directions, respectively. The program has the capability to take care of more general shapes as an isoparametric element is used for the analysis. In order to evaluate an integral numerically, the concept of three-point Gauss quadrature is utilized.

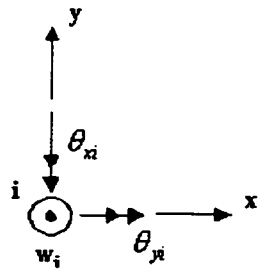

Figure 3.4 Co-ordinate system, deflection and rotations about the axes

3.2.1 Bending stiffness matrix for isotropic material

Stresses produce the following bending moments and transverse shear forces as shown in Figure 3.3:

$$M_x = \int_{-h/2}^{h/2} \sigma_x z\, dx \qquad M_y = \int_{-h/2}^{h/2} \sigma_y z\, dz \qquad M_{xy} = \int_{-h/2}^{h/2} \tau_{xy} z\, dx \tag{3.2}$$

$$Q_x = \int_{-h/2}^{h/2} \tau_{zx} dz \qquad Q_y = \int_{-h/2}^{h/2} \tau_{yz} dz \tag{3.3}$$

The moments are expressed in terms of moment per unit length and shear forces as forces per unit length.

Now, let x and y be the principal directions of the material. Stress σ_z is considered negligible in comparison with σ_x, σ_y and τ_{xy}. The strain-displacement relations of Mindlin plate theory can be expressed as follows,

$$\begin{aligned} u &= -z\theta_x \quad \varepsilon_x = -z\theta_{x,x} \quad \gamma_{xy} = -z\left(\theta_{x,y} + \theta_{y,x}\right) \\ v &= -z\theta_y \quad \varepsilon_y = -z\theta_{y,y} \quad \gamma_{yz} = w_{,y} - \theta_y \\ & \qquad\qquad\quad \gamma_{zx} = w_{,x} - \theta_x \end{aligned} \tag{3.4}$$

Accordingly the stress-strain relation for isotropic materials can be expressed as,

$$\begin{bmatrix}\sigma_x\\ \sigma_y\\ \tau_{xy}\\ \tau_{yz}\\ \tau_{zx}\end{bmatrix}=\begin{bmatrix}E_x^{'} & E^{"} & 0 & 0 & 0\\ E^{"} & E_y^{'} & 0 & 0 & 0\\ 0 & 0 & G_{xy} & 0 & 0\\ 0 & 0 & 0 & G_{yz} & 0\\ 0 & 0 & 0 & 0 & G_{zx}\end{bmatrix}\begin{pmatrix}-z\theta_{x,x}\\ -z\theta_{y,y}\\ -z(\theta_{x,y}+\theta_{y,x})\\ -\theta_y+w_{,y}\\ -\theta_x+w_{,x}\end{pmatrix} \tag{3.5}$$

where

$$E_x^{'}=E_y^{'}=\frac{E^{"}}{\nu}=\frac{E}{1-\nu^2} \quad \text{and} \quad G=\frac{E}{2(1+\nu)} \tag{3.6}$$

where E is the elastic modulus and ν is the Poisson's ratio.

The moment-curvature relation is obtained by substitution of equation (3.4) into equation (3.5) and the result into equations (3.2) and (3.3):

$$\{M\}=-[\,D_M\,]\{\kappa\} \tag{3.7}$$

Accordingly the [D_M] matrix can be derived as follows:

$$\begin{bmatrix}M_x\\ M_y\\ M_{xy}\end{bmatrix}=\int_{-h/2}^{h/2}\begin{bmatrix}\sigma_x\\ \sigma_y\\ \tau_{xy}\end{bmatrix}z\,dz \tag{3.8}$$

Substitution of the stress terms from equation (3.5) into equation (3.8) we have

$$\begin{bmatrix}M_x\\ M_y\\ M_{xy}\end{bmatrix}=\int_{-h/2}^{h/2}\begin{bmatrix}E_x^{'} & E^{"} & 0\\ E^{"} & E_y^{'} & 0\\ 0 & 0 & G_{xy}\end{bmatrix}\begin{bmatrix}-z\theta_{x,x}\\ -z\theta_{y,y}\\ -z(\theta_{x,y}+\theta_{y,x})\end{bmatrix}z\,dz \tag{3.9}$$

$$\begin{bmatrix} Q_y \\ Q_x \end{bmatrix} = -\int_{-h/2}^{h/2} \begin{bmatrix} G_{yz} & 0 \\ 0 & G_{zx} \end{bmatrix} \begin{bmatrix} \theta_y - w_{,y} \\ \theta_x - w_{,x} \end{bmatrix} dz \tag{3.10}$$

The shear stiffness terms $G_{yz}h$ and $G_{zx}h$ in equation (3.10) are replaced by $G_{yz}h/1.2$ and $G_{zx}h/1.2$ in order to permit the parabolic distributions of τ_{yz} and τ_{zx} to be replaced by uniform distributions. Thus the factor (1/1.2) attached with $G_{yz}h$ and $G_{zx}h$ is termed as shear correction factor. Assembly of the equations (3.9) and (3.10) yields

$$\begin{bmatrix} M_x \\ M_y \\ M_{xy} \\ Q_y \\ Q_x \end{bmatrix} = -\underbrace{\begin{bmatrix} & & & 0 & 0 \\ & [D_k] & & 0 & 0 \\ & & & 0 & 0 \\ 0 & 0 & 0 & G_{yz}h/1.2 & 0 \\ 0 & 0 & 0 & 0 & G_{zx}h/1.2 \end{bmatrix}}_{[D_M]} \underbrace{\begin{pmatrix} \theta_{x,x} \\ \theta_{y,y} \\ \theta_{x,y} + \theta_{y,x} \\ \theta_y - w_{,y} \\ \theta_x - w_{,x} \end{pmatrix}}_{\{\kappa\}} \tag{3.11}$$

where $\{\kappa\}$ is the curvature matrix. For isotropic material $[D_k]$ matrix can be represented as:

$$[D_k] = \begin{bmatrix} D & \nu D & 0 \\ \nu D & D & 0 \\ 0 & 0 & (1-\nu)\dfrac{D}{2} \end{bmatrix} \tag{3.12}$$

where

$$D = \frac{Eh^3}{12(1-\nu^2)} \tag{3.13}$$

3.2.2 Stiffness matrix for isotropic plate

The starting point for formulating an element stiffness matrix is an expression for strain energy U. With 'A' denoting the area of the plate at the mid-surface,

$$U = \frac{1}{2}\int_{-h/2}^{h/2}\{\varepsilon\}^T[E]\{\varepsilon\}dzdA \tag{3.14}$$

where $\{\varepsilon\}^T = [\varepsilon_x \quad \varepsilon_y \quad \gamma_{xy} \quad \gamma_{yz} \quad \gamma_{zx}]$, and the individual strains are stated in terms of displacements. Integration through the thickness yields

$$U = \frac{1}{2}\int_{A}\{\kappa\}^T[D_M]\{\kappa\}dA \tag{3.15}$$

where $[D_M]$ and $\{\kappa\}$ are the bending stiffness and curvature matrices. Since all the d.o.f are present at every node, the same shape functions N_i are used to interpolate w, θ_x and θ_y, that is,

$$\begin{bmatrix} w \\ \theta_x \\ \theta_y \end{bmatrix} = \sum_{i=1}^{N} \begin{bmatrix} N_i & 0 & 0 \\ 0 & N_i & 0 \\ 0 & 0 & N_i \end{bmatrix} \begin{bmatrix} w_i \\ \theta_{xi} \\ \theta_{yi} \end{bmatrix}$$

$$\{u\} \quad = \quad [N] \quad \{d\} \tag{3.16}$$

where N is the number of nodes per element and $\{d\} = [w_1, \theta_{x1}, \theta_{y1} \ldots\ldots w_N, \theta_{xN}, \theta_{yN}]^T$.

Curvature matrix $\{\kappa\}$ is stated as:

$$\{\kappa\} = \begin{bmatrix} \theta_{x,x} \\ \theta_{y,y} \\ \theta_{x,y} + \theta_{y,x} \\ \theta_y - w_{,y} \\ \theta_x - w_{,x} \end{bmatrix} = [\partial]\{u\} \tag{3.17}$$

where

$$[\partial] = \begin{bmatrix} 0 & \partial/\partial x & 0 \\ 0 & 0 & \partial/\partial y \\ 0 & \partial/\partial y & \partial/\partial x \\ -\partial/\partial y & 0 & 1 \\ -\partial/\partial x & 1 & 0 \end{bmatrix} \tag{3.18}$$

Thus

$$\{\kappa\} = [B]\{d\} \tag{3.19}$$

and

$$[B] = [\partial][N] = \begin{bmatrix} 0 & N_{1,x} & 0 & .... & .... & 0 & N_{8,x} & 0 \\ 0 & 0 & N_{1,y} & .... & .... & 0 & 0 & N_{8,y} \\ 0 & N_{1,y} & N_{1,x} & .... & .... & 0 & N_{8,y} & N_{8,x} \\ -N_{1,y} & 0 & N_1 & .... & .... & -N_{8,y} & 0 & N_8 \\ -N_{1,x} & N_1 & 0 & .... & .... & -N_{8,x} & N_8 & 0 \end{bmatrix} \tag{3.20}$$

Finally the strain energy and the elemental stiffness matrix are obtained:

$$U = \frac{1}{2}\{d\}^T[k]\{d\} \tag{3.21}$$

$$[k] = \int_A [B]^T[D_M][B]dA \tag{3.22}$$

It can be regarded that the stiffness matrix of a Mindlin plate element is composed of a bending stiffness term $[k_b]$ and a transverse shear stiffness term $[k_s]$. Thus equation (3.20) can be split into two parts as:

$$[B]=[B_b]+[B_s] \tag{3.23}$$

$[B_b]$ is associated with in-plane strains $\varepsilon_x, \varepsilon_y$ and γ_{xy} and is obtained by setting rows 4 and 5 of $[B]$ to zero. $[B_s]$ is associated with transverse shear strains γ_{yz} and γ_{zx}, and is obtained by setting rows 1,2 and 3 of $[B]$ to zero. The shape functions N_i are expressed in terms of isoparametric co-ordinates ξ and η.

The elemental stiffness matrix would be

$$[k]=\underbrace{\int_A [B_b]^T [D_M][B_b]dA}_{[k_b]}+\underbrace{\int_A [B_s]^T [D_M][B_s]dA}_{[k_s]} \tag{3.24}$$

where $dA=J\,d\xi\,d\eta$ (3.25)

and J is the Jacobian determinant.

3.2.3 Nodal force calculation

It has been shown in reference [47] that the application of a load on the laminate will not generate equal amount of load on each and every node on the plate. In that case all application problems involving different kinds of loading, have to be dealt with separately and nodal forces have to be calculated. When a distributed lateral load or a

moment load is acting on an element, then the respective element nodal loads can be calculated as follows:

$$f_{iq} = \int_A N_i q \, dA \qquad f_{iMx} = \int N_{i,x} M_x dy \qquad f_{iMy} = \int N_{i,x} M_{xy} dx \tag{3.26}$$

where i = 1,2...8, 'q' is the intensity of uniformly distributed load, M_x and M_y are prescribed boundary values of moments imposed over the plate. As an illustration, forces exerted at the nodes due to the application of uniformly distributed load is given in equations (3.27) and (3.28),

$$f_{1,2,3,4} = -(1/3)q|J| \tag{3.27}$$

and

$$f_{5,6,7,8} = (4/3)q|J| \tag{3.28}$$

where $f_{1,2,\ldots,8}$ correspond to the respective nodes of the element as shown below.

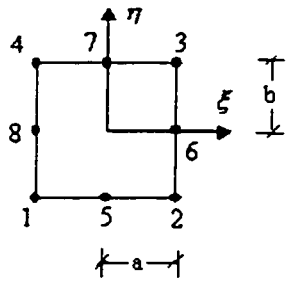

Figure 3.5 Eight-node plane isoparametric element in the local co-ordinate system

Finally the minimum number of simulations in the stochastic analysis is determined considering each of the stress components. The procedure is based on the flow-chart

presented in Figure 2.6. Application problems involving the calculation of mean and standard deviation values of the stress components are given in the following.

3.2.4 Program validation for isotropic case

To check the correctness of the program, an example is considered which involves the analysis of an isotropic square plate of length (a) $0.12m$ and thickness (h) $0.012m$ subjected to simply supported condition [59]. When a plate with a ratio of length to thickness a/h = 10 is considered, then the plate can be considered to be a thick plate. The bending stiffness matrix [D_M] for an isotropic plate is obtained using equation (3.11) in section 3.1.1.

Closed form solution

Navier solution for simply supported rectangular plates [60] subjected to uniformly distributed load is considered for comparing the results obtained from FEM solution. The final form of the equation (3.29) shown below is achieved using a rapidly converging series, which gives a reasonably approximate result by taking only the first term of the series. Thus the maximum deflection at the centre of the plate, would be:

$$w_{\max} = \frac{4qa^4}{\pi^6 D} = 0.00416\frac{qa^4}{D} \tag{3.29}$$

where

$$D = Eh^3/12(1-\nu^2) \tag{3.30}$$

Representing it in the non-dimensional form:

$$\overline{w} = w_{max} E h^3 \, x \, 10^2 / a^4 q \tag{3.31}$$

Assuming (Poisson's ratio) 'ν'as 0.3, (Young's Modulus) 'E' as $200\,GPa$, (shear modulus) 'G' as $80\,GPa$ and (intensity of distributed load) 'q' as $18.5\,MPa$, the maximum displacement of the plate, non-dimensional form of the maximum displacement $\overline{w}$ obtained from closed form and FEM solutions are tabulated in Table 3.1 as follows.

Reference	Mean $w_{max}(m)$	Mean $\overline{w}$
Navier solution	-0.000492	- 4.432
Matlab (FEM)	-0.000461	- 4.153
Ref. [59]	-0.000498	- 4.770

Table 3.1 Mean values of maximum displacement and non-dimensional maximum displacement

It has been shown in reference [59] that the 9-node rectangular element gives virtually the same results as the exact solution considering full (3 x 3 Gauss rule) integration. As seen from Table 3.1, maximum deflection obtained from MATLAB® program is varying by 6.3% from the Navier solution. This variation in the value can be attributed to the fact that an 8-noded isoparametric element produces less accurate results as compared to a 9-noded rectangular element. At the same time the thickness of the plate and the finite element mesh employed will also contribute to the variation in the result.

3.3 Formulation of plate bending analysis for composite laminates

The present formulation uses a five-degrees of freedom (d.o.f.) system at each and every node, with displacements in 'u' and 'v'directions, one translation 'w' in the direction of

z-axis and two rotations θ_x and θ_y about 'y' and 'x' axes respectively. Sign conventions similar to those expressed in section 3.1.1 are retained.

The displacement field of the laminate in the first order shear deformation theory, is given by,

$$u(x,y,z) = u_o - z\theta_x(x,y)$$

$$v(x,y,z) = v_o - z\theta_y(x,y) \tag{3.32}$$

$$w(x,y,z) = w_o(x,y)$$

Linear strain-displacement relation is given by,

$$\varepsilon_x = \frac{\partial u}{\partial x}\ ;\ \varepsilon_y = \frac{\partial v}{\partial y}\ ;\ \gamma_{xy} = \frac{\partial v}{\partial x} + \frac{\partial u}{\partial y}\ ;\ \gamma_{yz} = \frac{\partial w}{\partial y} + \frac{\partial v}{\partial z}\ ;\ \gamma_{xz} = \frac{\partial w}{\partial x} + \frac{\partial u}{\partial z} \tag{3.33}$$

Substituting equation (3.32) in equation (3.33) we have;

$$\varepsilon_x = \frac{\partial}{\partial x}(u_o - z\theta_x) = \frac{\partial u_o}{\partial x} - z\frac{\partial \theta_x}{\partial x} = \varepsilon_x^o - z\theta_{x,x} = \varepsilon_x^o - z\kappa_x \tag{3.34}$$

Similarly we have,

$$\varepsilon_y = \varepsilon_y^o - z\theta_{y,y} = \varepsilon_y^o - z\kappa_y \tag{3.35}$$

$$\gamma_{xy} = \gamma_{xy}^o - z(\theta_{x,y} + \theta_{y,x}) = \gamma_{xy}^o - z\kappa_{xy} \tag{3.36}$$

$$\gamma_{yz} = w_{,y} - \theta_y \tag{3.37}$$

$$\gamma_{xz} = w_{,x} - \theta_x \tag{3.38}$$

The ply stiffness matrix coupling the stress and strain matrices can be expressed as,

$$\begin{bmatrix}\sigma_x\\ \sigma_y\\ \tau_{xy}\\ \tau_{yz}\\ \tau_{xz}\end{bmatrix}=\begin{bmatrix}\overline{Q}_{11} & \overline{Q}_{12} & \overline{Q}_{13} & 0 & 0\\ \overline{Q}_{21} & \overline{Q}_{22} & \overline{Q}_{23} & 0 & 0\\ \overline{Q}_{31} & \overline{Q}_{32} & \overline{Q}_{33} & 0 & 0\\ 0 & 0 & 0 & \overline{Q}_{44} & \overline{Q}_{45}\\ 0 & 0 & 0 & \overline{Q}_{54} & \overline{Q}_{55}\end{bmatrix}\begin{pmatrix}\varepsilon_x\\ \varepsilon_y\\ \gamma_{xy}\\ \gamma_{yz}\\ \gamma_{xz}\end{pmatrix} \tag{3.39}$$

where $\overline{Q}_{ij}$ are the transformed reduced stiffness coefficients of the ply.

3.3.1 Bending stiffness matrix for composite laminate

Proceeding in a similar way as described in section 3.1.1, stiffness matrix $[D_M]$ for the composite laminate can also be deduced. The force and moment resultants N_i and M_i are defined as

$$(N_i, M_i) = \int_{-h/2}^{h/2} \sigma_i(1, z)dz \quad (i = 1,2,6) \tag{3.40}$$

The resultants (N_i, M_i, Q_i) can be expressed in terms of the strain components as follows:

$$N_i = A_{ij}\varepsilon_j^o + B_{ij}k_j \quad (i, j = 1,2,6) \tag{3.41}$$

$$M_i = B_{ij}\varepsilon_j^o + D_{ij}k_j \quad (i, j = 1,2,6) \tag{3.42}$$

$$Q_x = A_{4j}\varepsilon_j^o \qquad (j = 4,5) \tag{3.43}$$

$$Q_y = A_{5j}\varepsilon_j^o \qquad (j = 4,5) \tag{3.44}$$

where

$\varepsilon_1^o = \varepsilon_x^o,\ \varepsilon_2^o = \varepsilon_y^o,\ \varepsilon_6^o = \gamma_{xy}^o,\ \varepsilon_4^o = \gamma_{yz},\ \varepsilon_5^o = \gamma_{zx},\ k_1 = \kappa_x,\ k_2 = \kappa_y$ *and* $k_6 = \kappa_{xy}$.

Further A_{ij}, B_{ij} and D_{ij} are the laminate stiffness coefficients given by,

$$A_{ij}, B_{ij}, D_{ij} = \int_{-h/2}^{h/2} \overline{Q}_{ij}(1, z, z^2)dz \quad (i, j = 1,2,6) \tag{3.45}$$

Thus the force and moment resultants can be written as

$$\begin{bmatrix} N_x \\ N_y \\ N_{xy} \\ M_x \\ M_y \\ M_{xy} \\ Q_x \\ Q_y \end{bmatrix} = \underbrace{\begin{bmatrix} A_{11} & A_{12} & A_{16} & B_{11} & B_{11} & B_{16} & 0 & 0 \\ A_{21} & A_{22} & A_{26} & B_{21} & B_{22} & B_{26} & 0 & 0 \\ A_{61} & A_{62} & A_{66} & B_{61} & B_{62} & B_{66} & 0 & 0 \\ B_{11} & B_{12} & B_{16} & D_{11} & D_{12} & D_{16} & 0 & 0 \\ B_{21} & B_{22} & B_{26} & D_{21} & D_{22} & D_{26} & 0 & 0 \\ B_{61} & B_{62} & B_{66} & D_{61} & D_{62} & D_{66} & 0 & 0 \\ 0 & 0 & 0 & 0 & 0 & 0 & F_{44} & F_{45} \\ 0 & 0 & 0 & 0 & 0 & 0 & F_{54} & F_{55} \end{bmatrix}}_{[D_M]} \underbrace{\begin{bmatrix} \varepsilon_x^o \\ \varepsilon_y^o \\ \gamma_{xy}^0 \\ \kappa_x \\ \kappa_y \\ \kappa_{xy} \\ \gamma_{yz} \\ \gamma_{zx} \end{bmatrix}}_{\{k\}} \tag{3.50}$$

where $[D_M]$ corresponds to the stiffness matrix associated with a composite laminate. Since the shear correction factor K_s is also associated with the composite material, the coefficients F_{ij} where i, j = 4,5 are given by:

$$F_{44} = K_s A_{44} \; ; \; F_{45} = K_s A_{45} ; \; F_{54} = K_s A_{54} ; \; F_{55} = K_s A_{55} \tag{3.51}$$

It is to be noted that, if a symmetric laminate configuration is considered then the matrix [B] is a null matrix.

3.3.2 Stiffness matrix for composite laminate

The stiffness matrix is derived as presented in section 3.2.2. Accordingly we can express the displacements in terms of the interpolation functions as follows:

$$u_o = \sum_{i=1}^{8} N_i u_{oi};\ v_o = \sum_{i=1}^{8} N_i v_{oi};\ w_o = \sum_{i=1}^{8} N_i w_{oi};\ \theta_x = \sum_{i=1}^{8} N_i \theta_{xi};\ \theta_y = \sum_{i=1}^{8} N_i \theta_{yi} \tag{3.52}$$

Thus,

$$\begin{bmatrix} u_o \\ v_o \\ w_o \\ \theta_x \\ \theta_y \end{bmatrix} = \sum_{i=1}^{8} \begin{bmatrix} N_i & 0 & 0 & 0 & 0 \\ 0 & N_i & 0 & 0 & 0 \\ 0 & 0 & N_i & 0 & 0 \\ 0 & 0 & 0 & N_i & 0 \\ 0 & 0 & 0 & 0 & N_i \end{bmatrix} \begin{bmatrix} u_{oi} \\ v_{oi} \\ w_{oi} \\ \theta_{xi} \\ \theta_{yi} \end{bmatrix} \tag{3.53}$$

which is of the form,

$$\{u\} = [N]\{d\} \tag{3.54}$$

and matrix $\{d\}$ is given by,

$$\{d\} = \lfloor u_1\ v_1\ w_1\ \theta_{x1}\ \theta_{y1} \ldots\ldots\ldots u_8\ v_8\ w_8\ \theta_{x8}\ \theta_{y8} \rfloor^T$$

Also the matrix $\{k\}$ can be expressed as,

$$\{k\}_{8x1} = [B]_{8x40}\ \{d\}_{40x1} \tag{3.55}$$

Matrix [B] can further be expressed as,

$$\{k\}_{8x1} = [\partial]_{8x5}\ [N]_{5x40}\ \{d\}_{40x1} \tag{3.56}$$

Equation (3.57) represents the $[\partial]$ matrix employed in equation (3.56);

$$[\partial]=\begin{bmatrix} \frac{\partial}{\partial x} & 0 & 0 & 0 & 0 \\ 0 & \frac{\partial}{\partial y} & 0 & 0 & 0 \\ \frac{\partial}{\partial y} & \frac{\partial}{\partial x} & 0 & 0 & 0 \\ 0 & 0 & 0 & \frac{\partial}{\partial x} & 0 \\ 0 & 0 & 0 & 0 & \frac{\partial}{\partial y} \\ 0 & 0 & 0 & \frac{\partial}{\partial y} & \frac{\partial}{\partial x} \\ 0 & 0 & \frac{\partial}{\partial y} & 0 & -1 \\ 0 & 0 & \frac{\partial}{\partial x} & -1 & 0 \end{bmatrix} \tag{3.57}$$

Thus the matrix [B] is given by:

$$[B]=\begin{bmatrix} N_{1,x} & 0 & 0 & 0 & 0 & . & . & N_{8,x} & 0 & 0 & 0 & 0 \\ 0 & N_{1,y} & 0 & 0 & 0 & . & . & 0 & N_{8,y} & 0 & 0 & 0 \\ N_{1,y} & N_{1,x} & 0 & 0 & 0 & . & . & N_{8,y} & N_{8,x} & 0 & 0 & 0 \\ 0 & 0 & 0 & N_{1,x} & 0 & . & . & 0 & 0 & 0 & N_{8,x} & 0 \\ 0 & 0 & 0 & 0 & N_{1,y} & . & . & 0 & 0 & 0 & 0 & N_{8,y} \\ 0 & 0 & 0 & N_{1,y} & N_{1,x} & . & . & 0 & 0 & 0 & N_{8,y} & N_{8,x} \\ 0 & 0 & N_{1,y} & 0 & -N_1 & . & . & 0 & 0 & N_{8,y} & 0 & -N_8 \\ 0 & 0 & N_{1,x} & -N_1 & 0 & . & . & 0 & 0 & N_{8,x} & -N_8 & 0 \end{bmatrix} \tag{3.58}$$

The elemental stiffness matrix can be written as shown in equation (3.59):

$$[k]=\int_A [B]^T[D_M][B]dA \tag{3.59}$$

3.3.3 Program validation for composite laminate

The MATLAB® program developed in this chapter is now demonstrated through an application to a composite square laminate. Accordingly a cross-ply laminate of configuration $[0/90]_{24s}$ having dimensions of 0.12 m x 0.12 m is employed. The ply thickness is chosen to be 1.25 x 10^{-4} m, which makes the total thickness of the laminate to be 0.012 m. Thus the length to thickness ratio (a/h) is 10. It is subjected to a uniformly distributed load 'q' of intensity $18.5\,MPa$. The shear correction factor K_s is set to a value of (5/4).

The bending stiffness matrix $[D_M]$ for the composite laminate is calculated using equation (3.50) in section 3.2.1. Using the test data on elastic constants of the composite material, presented in Table 2.5, the stochastic field realizations of all the material properties are obtained at each Gauss point. In the present thesis, a three-point Gaussian numerical integration is used as it gives the most accurate results. Considering any typical element in the structure, nine different sample realizations of each of the stochastic processes are generated corresponding to the nine Gauss points in the element. Figure 3.6 depicts the geometry, finite element mesh, boundary condition and loading used for the present analysis. Accordingly we have 16 elements thus developing 16 x 9 Gauss points. Table 3.2 gives a comparison of nodal displacement values between the MATLAB® program results and closed form solution. The last column of the table provides the variation in their values.

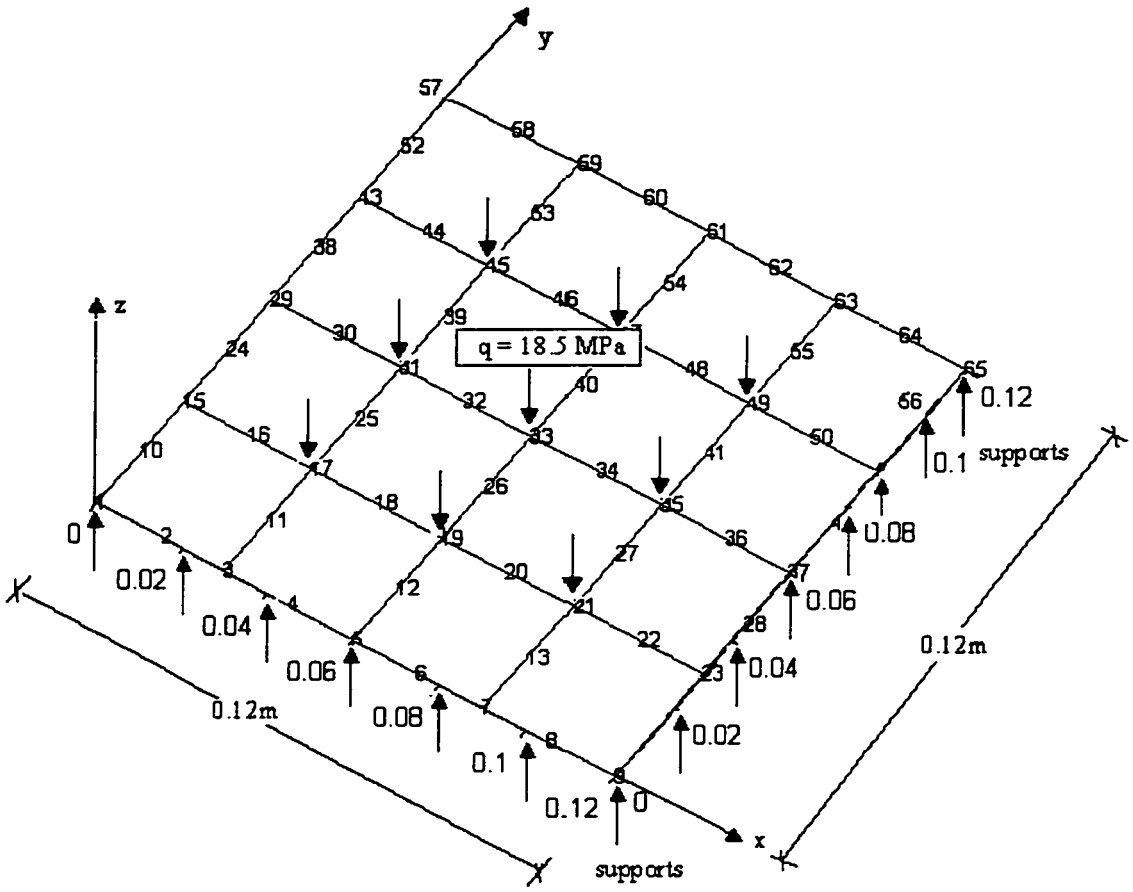

Figure 3.6 Geometry, finite element mesh, boundary conditions and loading for the $[0/90]_{24s}$ laminate

Closed form solution:

In determining the deflection at any point in the laminate, when subjected to uniformly distributed load, equation (3.60) is used [61,62]:

$$w = (R^4 b^4 / \pi^4) \sum_{m=1}^{\infty} \sum_{n=1}^{\infty} q_{mn} \frac{\sin(m\pi x / a) \sin(n\pi y / b)}{[D_{11}(m^4 + n^4 R^4) + 2(D_{12} + 2D_{66}) m^2 n^2 R^2]} \tag{3.60}$$

where

R = a/b (ratio of length to width)

$$q_{mn} = \frac{16q}{\pi^2 mn} \tag{3.61}$$

where q is the intensity of uniformly distributed load.

Upon substituting the appropriate values for the variables in equation (3.60), the closed form solution is obtained and the values are shown in Table 3.2. The finite element solution obtained from the MATLAB® program is also shown in the same table. Expressing in non-dimensional format we have the closed form and FEM results as presented in Table 3.3 in the last column. Equation (3.62) is used in finding out the non-dimensional values.

$$\bar{w} = \frac{w_{\max} E_2 h^3 x 10^2}{qa^4} \tag{3.62}$$

In Table 3.2, nodal displacement at the centre of the laminate (node 33) corresponds to the mean nodal deflection value at 300 simulations, and all other nodal deflection values correspond to 300th simulation. The mean maximum deflection obtained over 300 simulations is presented in Table 3.3 and its non-dimensional form value is also given. It is observed that the MATLAB® program result for mean maximum deflection of a cross-ply laminate subjected to uniformly distributed load under simply supported condition differs from the closed form solution by 7.4%. It can be concluded that the obtained results are in good agreement with the closed form solution.

Node number	$w_{max.closed\ form}$	$w_{max.fem}$	% Variation
11	-0.00072	-0.00074	2.95
19	-0.00181	-0.00197	8.42
26	-0.00238	-0.00252	7.25
32	-0.00236	-0.00252	7.22
33	-0.00256	-0.00275*	7.42
34	-0.00234	-0.00252	7.23
41	-0.00185	-0.00188	1.59
44	-0.00072	-0.00075	2.96

Table 3.2 Comparison of nodal deflection values for the $[0/90]_{24s}$ laminate subjected to uniformly distributed load under simply supported condition
* Mean value of maximum deflection

Reference	Mean max. deflection w_{max} (m)	Non-dimensional mean maximum deflection $\overline{w}$
Ref. [61]	-0.00256	-0.8381
Matlab (FEM)	-0.00275	-0.8934

Table 3.3 Comparison of mean maximum deflection and non-dimensional mean maximum deflection values

3.3.4 Line load and four-point bending analyses

The program developed is extended further to illustrate few more application problems, performed on a composite laminate. The analysis involves a symmetric cross-ply laminate of 96 layers having a configuration of $[0/90]_{24s}$. The dimensions of the laminate are considered to be 0.12 m in length, 0.12 m in width and 0.012 m in thickness. Figure 3.7 shows the finite element mesh employed in modeling the laminate and application of line load over the laminate. Laminate is subjected to a uniformly distributed load of 2 MPa.

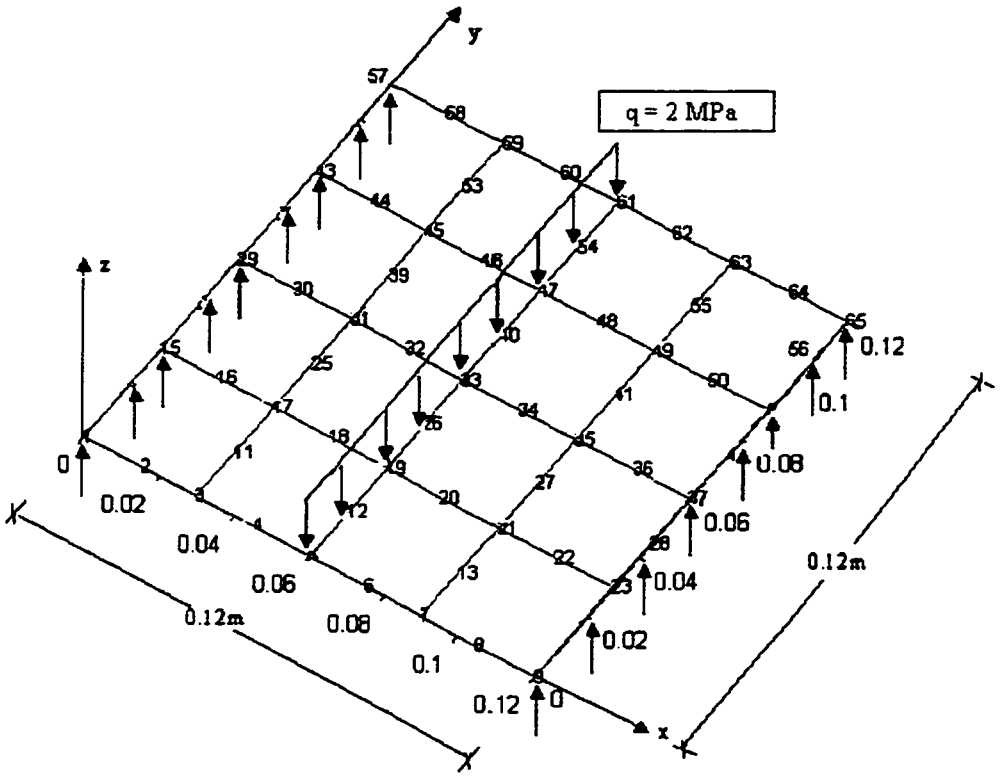

Figure 3.7 Geometry, finite element mesh, boundary conditions and loading for the $[0/90]_{24s}$ laminate

3.3.4.1 Line load analysis results

MATLAB® program results are listed in Table 3.4 which gives the displacement values at the nodes specified over the laminate as shown in Figure 3.7. These values are plotted with respect to the node numbers and resulting graph is shown in Figure 3.8. Mean maximum deflection value as calculated by conducting the simulation over 300 laminates is 0.00727 m acting in a direction opposite to the z-axis. Its standard deviation and coefficient of variation values are 0.000143 m and 0.0196 respectively.

Global node number	Nodal Displacement (m)
29	0.00000
30	-0.00237
31	-0.00448
32	-0.00609
33	-0.00727*
34	-0.00609
35	-0.00449
36	-0.00237
37	0.00000

Table 3.4 Displacement values for the $[0/90]_{24s}$ laminate
* Mean maximum displacement value

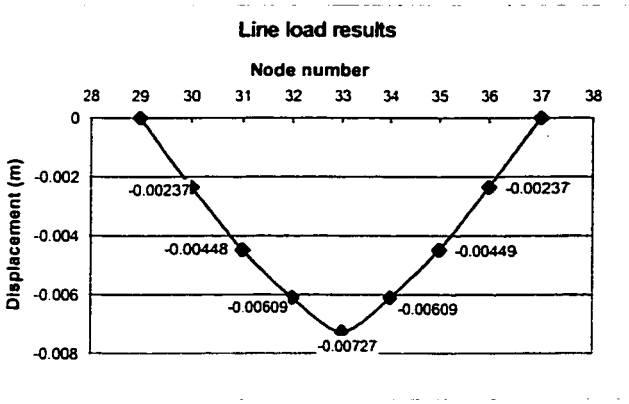

Figure 3.8 Plot of node number *vs* displacement for line load

3.3.4.2 Four-point bending analysis results

Considering the same laminate configuration of $[0/90]_{24s}$, dimensions and imposition of load as employed in section 3.3.4, displacement values obtained in the four-point bending analysis are listed in Table 3.5. A graph is plotted with displacement versus node number as shown in Figure 3.9. It is to be noted that the nodal force estimation for the four-point bending analysis assumes the same formulation as described for line load analysis. It is observed that the mean value of maximum displacement is 0.0094 m acting in a direction

opposite to the z-axis. Accordingly the standard deviation and coefficient of variation are 0.000193 m and 0.0205 respectively.

Global node number	Nodal Displacement (m)
29	0.0000
30	-0.0037
31	-0.0069
32	-0.0085
33	-0.0094*
34	-0.0084
35	-0.0069
36	-0.0037
37	0.0000

Table 3.5 Four-point bending analysis results for the $[0/90]_{24s}$ laminate
* Mean maximum displacement value

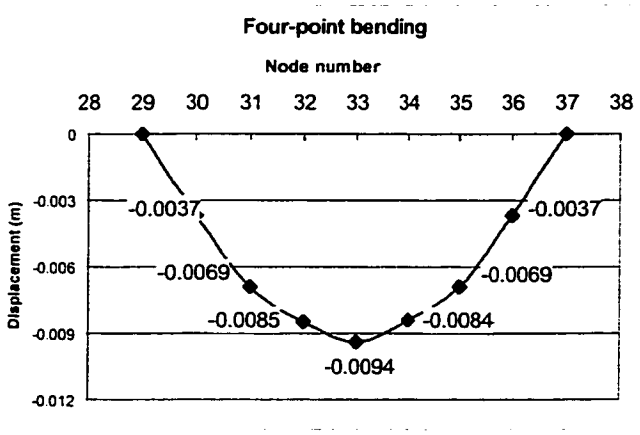

Figure 3.9 Plot of node number *vs* displacement for four-point bending

From the line load analysis and four-point bending analysis results, it is clear that, the deflection of the laminate takes a parabolic path. The former case results in sharper deflection at the centre of the laminate where the application of the load is imposed. In the later case a smooth deflection curve can be seen, as the points of application of load are at a distance away from the centre of the laminate along the x-axis.

3.4 Conclusions and discussions

The stochastic finite element method based on Markov correlation model is utilized for the probabilistic analysis of composite laminates in which mechanical properties have uncertainty and variability. The first-order shear deformable plate element is employed. Considering the randomness in the material properties the statistics of displacements, strains and stresses, are determined.

A MATLAB® program has been developed to calculate the mean nodal deformations and stresses for a plate without a hole subjected to out-of-plane uniformly distributed load. Program is capable of handling both isotropic and composite material analyses.

Example problems are addressed in section 3.4 to compare the results obtained from the program. Results are found to be in excellent agreement with the reference solutions, thus confirming the validity of the formulation and program.

As an extension of the work described in previous sections, a stochastic finite element investigation of the effects of holes on the stress distribution in symmetric composite laminates subjected to bending moments is conducted in chapter 5. Accordingly, stresses around a circular hole are determined for laminates with different types of loading and stacking sequences.

Chapter 4

Experimental Characterization of Composite Laminates

4.1 Introduction

The presence of holes is well known to be a serious design problem and a major cause of structural failure. Traditional engineering solutions to this problem either involve massive reinforcements around the hole, which are often expensive in terms of weight and cost, or shape contouring to alleviate the effects of the hole, which is not always possible. In practical situations, it is difficult to achieve a hole with a perfect circular profile in composite laminates during the drilling operation. Also the problem of hole being offset from the desired co-ordinates is encountered. Because of the above-mentioned reasons, a study of stress concentration at the hole boundary and the stress distribution at a distance from the hole boundary in finite elastic plates subjected to uniform uniaxial and biaxial loads have to be conducted. Information about stress concentration factor provides the designer with useful worst-case information regarding the influence of the uncertainty in the hole shape on the resulting stress concentration factor.

Before actually delving into the problem, it is important to make a note that, direct application of the mechanics of metallic structures to fiber reinforced composite

laminates would produce some abnormal results, such as hole-size effect. These anomalies apparently stem from the fact that, the methodology for metallic structures is based on the conditions at a point on hole the boundary, while the strength of a perforated composite laminate seems to be related to the in-plane elastic stresses within a region defined by the characteristic length a_o adjacent to the hole boundary. Thus SCF itself is not an adequate measure of strength for a composite laminate containing a circular hole. Also, previous analyses [46,63] have shown that in the case of composite laminates, stress concentration decreases more gradually away from the hole for a large hole than for a small hole.

As the characteristic length value varies from one laminate configuration to another, it becomes necessary to conduct experiments on all the selected laminate configurations. On an average, 25 samples of notched and another 25 samples of un-notched laminates are tested, for each laminate configuration, in the present work. At this stage we consider a failure criterion to calculate the characteristic length. Accordingly we have two major criteria [1]:

1) Point stress criterion
2) Average stress criterion

A brief description of the two criteria and the appropriate selection of the criterion follow our discussion.

4.2 Point stress criterion

The point stress failure criterion [1] assumes that failure occurs when the stress, σ_y, at some distance d_o, away from the opening is equal to or greater than the strength of the un-notched laminate. A pictorial representation is shown in Figure 4.1.

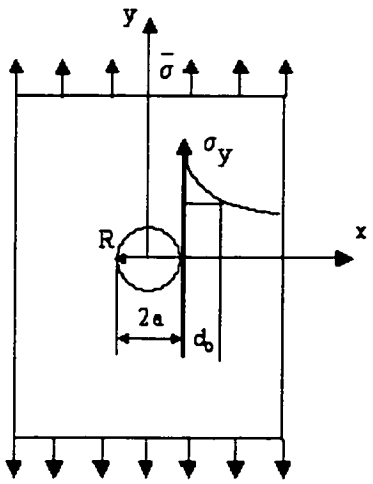

Figure 4.1 Graphical representation of the point stress criterion

Mathematically an equation can be expressed as follows:

$$\sigma_y(x,0)|_{x=R+d_o} = \sigma_o \tag{4.1}$$

where

σ_o is the un-notched strength of the laminate and 'R' is the radius of the opening.

In the point stress criterion, it is considered that a larger volume of material is subjected to high stress in the case of the plates containing a larger hole. Therefore, instead of considering the stress at a point, the average stress criterion considers the average stress over a characteristic length. Further details are provided in the next section.

Also the choice of analysis, either micro mechanics or macro mechanics, is based on the consideration as to whether an improvement is to be made in terms of design and material of unidirectional laminate or for a structural design improvement. It is a known fact that in composite laminates it is highly impossible to know exactly the degree of inhomogeneity, and the distribution and locations of fibers. Variability in test data is basically due to these reasons in addition to human error and machine misalignment. Averaging the measured strength data can reduce the effects of these factors. Thus it is logical to adopt the macro structural study rather than the micro structural study.

4.3 Average stress criterion

According to this criterion [1], it is assumed that the laminate would fail when the normal stress averaged over some length a_o of a notched specimen, away from the opening edge and on the axis normal to the applied load, reaches or is greater than the strength of an un-notched specimen (σ_o).

$$\frac{1}{a_o}\int_{R}^{R+a_o}\sigma_y(x,0)dx \geq \sigma_o \tag{4.2}$$

where

'R' is the radius of the hole, a_o is the characteristic length value, σ_o is the un-notched strength of the laminate and $\sigma_y(x,0)$ is the approximate solution for the stress distribution in orthotropic notched plate [55].

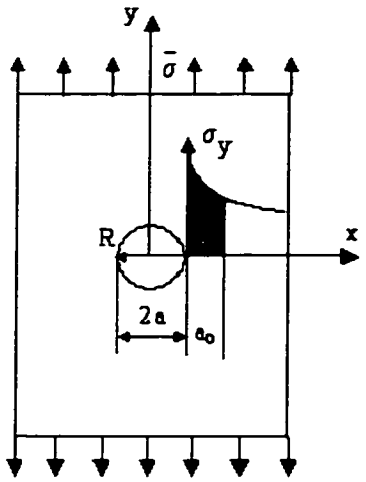

Figure 4.2 Graphical representation of average stress criterion

It is to be noted that, for the sake of convenience, the term 'Average stress', as used in most of the references is replaced by the term 'Equivalent stress'.

Considering the case of an orthotropic plate containing a hole, the approximate solution [1] is given by equation (4.3):

$$\sigma_y(x,0)=\frac{\bar{\sigma}}{2}\left\{2+\left(\frac{R}{x}\right)^2+3\left(\frac{R}{x}\right)^4-\left(K_T^{\infty}-3\right)\left[5\left(\frac{R}{x}\right)^6-7\left(\frac{R}{x}\right)^6\right]\right\} \quad where\ x>R \tag{4.3}$$

where

$$K_T^{\infty}=1+\sqrt{\frac{2}{A_{22}}\left[\sqrt{A_{11}A_{22}}-A_{12}+\frac{A_{11}A_{22}-A_{12}^2}{2A_{66}}\right]} \tag{4.4}$$

K_T^{∞} denotes the stress concentration factor at the edge of the hole; $A_{ij}, i, j = 1,2,6$ are the

components of the in-plane stiffness matrix with axes 1 and 2 parallel and transverse to the loading direction respectively.

Substituting equation (4.3) into equation (4.2) and considering the case when the left hand side terms of equation (4.2) equal right hand side terms we have:

$$\frac{\bar{\sigma}}{\sigma_o} = \frac{2(1-\xi_2)}{2-\xi_2^2-\xi_2^4+(K_T^\infty-3)(\xi_2^6-\xi_2^8)} = \frac{\sigma_N^\infty}{\sigma_o} \tag{4.5}$$

where

$$\xi_2 = \frac{R}{R+a_o} \tag{4.6}$$

and σ_N^∞ is the ultimate strength of notched laminate.

The two unknowns i.e. the un-notched strength σ_o and the characteristic length a_o are determined experimentally. The procedure is to first obtain a set of un-notched and notched strengths from the experiments and subsequently substitute them into the equation (4.5) to solve for a_o.

4.4 Experiments on notched and un-notched composite laminates

In the following sections, details as to the selection of laminate configuration, specimen preparation and dimensions of the specimen for uniaxial tensile testing are provided. Tensile testing is carried out on 25 samples for each case of un-notched and notched laminates and for each configuration.

Laminate configuration:

Extensive use of 0°, 90° and $\pm 45°$ ply orientations in the laminate configuration has been made in the previous works [1]. Symmetric cross-ply laminates and quasi-isotropic laminates are used in the present study as they are employed in many practical applications. Based on these facts, testing is carried out on laminates with $[0_2/\pm 45]_{2s}$ and $[0/90]_{4s}$ configurations.

Specimen preparation:

A thick aluminum plate is used to support laminates during curing. Release agent is applied over the cure area of the plate for permanent tool release. Preparation of the cure assembly begins by placing resin damping material around the perimeter of the cure area on the aluminum plate. Once the release agent applied over the aluminum plate dries, fill-in sub-laminates are placed and subsequently two layers of peel ply are stacked over the fill-in sub-laminates. This is to ensure that, after curing in the autoclave, the laminate could easily be separated from the fill-in sub-laminate. The purpose of peel ply is also to isolate the excess resin from the aluminum plate. A sheet of porous Teflon fabric is added to allow the resin to flow away from the laminate to the bleeder material. Two sheets of paper bleeder are then placed on the assembly to absorb the majority of the excess resin from the laminate. A large section of synthetic fiber breather material is placed over the cure assembly and beneath the surface of the vacuum plate to allow gases to vent away from the assembly. On the vacuum plate around the perimeter of the cure assembly, vacuum bag sealant is placed. Finally, a large section of bagging film, with a quick disconnect vacuum valve attached, is placed over the assembly and pressed onto the

sealant. A cross-section of typical lay-up prepared for autoclave processing is shown in Figure 4.3

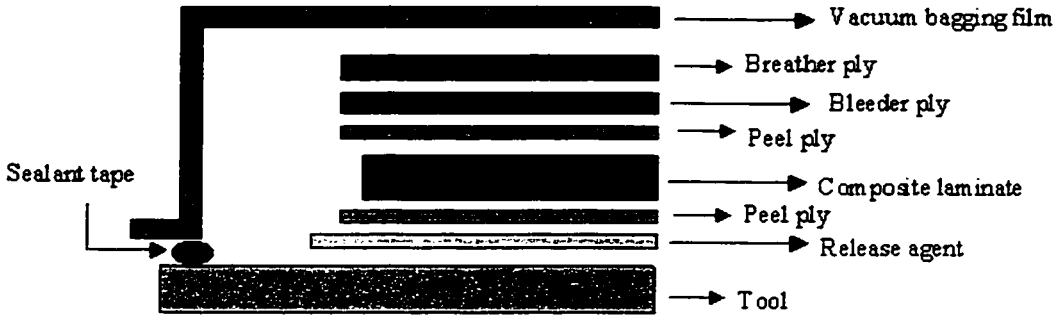

Figure 4.3 Typical cross-section of the lay-up

An electrically heated autoclave is used to cure the laminate. The laminate is cured according to the manufacturer's specifications. Full vacuum of 28 in. Hg is drawn over the cure assembly and the bag is inspected for leaks. The entire assembly is then placed in the autoclave and the door is closed and secured. The cure cycle adopted for NCT-301 graphite/epoxy composite material is depicted in Figure 4.4.

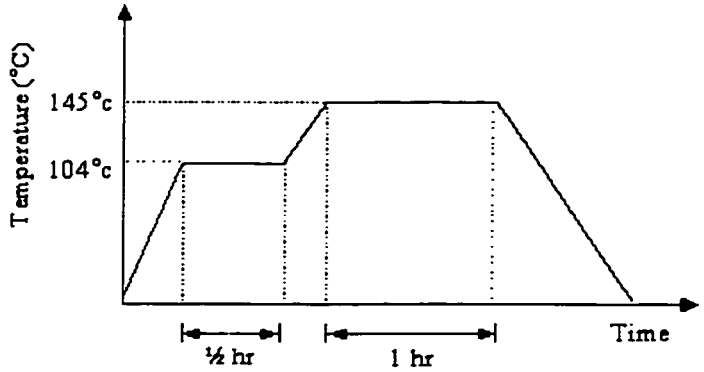

Figure 4.4 Cure cycle for NCT-301 graphite/epoxy composite material

The cure cycle is a two-step process. The laminate is heated from room temperature to 104° C and it is held at this temperature for a period of 30 minutes (first dwell). The

purpose of the first dwell is to allow the entrapped air, water vapor or volatiles to escape from the matrix material and to allow a matrix flow, resulting in the compaction of the part. Afterwards, the temperature is again increased to 145° C and held constant for one hour (second dwell). The cross-linking of the resin takes place and the related material properties are developed during the second dwell. A constant pressure of 60 psi is maintained inside the autoclave throughout the processing time. Later the laminate is cooled to room temperature at constant rate and post-cured for ten hours. Finally the laminate is removed from the aluminum plate. Excess resin on the laminate is trimmed off with a circular sander using medium grit sand paper. Laminate thus prepared is cut to the required size using the diamond cutter. A drilling operation is performed to prepare a notched laminate. The center point of the coupon is located and using the center punch a mark is made at the desired co-ordinate. Using the HSS drill bit, without the coolant, a drilling operation is performed. A laminate with a hole is shown in Figure 4.5.

Basis for the specimen dimensions:

Since there are no ASTM standards for the tensile testing of anisotropic materials with notch, we refer to the works of Tan S.C [1] and Nuismer, R.J. and Whitney J.M. [64] who have conducted studies on plates with circular openings for different laminate configurations. Accordingly, they have come to a conclusion that, the ratio of diameter to width of the plate (2a/W) should lie between 0 and 0.4. Otherwise, the stress concentration factor tends to deviate from the exact value for regions away from the hole. This is true, as the theory is developed to find out only the maximum stress around the hole region. Based on these considerations, we have set the dimensions of the coupon as follows: width as 37.9 mm, gauge length as 180 mm and hole diameter (2a) as 5.1 mm.

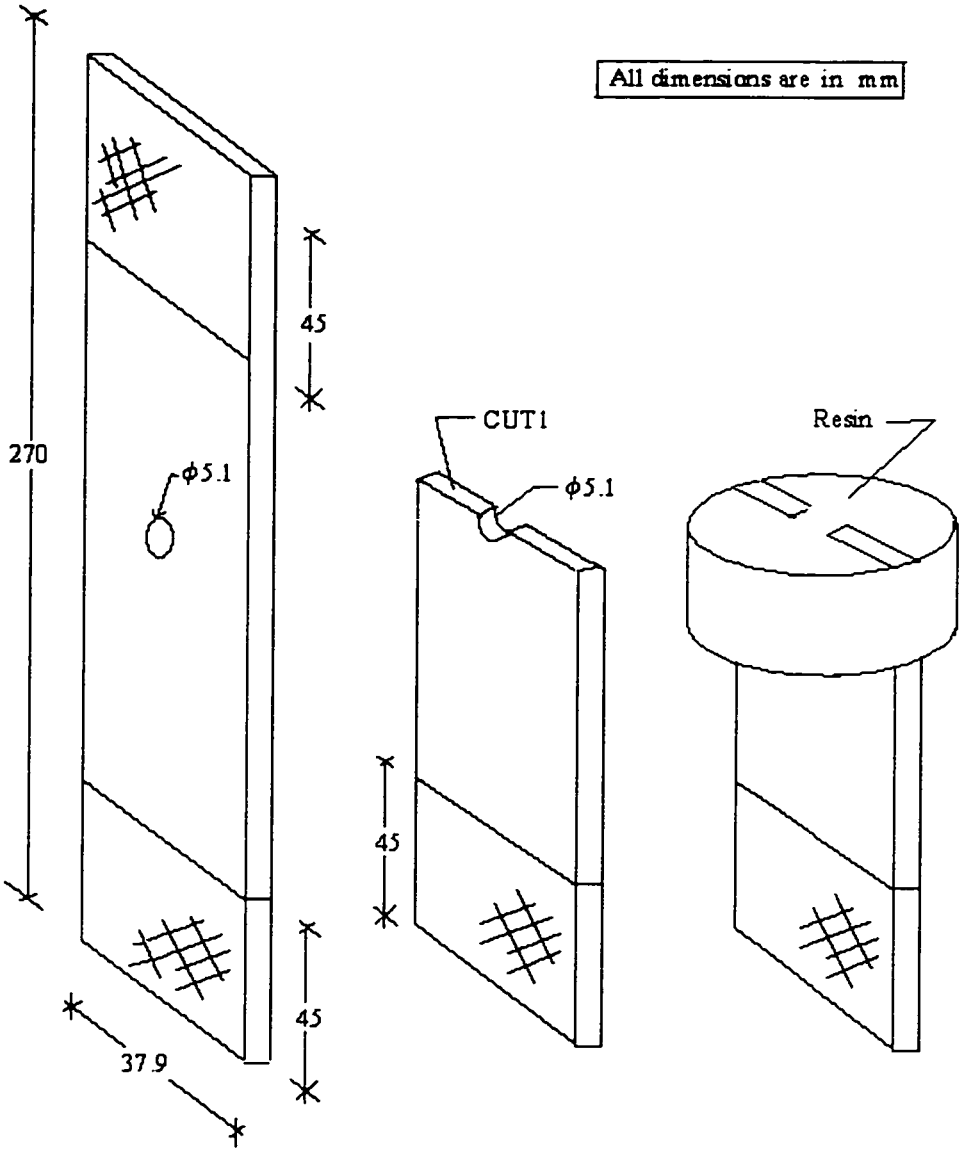

Figure 4.5 Sketch showing a section taken at the hole region of the specimen and a resin block covering the cut out region

4.5 Micro structural study

Before conducting the test, specimens are checked for any defects, such as, delamination and voids. These defects are developed as a result of uneven rolling while laying up the plies, poor vacuum bagging, improper pressurization in furnace during curing and so on.

To observe these defects, a micro structural study is conducted. As most of the defects are expected to occur at the hole region, a cross-section is taken accordingly at this region. Since the specimens for micro structural study are quite small, the region of interest is immersed in a bowl containing resin. It is heated to 80°C in a furnace for nearly 40 minutes, which evaporates all the moisture content present in the resin and is allowed to cool down at room temperature. This in-turn creates a bigger surface and hence a better grip for polishing. Now the surface generated is polished with the grinding operation. Initially it is treated with 200 grit SiC paper and subsequently with SiC papers that have 300, 600, 800 grit levels. It has to be noted at this point, that, while grinding the specimen, care is taken to maintain a perfect horizontal surface. Finally polishing is done using diamond paste to obtain a very smooth surface for micro structural analysis. Two specimens from each of the configuration are studied for any defects under an optical microscope by setting a magnification factor of 100x. In all the specimens, a slight delamination is observed near the hole region (CUT1) as shown in Figure 4.6. It is quite obvious that these defects are due to the drilling operation. Figures 4.6 and 4.7 show the images captured for $[0_2/\pm 45]_{2s}$ and $[0/90]_{4s}$ laminate configurations using the Clemex Vision Software, which is connected to the optical microscope. It is observed that, for a $[0_2/\pm 45]_{2s}$ laminate configuration the delamination occurs mostly between the +45° and -45° layers. Delaminations of length 500 μm and width 40 μm are measured. It is felt that a delamination area of 500 μm x 40 μm is small when compared with the overall area of the laminate and thus it is not that significant. Also the delamination caused, will not contribute to a change in the experimental value obtained. Observing Figure 4.7 for $[0/90]_{4s}$ laminate a slight delamination in between the 0° layers is noticed. It is to be

noted that any delaminations observed near the periphery of the hole (CUT1) would continue in the circumferential region of the opening.

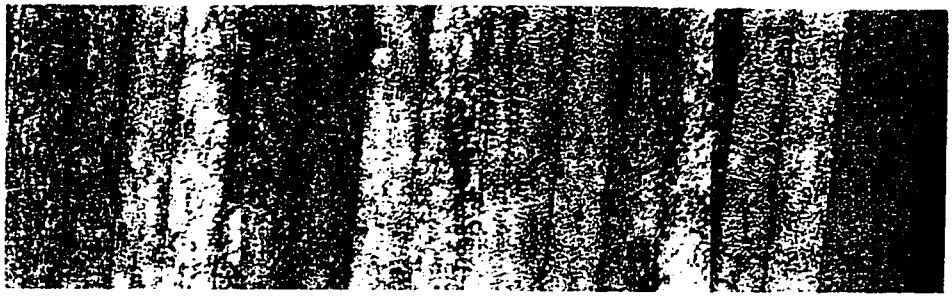

0 0 +45 –45 0 0 +45 –45 -45 +45 0 0 -45 +45 0 0

Figure 4.6 Cross-section of $[0_2/\pm 45]_{2s}$ laminate observed under a microscope having a magnification of 100x.

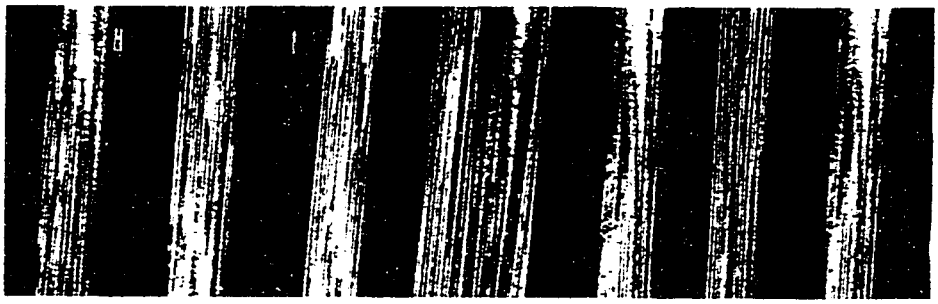

0 90 0 90 0 90 0 90 90 0 90 0 90 0 90 0

Figure 4.7 Cross-section of $[0/90]_{4s}$ laminate observed under a microscope having a magnification of 100x.

4.6 Uni-axial tensile testing of composite laminates

Experiments are conducted on MTS machine having a loading capacity of 25 tons. For our application laminates are loaded at a speed of 25 lb/sec. Readings are recorded online automatically at every one-second interval till failure. Equipments used while testing is shown Figure 4.8a.

(a) Experimental set-up

(b) Before failure

(c) After failure

Figure 4.8 The tensile testing of laminate coupons

Figure 4.8a shows the set-up for the tensile testing of laminate coupons. Also Figures 4.8b and 4.8c depict the pre-failure and post-failure states of a notched laminate under test. Ultimate loads experienced by notched and un-notched laminates of both the ply configurations are listed in tables to follow. The ultimate failure is defined as the state when the specimen abruptly loses its load-carrying capability and cannot recover.

4.6.1 Experimental results for $[0/90]_{4s}$ laminate

Table 4.1 lists the experimental results for $[0/90]_{4s}$ laminate with a circular opening. An effort has been made to control the width and hole diameter of the laminate to a constant value of 37.9 mm and 5.1 mm respectively.

Specimen No.	Width (mm)	Diameter (mm)	Ultimate load (lb)	Ultimate stress (*GPa*)
2H	37.59	5.08	9867	0.6754
3H	37.90	5.08	9282	0.6293
4H	37.78	5.08	9316	0.6340
5H	36.99	5.08	9584	0.6684
6H	37.83	5.08	9732	0.6613
7H	37.96	5.08	9406	0.6366
8H	37.56	5.08	9482	0.6496
9H	37.69	5.08	9577	0.6535
10H	37.66	5.08	9110	0.6222
11H	37.86	5.08	9450	0.6415
12H	37.86	5.08	9214	0.6255
13H	37.92	5.08	8968	0.6077
14H	37.96	5.08	9486	0.6420
15H	37.54	5.08	9536	0.6537
16H	37.83	5.08	9817	0.6670
17H	37.43	5.08	10223	0.7032
18H	37.89	5.08	9284	0.6297
19H	37.96	5.08	9482	0.6417
20H	38.08	5.08	9276	0.6255
21H	37.97	5.08	9312	0.6300
22H	37.09	5.08	9382	0.6522
23H	37.14	5.08	8928	0.6197
24H	37.46	5.08	9136	0.6279
25H	37.24	5.08	9582	0.6630
26H	37.66	5.08	9678	0.6610

Table 4.1 Experimental results for $[0/90]_{4s}$ laminates with a circular opening

It is to be noted that all the specimens tested in tensile mode belong to the same lot viz. Lot-1. Specimen number 1 is used to prepare an un-notched sample. The notation 'H' in the specimen numbering represents, that a hole is present in the laminate. The mean

ultimate load and mean ultimate stress values achieved for a notched $[0/90]_{4s}$ laminate are calculated from Table 4.1 and they are 9444 lb and 0.6448 GPa respectively.

Specimen No.	Width (mm)	Ultimate load (lb)	Ultimate stress (GPa)
1	38.35	15591	0.9042
27	37.53	13929	0.8255
28	37.70	14195	0.8374
29	37.27	15857	0.9463
30	37.83	15139	0.8901
31	37.68	14025	0.8278
32	37.72	16114	0.9501
33	37.65	15735	0.9295
34	37.72	16639	0.9811
35	37.45	16702	0.9919
36	37.74	16234	0.9567
37	37.68	16122	0.9516
38	37.16	15998	0.9575
39	37.73	16454	0.9699
40	37.30	16505	0.9841
41	37.66	16488	0.9737
42	37.83	17818	1.0476
43	37.84	15807	0.9291
44	37.47	17446	1.0355
45	37.75	16582	0.9770
46	37.26	13004	0.7762
47	36.75	16789	1.0161
48	38.12	16668	0.9725
49	38.39	16876	0.9777
50	37.42	17626	1.0476

Table 4.2 Experimental results for $[0/90]_{4s}$ laminates without a circular opening

In Table 4.2, specimen number 1 is taken from Lot-1 and all other specimens are taken from Lot-2. This is to ensure that samples from all lots behave in a consistent manner and produce results that are consistent among themselves. Columns 3 and 4 of Table 4.2 represent the ultimate load and ultimate stress that each sample has experienced. Thus, the mean load and mean stress values are 16058 lb and 0.9462 GPa respectively.

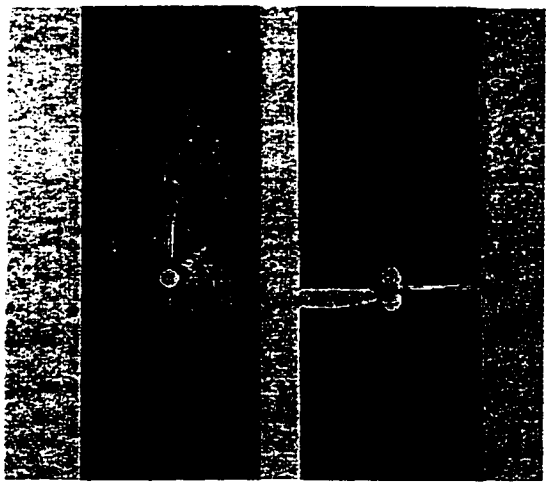

Figure 4.9 The typical failure of $[0/90]_{4s}$ notched laminate. Sample before and after failure is shown

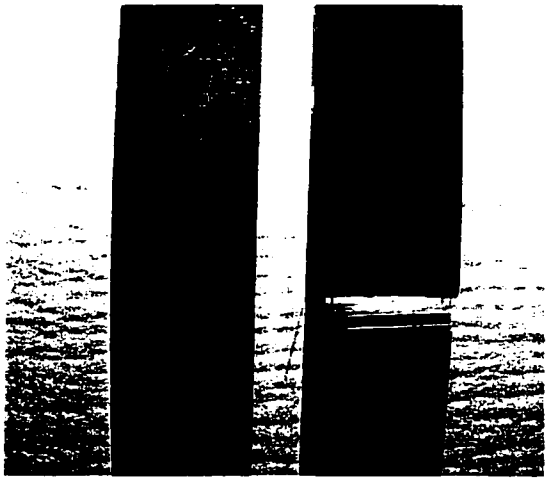

Figure 4.10 The typical failure of $[0/90]_{4s}$ un-notched laminate. Sample before and after failure is shown

From Figures 4.9 and 4.10 we can make out that the failure of notched and un-notched $[0/90]_{4s}$ laminates take place in a direction perpendicular to the loading direction and across the circular cutout. This is due to the presence of 90° ply in the laminate configuration. Failure begins with the matrix cracking followed by fiber breakage.

4.6.2 Experimental results for $[0_2/\pm 45]_{2s}$ laminate

Table 4.3 lists the experimental results for $[0_2/\pm 45]_{2s}$ laminate with a circular opening. Due attention was given to control the width and hole diameter of the laminate to constant values of 37.9 mm and 5.1 mm respectively.

Specimen No.	Width (mm)	Diameter (mm)	Ultimate load (lb)	Ultimate stress (*GPa*)
1H	37.71	5.08	12554	0.8536
2H	37.05	5.08	11286	0.8084
3H	37.54	5.08	12379	0.8461
5H	37.71	5.07	11749	0.7988
6H	37.57	5.08	11259	0.7688
7H	37.78	5.07	12764	0.8660
8H	37.70	5.08	11396	0.7751
10H	37.45	5.08	12858	0.8549
11H	37.68	5.08	11554	0.7863
12H	37.60	5.08	12203	0.8325
14H	37.65	5.07	11734	0.7993
16H	37.54	5.08	11825	0.8082
17H	37.82	5.08	12474	0.8453
18H	37.54	5.08	12383	0.8463
19H	37.78	5.08	12380	0.8399
20H	37.51	5.08	12490	0.8544
21H	37.13	5.08	12163	0.8419
22H	37.02	5.08	11574	0.8039
23H	37.69	5.08	11546	0.7855
24H	37.46	5.08	12564	0.8608
25H	37.32	5.08	10055	0.6919
26H	37.32	5.08	12613	0.8679
27H	37.41	5.08	10988	0.7540
28H	37.33	5.08	11939	0.8213
29H	37.22	5.08	11235	0.7755

Table 4.3 Experimental results for $[0_2/\pm 45]_{2s}$ laminates with a circular opening

The mean ultimate load and mean ultimate stress values achieved for a notched $[0_2/\pm 45]_{2s}$ laminate are calculated from Table 4.3 and they are 12093 lb and 0.8272 GPa respectively.

Specimen No.	Width (mm)	Ultimate Load (lb)	Ultimate stress (*GPa*)
1	37.75	16590	0.9774
2	37.33	16392	0.9766
3	37.06	17828	1.0699
4	37.79	16609	0.9775
6	37.88	16666	0.9785
7	37.69	17825	1.0519
8	37.72	16728	0.9863
9	37.48	17664	1.0482
10	36.75	16637	1.0069
11	37.60	16887	0.9989
13	37.12	15854	0.9499
14	37.23	16195	0.9675
15	37.10	16011	0.9598
16	37.44	16327	0.9699
17	37.55	16420	0.9726
20	37.35	17160	1.0218
21	37.36	16566	0.9862
22	37.85	16745	0.9840
23	37.74	16983	1.0008
25	37.77	16735	0.9854
26	37.34	16148	0.9618
27	37.43	16216	0.9636
28	37.45	16110	0.9567
29	37.51	17128	1.0156
30	37.64	17082	1.0094

Table 4.4 Experimental results for $[0_2/\pm 45]_{2s}$ laminates without a circular opening

Columns 3 and 4 of Table 4.4 represent the ultimate load and ultimate stress that each sample has experienced. Thus, the mean ultimate load and mean ultimate stress values for an un-notched $[0_2/\pm 45]_{2s}$ laminate are 16520 lb and 0.9784 GPa respectively.

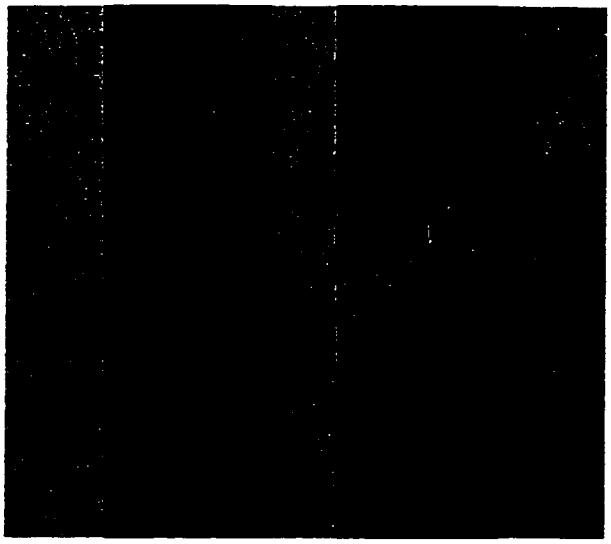

Figure 4.11 The typical failure of $[0_2/\pm 45]_{2s}$ notched laminate. Sample before and after failure is shown

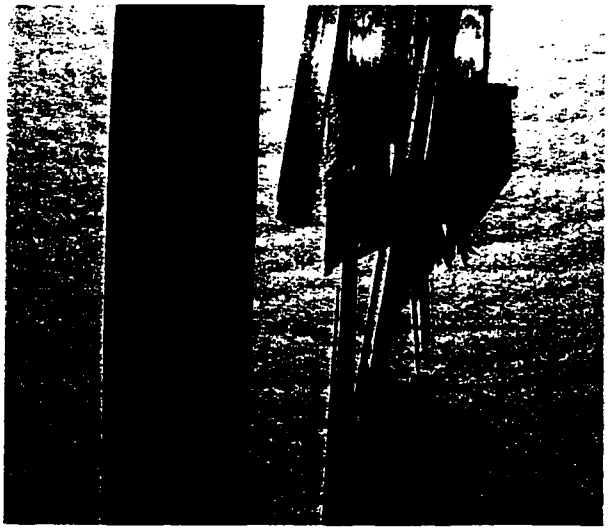

Figure 4.12 The typical failure of $[0_2/\pm 45]_{2s}$ un-notched laminate. Sample before and after failure is shown

From Figure 4.11 it is clear that the failure of a notched $[0_2/\pm 45]_{2s}$ laminate takes place approximately at an angle of 45° from the horizontal axis. Similar observation can be made from the rest of the samples tested. Due to the presence of +45° ply and -45° ply

along with 0° ply, a better reinforcement in terms of resistance to the application of load is established, thereby accepting higher loads as opposed to a $[0/90]_{4s}$ laminate. Observing Figure 4.12, the un-notched $[0_2/\pm 45]_{2s}$ laminate fails in a region close to the center of the laminate but not exactly at the center. It is to be noted that some samples failed near the tab region during the test and those data are not taken into account.

Figure 4.13 distinguishes clearly the failure modes of $[0_2/\pm 45]_{2s}$ and $[0/90]_{4s}$ notched laminates.

Figure 4.13 The typical failures of $[0_2/\pm 45]_{2s}$ and $[0/90]_{4s}$ notched laminates respectively

4.7 Characteristic length (a_o) calculation

As mentioned in section 4.2, in order to find out the characteristic length value of a laminate, a set of un-notched and a set of notched strength values have to be found out. Tables 4.1 to 4.4, list the ultimate stress values obtained experimentally for different

laminate configurations considering both notched and un-notched laminates. Characteristic length a_o is found using equation (4.5). For example from Table 4.1, considering specimen number 10, the ultimate stress value for a notched laminate of $[0/90]_{4s}$ configuration is 0.6222 GPa. Now from Table 4.2, for specimen number 29, the ultimate stress value for an un-notched laminate of the same configuration is 0.9463 GPa. These values are used in equation (4.5) to calculate the corresponding value of characteristic length of the $[0/90]_{4s}$ laminate. A similar procedure is adopted for the $[0_2/\pm 45]_{2s}$ laminate configuration also. Sub-routine *A0CAL.m* given in Appendix-D is used to calculate the value of the characteristic length. Sample values of a_o can be calculated for each laminate coupon in a similar manner.

Table 4.5 lists, a series of characteristic length values for $[0/90]_{4s}$ laminate coupons. It is to be noted that the ratio $\frac{\sigma_N^{\infty}}{\sigma_o}$ (ultimate stress value of a notched laminate to ultimate stress value of an un-notched laminate) on the left hand side of the equation (4.5) is very sensitive when used to calculate the value of characteristic length for any laminate configuration. The value of characteristic length depends mainly on the experimental results obtained for notched and un-notched laminates. The ensemble mean and standard deviation values of the characteristic length are 4.44 mm and 1.392 mm respectively and they are shown in Table 4.6 along with the coefficient of variation (C.O.V) value.

Serial No.	a_o (mm)
1	6.39
2	7.04
3	6.80
4	5.02
5	6.23
6	7.34
7	4.42
8	4.93
9	3.37
10	3.60
11	3.74
12	3.45
13	4.10
14	4.18
15	4.27
16	5.51
17	2.82
18	4.59
19	2.87
20	3.57
21	2.24
22	3.57
23	3.58
24	4.28
25	3.31

Table 4.5 Values of characteristic length a_o obtained for $[0/90]_{4s}$ laminate

Laminate configuration	Mean a_0 (mm)	Std. dev. (mm)	C.O.V
$[0/90]_{4s}$	4.44	1.392	0.3135

Table 4.6 Statistics of characteristic length a_0 for $[0/90]_{4s}$ laminate

Table 4.7 gives the values of characteristic length for $[0_2/\pm 45]_{2s}$ laminate coupons. The ensemble mean and standard deviation values obtained from Table 4.7 are 10.63 mm and 2.21 mm respectively. These values and the corresponding coefficient of variation value are listed in Table 4.8.

Serial No.	a_o (mm)
1	12.58
2	11.03
3	8.44
4	10.18
5	8.15
6	10.66
7	8.16
8	10.06
9	13.78
10	11.53
11	12.30
12	12.70
13	12.36
14	12.32
15	13.58
16	11.78
17	13.63
18	4.88
19	8.10
20	8.86
21	11.90
22	11.61
23	8.28
24	9.57
25	9.40

Table 4.7 Values of characteristic length a_o obtained for $[0_2/\pm 45]_{2s}$ laminate

Laminate configuration	Mean a_0 (mm)	Std. dev. (mm)	C.O.V
$[0_2/\pm 45]_{2s}$	10.63	2.21	0.2079

Table 4.8 Statistics of characteristic length a_0 for $[0/90]_{4s}$ laminate

Comparing the coefficient of variation values from Tables 4.6 and 4.8, it is clear that, the value of characteristic length of $[0_2/\pm 45]_{2s}$ laminate configuration is more consistent as compared to $[0/90]_{4s}$ laminate configuration.

It is important to highlight that the values of characteristic length obtained are based on different combinations of ultimate stress value of notched laminate to ultimate stress value of un-notched laminate obtained experimentally. This means to say that, the notched laminate numbered 1H in Table 4.3 need not be considered together with the un-notched laminate numbered 1 in Table 4.4 to find out the value of characteristic length. In certain situations, it is observed that considering a similar pair of laminates in Tables 4.3 and 4.4 may result in a higher value of characteristic length, which is not feasible, as it might have exceeded the half width dimension of the laminate. Thus, the program developed, checks for the value of characteristic length and compares it with the half width dimension. If the value of characteristic length exceeds the half width dimension, then a different pair of ultimate stress values is chosen and the value of characteristic length is found out. The procedure is continued till it is within the half width dimension value.

4.8 Conclusions and discussions

It is clear from the test data that $[0_2/\pm 45]_{2s}$ laminate has the capability to withstand more loads in both notched and un-notched cases, when compared with $[0/90]_{4s}$ laminate configuration and hence a higher value of a_0 is attained. This is evident from the Tables 4.1, 4.2, 4.3 and 4.4.

The two configurations used in the experiments are fiber dominated laminates. Microscopic study is conducted on both the laminates by taking a cross-section exactly at the hole region and details are given in section 4.5. The failure modes of $[0/90]_{4s}$ and

$[0_2/\pm 45]_{2s}$ laminates under tensile load are depicted in Figures 4.9, 4, 10, 4.11, 4.12 and 4.13. It is observed that $[0/90]_{4s}$ laminate undergoes a failure in a direction that is exactly perpendicular to that of the application of the load i.e. at 0°, while the failure takes place at an angle of 45° in $[0_2/\pm 45]_{2s}$ laminate considering x-axis as the reference. In the tensile testing, specimens fail with total separation. In both the notched laminate configurations, failure occurs at the weakest region i.e. at the circular cutout area. The gross strength of the specimen is the ultimate load divided by the total cross-sectional area of the specimen.

The value of characteristic length thus obtained will be used to find out the equivalent stress value. Further simulation is carried out to calculate the mean and standard deviation values of the equivalent stress parameter. A stochastic analysis of the laminates subjected to different types of loading, boundary conditions and laminate configurations addressing both the cases of controlled and uncontrolled hole laminates is conducted in chapter 5.

Chapter 5

Stochastic Simulation of Notched Composite Laminates

5.1 Introduction

A need for implementing the simulation process in the present work arises due to the fact that there is significant randomness in the stress distribution, which is ascribed to the material and geometric properties of the composite laminate. Variations in the material properties occur due to the variations in the properties of the constituent fibers, matrices and interfaces, in the orientation of the fibers, in the void content and in the ply thickness. These variations are quite unavoidable and most of them are induced during manufacturing. Although composite materials have attractive features, such as high ratios of strength-to-weight and stiffness-to-weight, they are easily damaged when they are machined. A typical damage is delamination, which can occur when fiber reinforced composite laminates are drilled. This in turn creates an irregularity around the circumference of the hole and hence a geometric variation results. Because of the above stated unpredictable variations, a study on stress distribution near the hole edge of the laminate is conducted. The MATLAB® program developed is capable of handling the probabilistic distributions of these variations and calculates the stresses over the laminate.

The MATLAB® program developed in chapter 2 is used in the current analysis, of course with an addition of subroutine *AVGSTR.m* and suitable modifications in the main program *MODIFYSTIFPS.m* which is given in Appendix-E. The generalized program thus developed is capable of accepting any laminate configuration, geometry and number of laminates to be analyzed. In this chapter, two stress parameters i.e. equivalent stress and maximum stress values, which are considered to be the prime design parameters, are calculated. Section 5.2 is completely devoted to the calculation of equivalent stress parameter σ_{equ} and the subroutine *AVGSTR.m* achieves the objective by calculating the equivalent stress value for each and every laminate and stores them automatically into a MATALB® file. Simultaneously the maximum stress developed in the laminate due to the application of a load is also collected and stored in the same file. Depending on the type of the laminate configuration, a corresponding MATALB® file name is created. For example, if a $[0/90]_{4s}$ laminate is analyzed, then the MATALB® file name would be *SIGMA090.m*.

Considering practical situations, two categories of notched laminates are analyzed:

(1) Controlled hole laminate (CHL)

(2) Uncontrolled hole laminate (UCHL)

In a controlled hole laminate it is assumed that the geometric variation and eccentricity of the hole do not exist while the uncontrolled hole laminate takes into account the above variations, which can exist in any practical application. Accordingly, for the uncontrolled hole laminates, appropriate equations are taken from reference [65], which express the imperfection around the hole boundary in the form of an algebraic equation. Using the Gaussian random value generating function, the coordinates associated with the

circumference of the hole are varied and thus eccentricity in the hole is achieved. An acceptable tolerance for the eccentricity of the hole from the central co-ordinates is fixed. These equations are introduced in section 5.4. First order auto regressive correlation model or Markov model is employed, to bring in the stochastic variation of the material properties, which has been already discussed in section 2.4 of chapter 2 and used in the flowchart in Figure 2.6.

The following ply configurations are analyzed for controlled and uncontrolled hole laminate cases:

(1) Symmetric angle-ply laminate $[0_2/\pm 45]_{2s}$

(2) Symmetric cross-ply laminate $[0/90]_{4s}$

It is a fact that the stress distribution in the laminate varies depending on the type of load imposed on the laminate. Thus an extensive study on controlled and uncontrolled hole laminates subjected to the application of different types of load is carried out. In the present work, laminates are subjected to the following load types:

(1) Uniaxial load

(2) Biaxial load

(3) Shear load

(4) Bending load

In the chart below, program layout is delineated which explicitly shows the equivalent and maximum stress parameters being calculated for controlled and uncontrolled hole laminate subjected to in-plane or out-of-plane load for any laminate configuration under consideration.

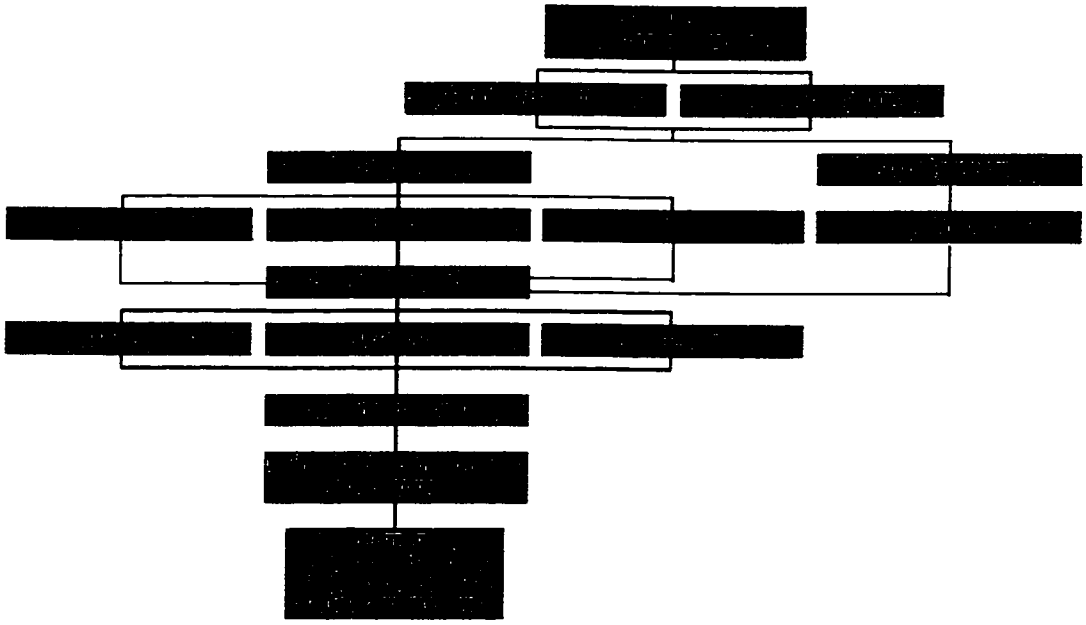

Figure 5.1 MATLAB® program layout

Since the simulation is performed over a number of laminates, adequate provisions are made in the program to calculate the equivalent and maximum stresses for each and every laminate. Simulation is carried out, till the fluctuations in the equivalent and maximum stress parameter values culminate. Standard deviation and hence the coefficient of variation are calculated based on the mean value obtained.

5.2 Explanation for equivalent stress calculation

In Figure 5.2, only a portion of the mesh is shown and elements that contribute to the stress distribution are highlighted. Common node numbers 157,149 and 106 belong to elements 40 and 41, and nodes 106,119 and 132 belong to elements16 and 18.

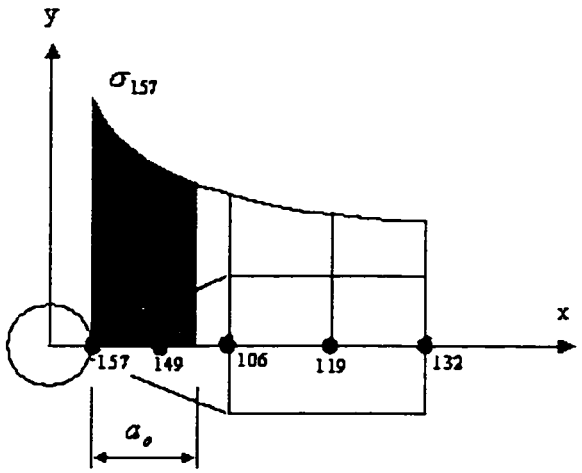

Figure 5.2 Equivalent stress calculation

From the MATLAB® program stresses are calculated at the Gaussian points. Nodal stresses in turn are found out using the stresses that contribute to the corresponding nodes.

The stress value at any node is expressed as

$$\sigma_{node\ i} = b_0 + b_1 x_i + b_2 x_i^{\ 2} + b_3 x_i^{\ 3} + b_4 x_i^{\ 4} \tag{5.1}$$

where

$$x_i = x|_{node\ i} - x|_{node\ 157}$$

and

i = 157,149,106,119 and 132

Stresses at nodes 157,149,106,119 and 132 are calculated using this equation. Expressing in the matrix form:

$$[y]=\begin{bmatrix}\sigma_{157}\\ \sigma_{149}\\ \sigma_{106}\\ \sigma_{119}\\ \sigma_{132}\end{bmatrix} = [x]^T[b] = \begin{bmatrix}1 & 1 & 1 & 1 & 1\\ x_1 & x_2 & x_3 & x_4 & x_5\\ x_1^2 & x_2^2 & x_3^2 & x_4^2 & x_5^2\\ x_1^3 & x_2^3 & x_3^3 & x_4^3 & x_5^3\\ x_1^4 & x_2^4 & x_3^4 & x_4^4 & x_5^4\end{bmatrix}^T \begin{bmatrix}b_o\\ b_1\\ b_2\\ b_3\\ b_4\end{bmatrix} \tag{5.2}$$

From the above equations, constants of the vector $[b]$ are calculated. Substituting back into the base equation, we obtain a general expression for the stress distribution. Using the average stress failure criterion, equivalent stress over the characteristic length is calculated. Sub-routine *AVGSTR.m* is written for this purpose and is called, whenever a new laminate analysis is conducted during the simulation process.

In the controlled hole laminates, only the spatial material properties are varying, while the geometric properties and value of characteristic length are held constant. On the other hand, uncontrolled laminates experience both the material and geometric property variations and thus the value of characteristic length also varies based on Gaussian distribution. Fluctuations in the material properties are expressed using stochastic processes as explained in chapter 2.

5.3 Case 1: Controlled hole laminate analysis

This section aims at analyzing the response of $[0_2/\pm 45]_{2s}$ and $[0/90]_{4s}$ laminates that have stochastic variation of material properties and under the application of uniaxial and biaxial load conditions. Simulation is carried out and the resulting plots are shown in subsequent sections.

5.3.1 Uniaxial load on $[0_2/\pm 45]_{2s}$ controlled hole laminate

Analysis is performed on a laminate having a width of 37.9 mm, length of 151.6 mm and ply thickness of 0.125 mm. Finite element mesh utilized for the laminate analysis is shown in Figure 2.7. The material properties are taken from chapter 2, Table 2.5. The mean ultimate tensile load at which the specimen fails as recorded from the tensile testing experiment for $[0_2/\pm 45]_{2s}$ notched coupons is used for the simulation. In the following analysis, a factor of safety of 1.2 is assumed on the failure load of the notched sample. Accordingly, a uniformly distributed load value of 1.35 MN/m is applied on the laminate in the direction parallel to the y-axis. The influence of the number of simulations, within the range of 1 to 300 on the probabilistic moments i.e. the mean value and variance and hence the standard deviation of the equivalent stress (σ_{equ}) and maximum stress (σ_{max}) parameters has been studied. The variations in the mean values and standard deviation values with the number of simulations for the two parameters have been presented in Figures 5.3-a – 5.3-d. The abbreviation used for controlled hole laminate is CHL.

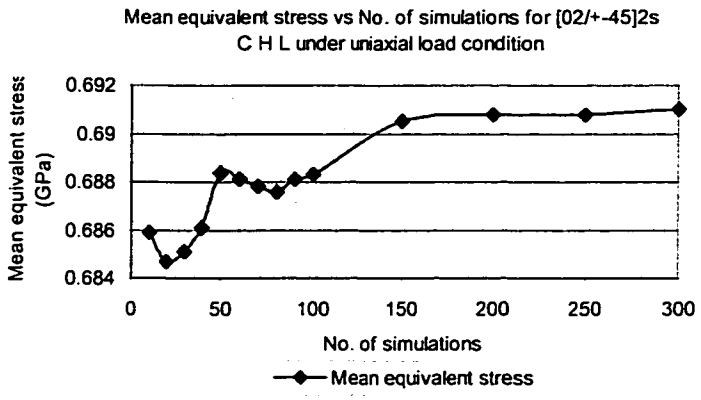

(a)

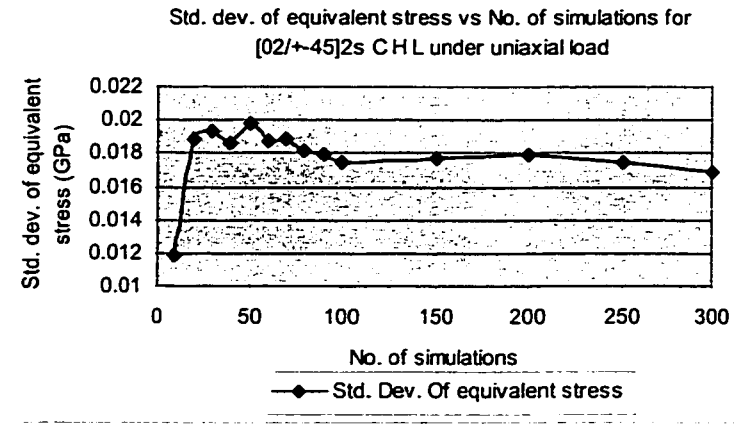

(b)

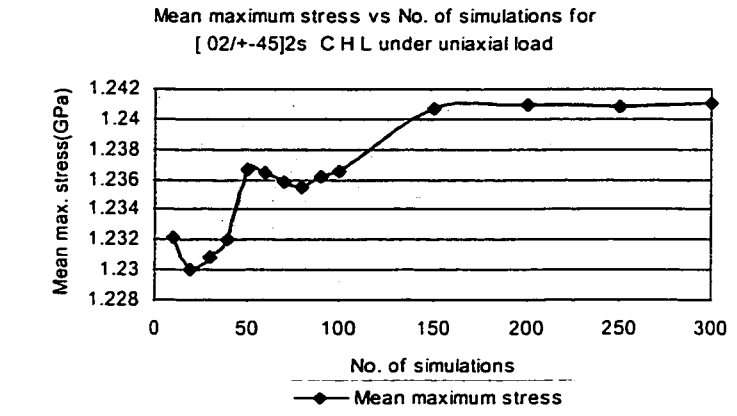

(c)

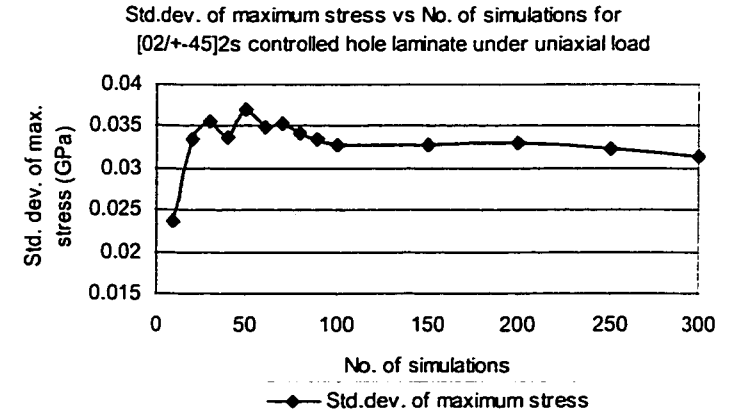

(d)

Figure 5.3 Stress analysis of $[0_2/\pm 45]_{2s}$ controlled hole laminate subjected to uniaxial load: (a) mean values of equivalent stress, (b) standard deviation values of equivalent stress, (c) mean values of maximum stress, (d) standard deviation values of maximum stress.

5.3.1.1 Observations

Simulation is carried out on a controlled hole $[0_2/\pm 45]_{2s}$ laminate subjected to uniaxial load. Our main aim is to see that the mean value of any stress parameter does not change with further increase in the number of simulations. From Figure 5.3-a it is observed that after 150 simulations the mean value of equivalent stress (σ_{equ}) converges to a constant value of 0.691 GPa. In the first 100 simulations, fluctuation is high, but as the number of simulation approaches 200 a steady state mean equivalent stress value is achieved. This implies that a minimum of 200 samples of $[0_2/\pm 45]_{2s}$ configuration under uniaxial load need to be simulated to achieve a mean equivalent stress value. Corresponding standard deviation value also has some variation in the first 100 simulations and attains a constant value at 200 simulations. This can be observed from Figure 5.3-b. Similarly, the maximum stress (σ_{max}) curve in Figure 5.3-c gains a steady state after 150 simulations and the corresponding mean maximum stress value is 1.241 GPa. Accordingly, the standard deviation value for maximum stress parameter almost reaches a constant value at about 150 simulations as can be seen from Figure 5.3-d. The initial variation of values in the first 150 simulations can be attributed to the stochastic variation in the material properties induced using the Markov correlation model. Comparing the mean equivalent stress and mean maximum stress curves from Figures 5.3-a and 5.3-c respectively, it is clear that, both the trajectories almost follow the same path. A similar observation can be made when a comparison is sought between the standard deviation of equivalent stress curve and standard deviation of maximum stress curve as shown in Figures 5.3-b and 5.3-d.

5.3.2 Uniaxial load on $[0/90]_{4s}$ controlled hole laminate

The geometry, material properties and the finite element mesh for the laminate as described in section 5.3.1 are retained for the analysis. The mean ultimate tensile load obtained from the tensile testing experiment for $[0/90]_{4s}$ notched coupons as shown in Table 4.1, chapter 4 is used as a reference load for the simulation. A factor of safety of 1.2 is assumed on the failure load of notched sample. Accordingly, a uniformly distributed load value of 0.92 MN/m is applied on the laminate in the direction parallel to the y-axis. All the d.o.f. corresponding to the nodes lying on the lower edge of the laminate are constrained as shown in Figure 2.7.

The variations in the mean values and standard deviation values with the number of simulations for equivalent stress and maximum stress parameters have been presented in Figures 5.4-a – 5.4-d.

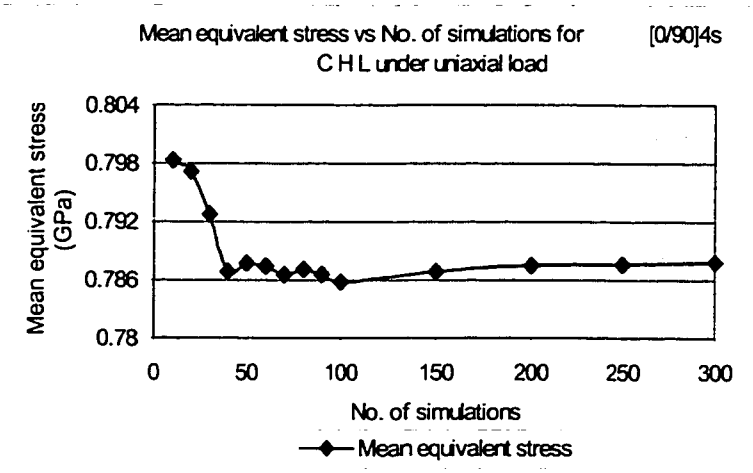

(a)

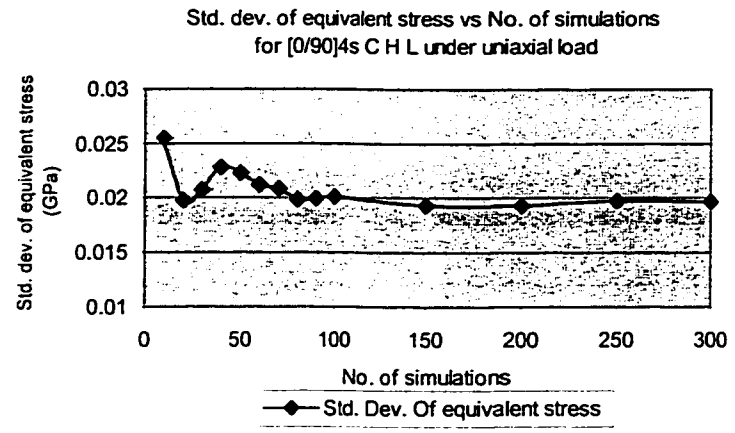

(b)

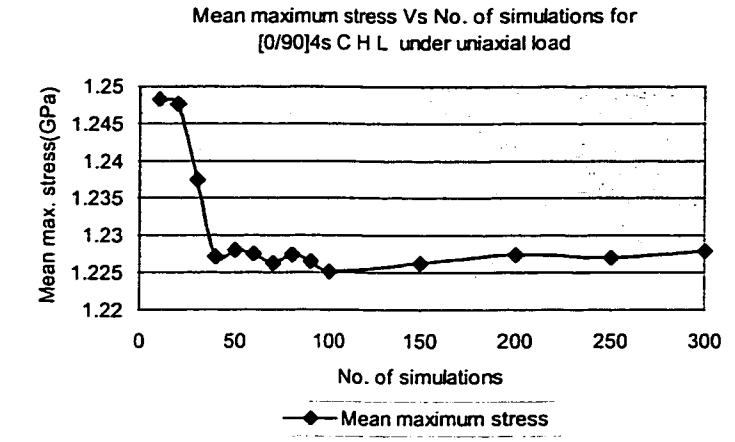

(c)

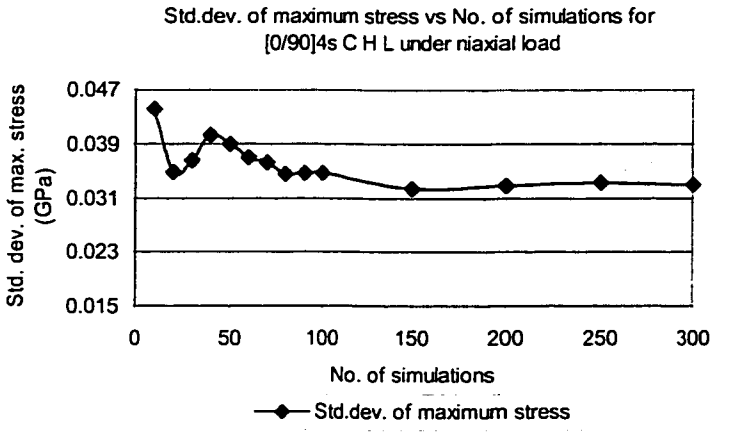

(d)

Figure 5.4 Stress analysis of $[0/90]_{4s}$ controlled hole laminate subjected to uniaxial load: (a) mean values of equivalent stress, (b) standard deviation values of equivalent stress, (c) mean values of maximum stress, (d) standard deviation values of maximum stress.

5.3.2.1 Observations

From Figure 5.4-a it is observed that the mean value of equivalent stress (σ_{equ}) converges nearly at 200 simulations attaining a constant value of 0.7877 GPa. High fluctuation in the values is observed in the first 100-150 simulations. The mean equivalent stress value initially attains a high value of 0.798 GPa and gradually reduces as the number of simulations increases. Thus a reverse trend can be noticed in the $[0/90]_{4s}$ laminate when compared with $[0_2/\pm 45]_{2s}$ laminate considering the equivalent stress parameter. The standard deviation curve also displays variation up to 150 simulations and attains a constant value of 0.0196 GPa at 200 simulations as shown in Figure 5.4-b. The maximum stress (σ_{max}) curve in Figure 5.4-c gains a constant value at about 200 simulations and the corresponding mean maximum stress value is 1.227 GPa. Variation of standard deviation value for maximum stress parameter is shown in Figure 5.4-d. On examining the overall trend of the curves, as pointed out in section 5.3.1.1, both the mean equivalent stress and mean maximum stress curves from Figures 5.4-a and 5.4-c respectively, attain a high value at the beginning, fluctuates rapidly between 50-100 simulations and attain a constant value at about 200 simulations.

In order to have a better understanding of the behavior of the laminates under consideration, Table 5.1 is prepared which clearly brings out a comparison of mean values of stress parameters, their standard deviation values and the values of coefficient of variation. Coefficient of variation is calculated by taking a ratio of standard deviation value to the corresponding mean value of the stress parameter.

Laminate Type	UDL MN/ m	No. of simulations	Mean value of max. stress (σ_{max}) (GPa)	Std. dev. of max. stress (GPa)	C.O.V of max. stress	Mean value of equ. stress (σ_{equ}) (GPa)	Std. dev. of equ. stress (GPa)	C.O.V of equ. stress
$[0_2/\pm 45]_{2s}$	1.35	150	1.241	0.0313	0.0252	0.6914	0.0169	0.0244
$[0/90]_{4s}$	1.06	200	1.227	0.0329	0.0268	0.7877	0.0196	0.0248

Table 5.1 Mean values, standard deviation values and coefficient of variation values of the parameters calculated for both laminate configurations for a controlled hole laminate under uniaxial load condition

From Table 5.1 we observe that:

1) Configuration $[0_2/\pm 45]_{2s}$ can bear a higher load in comparison with $[0/90]_{4s}$. Accordingly the mean value of maximum stress for the former configuration is high.

2) The $[0_2/\pm 45]_{2s}$ laminate requires less number of samples to be simulated to achieve a mean value of stress when compared to $[0/90]_{4s}$ configuration as the stresses converge at 150 simulations for $[0_2/\pm 45]_{2s}$ configuration and at 200 simulations for $[0/90]_{4s}$ configuration.

3) From Table 5.1, observing the values of coefficient of variation for both the laminate configurations, it can be concluded that the deviation is slightly more in $[0/90]_{4s}$ laminate as compared with $[0_2/\pm 45]_{2s}$ laminate.

4) It can be noticed from Table 5.2, that although the mean maximum stress value for $[0_2/\pm 45]_{2s}$ laminate is high when compared with $[0/90]_{4s}$ laminate, mean equivalent stress value for $[0_2/\pm 45]_{2s}$ laminate is less as opposed to $[0/90]_{4s}$ laminate. This is due to the reason that the equivalent stress value is obtained by taking a stress averaged over a large value of characteristic length, and the corresponding value is 10.63 mm and the value of characteristic length for $[0/90]_{4s}$ laminate is 4.44 mm.

5) As per the average stress criterion, the equivalent stress should be less than or equal to the strength of un-notched laminate. Accordingly both the laminate configurations display an equivalent stress value, which is well within the failure load limit.

5.3.3 Biaxial load on controlled hole laminate

It is recognized that, the internal damage in the laminate and its progression are affected by loading condition. Thus the material response under biaxial load is different from that under uniaxial load. Loading condition can significantly reduce the stiffness and strength properties of the laminate. The loading condition can also significantly reduce the reliability of the laminate.

The failure process under biaxial loading conditions has not yet been fully understood. Development of appropriate and accurate failure criterion for biaxial loading case is an on-going research activity. In determining the stress distribution in a composite laminate subjected to a biaxial load, it has been shown [1] that better results can be achieved using the first-ply failure criterion or lamina-based fibre failure criterion applied in conjunction with the models such as the point strength model or minimum strength model. In these

models, the strength distribution is analyzed point-by-point along the characteristic curve, which is at a distance of the value of characteristic length. Two points on this characteristic curve lie on the x-axis. In this regard, the value of characteristic length (along x-axis) is considered to be independent of the loading condition for the laminate configuration and thus it is assumed to be the same as in the case of uniaxial loading [1].

In the present thesis work, the main objective is to quantify the effects of randomness in hole geometry, eccentricity, and material properties on the reliability of the laminate. For this purpose, the equivalent stress calculated based on the characteristic length is used as the parameter. The reliability is related to the probabilistic parameters of the equivalent stress parameter. Information about the probabilistic parameters of the equivalent stress parameter corresponding to the uniaxial load case and the biaxial load case would help to understand how the reliability of the laminate is affected by the loading condition. To this end, a study has been conducted in the present work to analyze the effect of stress distribution due to biaxial loading near the hole edge and along the x-axis on the equivalent stress based on the average stress criterion itself. As mentioned before, two points on the characteristic curve lie on the x-axis. Thus the present analysis is applicable to these two points. In this regard, the value of characteristic length (along x-axis) is considered to be independent of the loading condition for the laminate configuration and thus it is assumed to be the same as in the case of uniaxial loading. As mentioned before, a similar assumption has been used in reference [1]. The load value imposed in uniaxial load case is used in the biaxial load case also and the analysis is performed. When a laminate with cutout is subjected to biaxial loading, the direction of the failure-propagating plane depends on the stress ratio and the lay-up configuration of the

laminate [1]. The stress ratio adopted in our case is $\sigma_x : \sigma_y = 1:1$. The case of a biaxial load is analyzed considering a square plate, rather than a rectangular plate. Figure 5.5 depicts the finite element mesh, boundary conditions and application of load on the laminate.

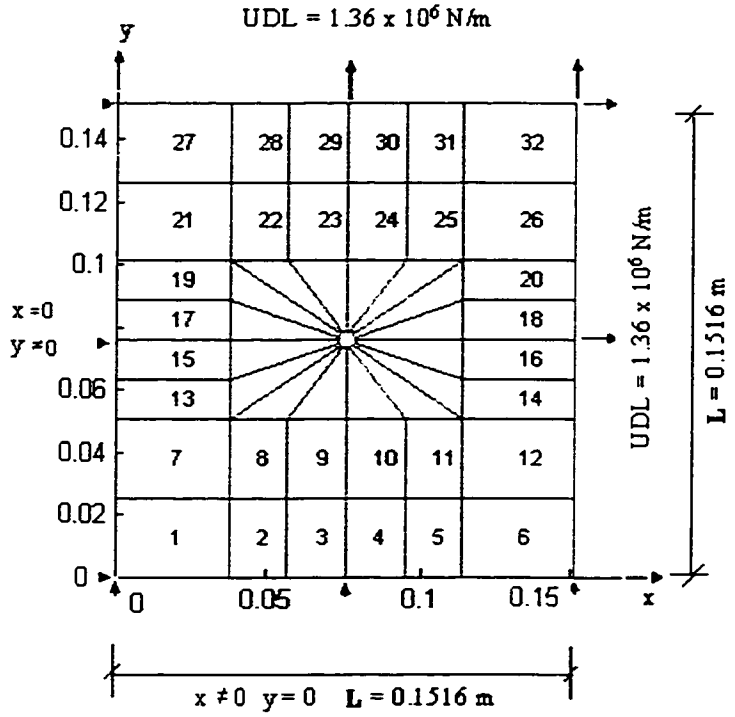

Figure 5.5 Boundary condition and finite element mesh for a square plate subjected to biaxial load

Table 5.2 shows the values of characteristic length employed for both the laminate configurations.

Laminate configuration	a_0 **(mm)**
$[0_2/\pm 45]_{2s}$	10.63
$[0/90]_{4s}$	4.44

Table 5.2 The value of characteristic length for the laminates

5.3.4 Biaxial load on $[0_2/\pm 45]_{2s}$ controlled hole laminate

Analysis is performed on a square laminate having a dimension of 151.6 x 151.6 mm^2. Since the ply thickness is considered to be 0.125 mm, the $[0_2/\pm 45]_{2s}$ laminate containing 16 layers, has a thickness of 2 mm. The finite element mesh utilized for the laminate analysis is depicted in Figure 5.5. A factor of safety (F.O.S) of 1.2 on the ultimate load of notched sample, as assumed in the previous cases is employed and simulation is performed. The application of the load on the laminate is shown in Figure 5.5. Since, stress ratio of $\sigma_x : \sigma_y = 1:1$ is used, we have same amount of load (1.35 MN/m) acting along the positive x and y-directions. Probabilistic quantities such as, mean, standard deviation and coefficient of variation for equivalent and maximum stress parameters are obtained from the simulation and the variations in the mean values and standard deviation values with the number of simulations for the two parameters have been presented in Figures 5.6-a – 5.6-d.

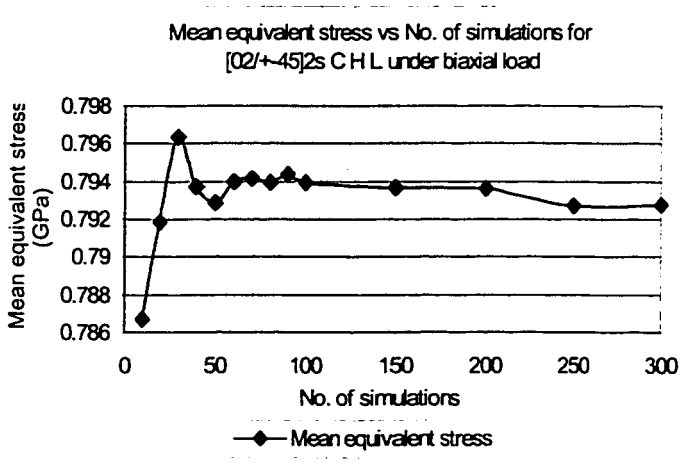

(a)

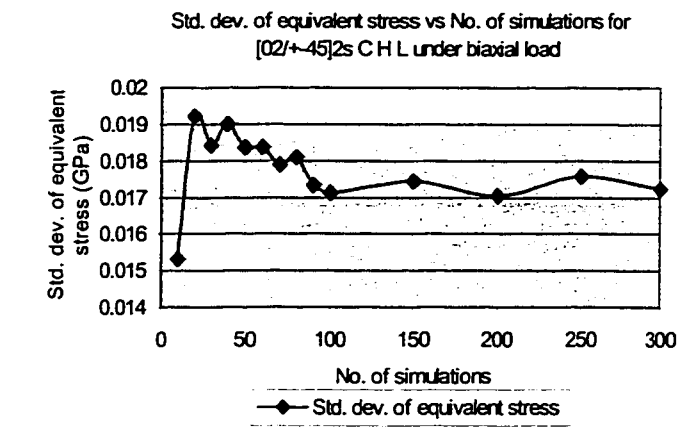

(b)

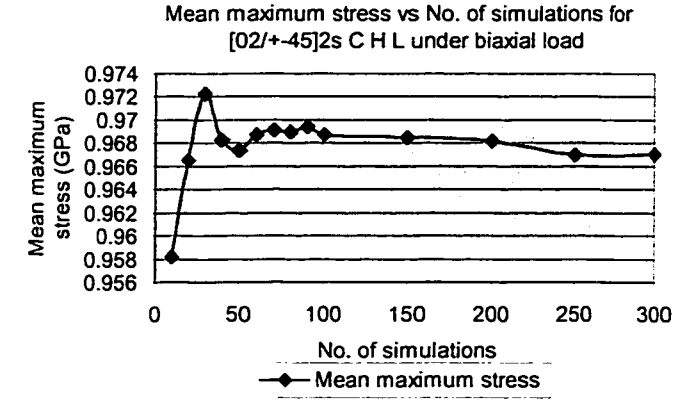

(c)

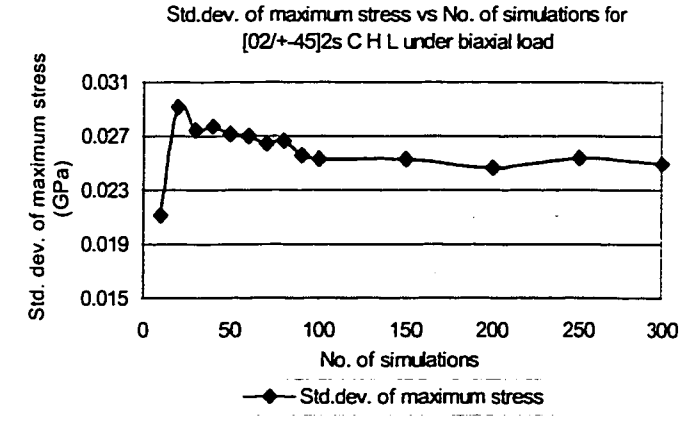

(d)

Figure 5.6 Stress analysis of $[0_2/\pm 45]_{2s}$ controlled hole laminate subjected to biaxial load: (a) mean values of equivalent stress, (b) standard deviation values of equivalent stress, (c) mean values of maximum stress, (d) standard deviation values of maximum stress.

5.3.4.1 Observations

It can be observed from Figure 5.6-a, that, there is a considerable amount of fluctuation in the mean value of equivalent stress (σ_{equ}) in the first 100 simulations. Subsequently the variation decreases as the number of simulation reaches 250 and finally converges at 300 simulations attaining a constant value of 0.7927 GPa. Noticing the standard deviation curve in Figure 5.6-b, we can make out that the influence of the number of simulations on the standard deviation values does not get reduced to the same order as that of the mean values, with the increase in number of simulations. But the variation is not predominant and due to the time considerations in the analysis the value is considered to be 0.0172 GPa. The maximum stress (σ_{max}) curve in Figure 5.6-c follows the same trend as the mean equivalent stress curve and gains a constant value at 300 simulations and the corresponding mean maximum stress value is 0.9670 GPa. Variation of standard deviation value for maximum stress parameter is shown in Figure 5.6-d.

On comparing the mean value of maximum stress (σ_{max}) developed in uniaxial and biaxial loading cases, for the same amount of load along the y-axis, a lesser value of maximum stress (σ_{max}) is generated in the case of biaxial loading, a reduction of the order of 274 MPa. But there is an increase in the mean value of equivalent stress (σ_{equ}), and it is of the order of 101.3 MPa. The variation in the value is due to the stochastic variation in the material properties and due to the addition of load in the x-direction along with the existing load in y-direction.

5.3.5 Biaxial load on $[0/90]_{4s}$ controlled hole laminate

In order to do a comparison of the stress values, a similarity in the condition of material properties, geometry, finite element mesh and boundary conditions is assumed for the analysis.

The variations in the mean values and standard deviation values with the number of simulations for equivalent stress and maximum stress parameters have been presented in Figures 5.7-a – 5.7-d.

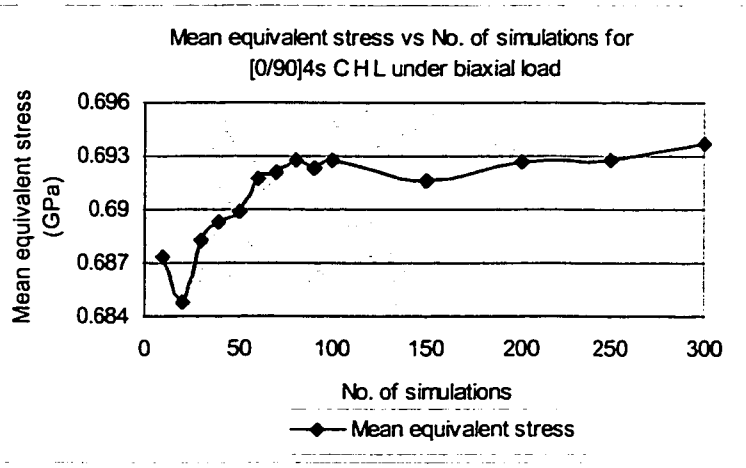

(a)

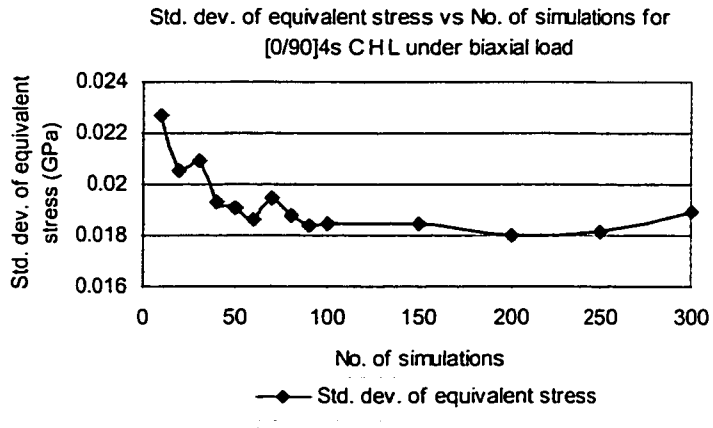

(b)

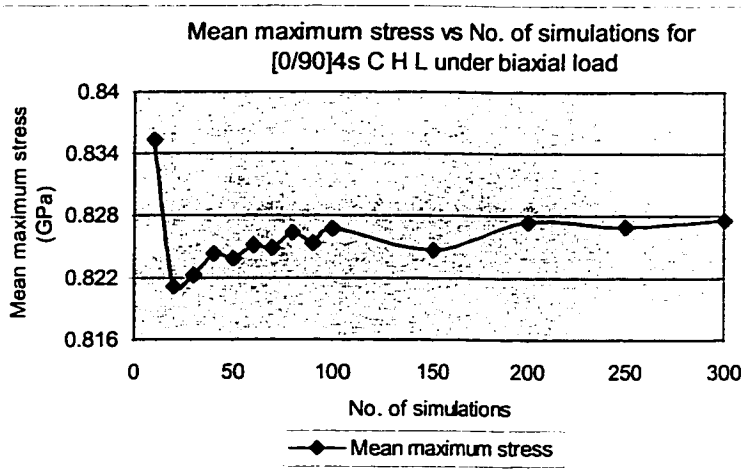

(c)

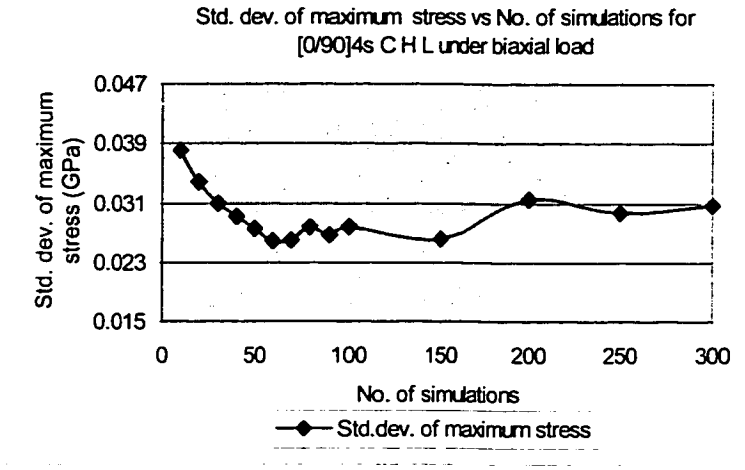

(d)

Figure 5.7 Stress analysis of $[0/90]_{4s}$ controlled hole laminate subjected to biaxial load: (a) mean values of equivalent stress, (b) standard deviation values of equivalent stress, (c) mean values of maximum stress, (d) standard deviation values of maximum stress.

5.3.5.1 Observations

It is clear from the Figures 5.7-a and 5.7-c that the mean values of equivalent stress (σ_{equ}) and the maximum stress values never converge with the increase in the number of simulations. High fluctuation in the values is observed up to 150 simulations. Later on the amount of variation reduces but never attains a constant value. Further increase in the

number of simulations would lead to a convergence in the value. Because of the time constraint, investigation on the exact number of simulations at which a steady state is achieved is not pursued and the value corresponding to 300 simulations is considered for further discussion. Thus the mean value of equivalent stress is 0.6936 GPa and mean value of maximum stress is 0.827 GPa. Also a reverse trend can be noticed in the $[0/90]_{4s}$ laminate case when compared with $[0_2/\pm 45]_{2s}$ laminate. The standard deviation curve for equivalent stress in Figure 5.7-b gains a high value of 0.023 GPa during the first 10 simulations and reduces to a value of 0.018 GPa and again rises. This means that a complete correlation between the previous value of standard deviation and the current value of standard deviation is still not achieved. Variation of standard deviation value for maximum stress parameter is shown in Figure 5.7-d.

Table 5.3 shows the mean value of the stress parameters, their standard deviation values and values of coefficient of variation. This aids in the study of response of the laminates under the application of biaxial loads.

Laminate Type	UDL MN/m	No. of simulations	Mean value of max. stress (σ_{max}) (GPa)	Std. dev. of max. stress (GPa)	C.O.V of max. stress	Mean value of equ. stress (σ_{equ}) (GPa)	Std. dev. of equ. stress (GPa)	C.O.V of equ. stress
$[0_2/\pm 45]_{2s}$	1.36	300	0.967	0.024	0.025	0.792	0.017	0.021
$[0/90]_{4s}$	1.06	300	0.827	0.030	0.037	0.693	0.018	0.027

Table 5.3 Mean values, standard deviation values and coefficient of variation values of the parameters calculated for both laminate configurations for a controlled hole laminate under biaxial load condition with the stress ratio as $\sigma_x : \sigma_y = 1:1$

From Table 5.3 we observe that:

(1) Configuration $[0_2/\pm 45]_{2s}$ can bear a higher load in comparison with $[0/90]_{4s}$. Accordingly the mean value of maximum stress for the former configuration exceeds the latter by 150 MPa. Similar observation can be made for mean value of equivalent stress of $[0_2/\pm 45]_{2s}$ laminate, which exceeds by 99 MPa that of $[0/90]_{4s}$ laminate.

(2) From Table 5.3, observing the values of coefficient of variation for both the laminate configurations, it can be concluded that the deviation is slightly more in $[0/90]_{4s}$ laminate as compared with $[0_2/\pm 45]_{2s}$ laminate.

(3) In biaxial load case, a considerable reduction in the mean value of maximum stress (σ_{max}) from that of the uniaxial load case is observed for both the laminates. Reduction of the order of 274 MPa is noticed in $[0_2/\pm 45]_{2s}$ laminate and 400 MPa in the case of $[0/90]_{4s}$ laminate.

5.4 Case 2: Uncontrolled hole laminate analysis

The application of systematic inspection of an uncontrolled hole laminate is performed. As it is highly impossible to achieve a perfect hole at the desired coordinates, it calls for an analysis to check for the change in the mean value of equivalent stress over the characteristic length and the mean value of maximum stress near the hole edge. Based on reference [65], a hypotrochoid variation in the hole shape is considered and the equation for variation is given by:

$$g(\theta) = \psi \cos(k+1)\theta \tag{5.3}$$

where the value of k is 7 (a non-negative integer). The equation is expanded in a power of ψ which is equal to 0.01. Here θ is the angle at which a node is created on the circle while developing a finite element mesh. Substituting the values for the variables in the above equation, a set of $g(\theta)$ values is obtained. It is by this factor the radius of the circular opening will be varying. Maximum tolerance for eccentricity of the hole is of the order of $\left(\frac{1}{20}\right)^{th}$ inch. Gaussian random values are generated and these values control the movement of the hole depending on the number of the nodes associated with the hole. Modifications in the circular opening are reflected in subroutines *MESHREFINE.m* and *MESHCIRCULAR.m*. Figure 5.8 given below, shows a portion of the finite element mesh representing the eccentricity and irregularity of the hole shape.

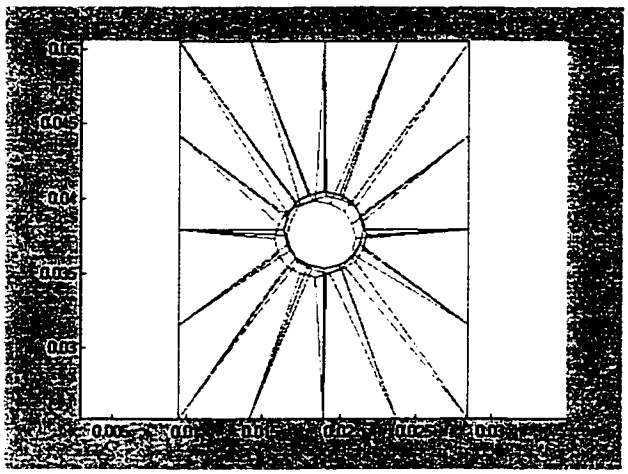

Figure 5.8 A portion of the finite element mesh representing the eccentricity and irregularity in the hole shape.

It is to be noted that, in the case of uncontrolled circular opening, as the hole location is not fixed, the value of characteristic length ceases to remain constant. Assuming the variation in the characteristic length to follow a Gaussian distribution, a series of values

are generated for the characteristic length a_o using the sub-routine *DISAO.m* in the MATLAB® program. Sub-routine *DISAO.m* in turn uses a MATLAB® sub-function:

$$[R] = a + (b-a) * \text{rand}(m, n) \tag{5.4}$$

where 'rand' is the sub-function, 'a' and 'b' are the maximum and minimum limits of the value of characteristic length respectively, 'm' is the number of rows of Gaussian random numbers to be generated and 'n' is the number of columns to be realized. In the present case 'm' is assigned a value equal to the number of laminates to be analyzed and 'n' = 1, giving matrix [R] a dimension (m*n).

5.4.1 Uniaxial load on $[0_2/\pm 45]_{2s}$ uncontrolled hole laminate

In order to compare the behavior of a controlled hole laminate with an uncontrolled hole laminate, the plate geometry, laminate configurations, boundary conditions and application of load for an uncontrolled hole laminate are kept the same as that for a controlled hole laminate. But it is to be noticed, that the finite element mesh close to the hole boundary assumes new co-ordinate values based on the tolerance value set. Referring to Tables 4.6 and 4.8, it is clear that the value of characteristic length a_o will not remain constant all the time. Assuming a Gaussian distribution variation, the value of characteristic length a_o can be varied and the probability distribution achieved is presented in Figure 5.9.

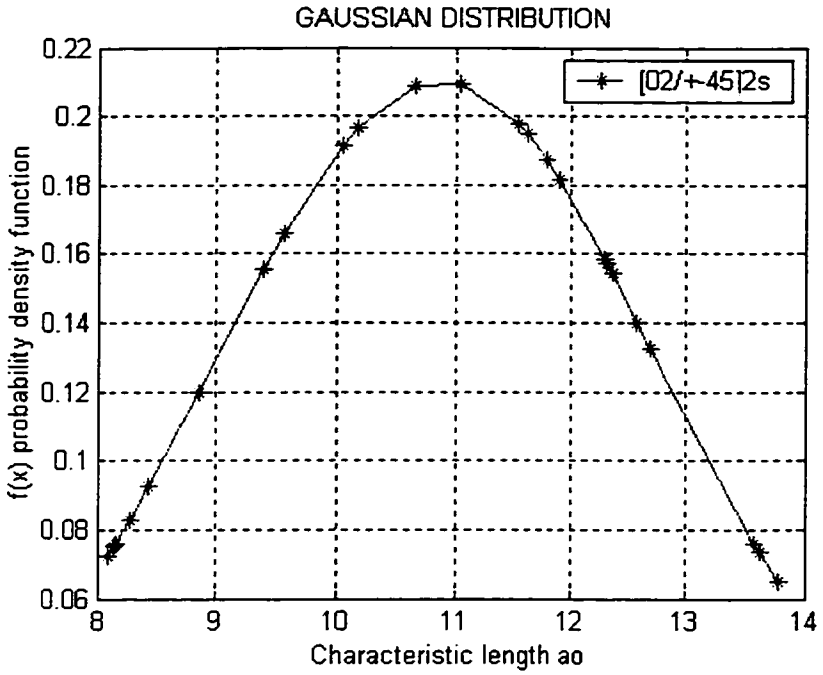

Figure 5.9 Gaussian distribution curve for the value of characteristic length a_o considering $[0_2/\pm 45]_{2s}$ configuration

The MATALB® program developed generates as many values of characteristic length as there are number of simulations and these values are based on the Gaussian distribution method.

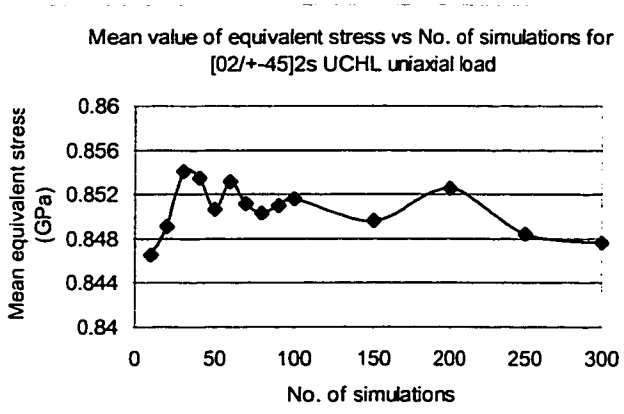

(a)

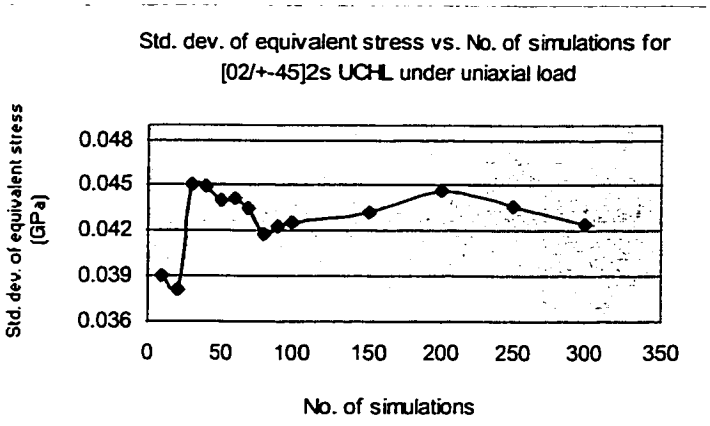

(b)

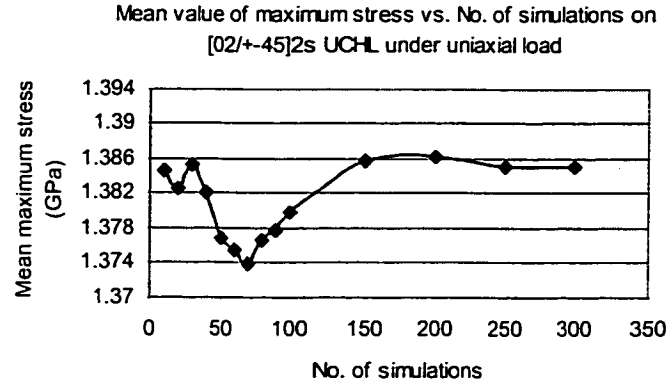

(c)

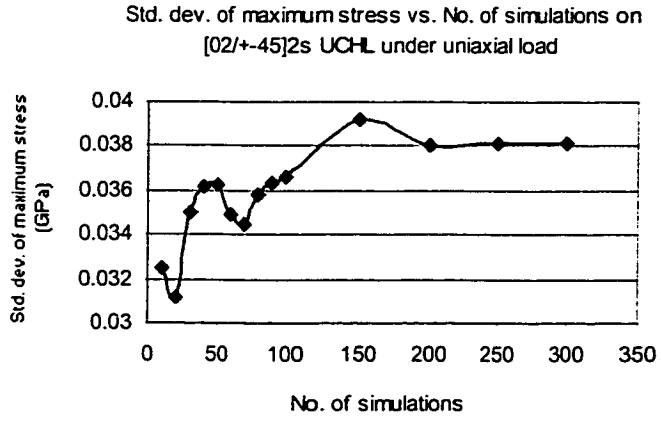

(d)

Figure 5.10 Stress analysis of $[0_2/\pm 45]_{2s}$ uncontrolled hole laminate subjected to uniaxial load: (a) mean values of equivalent stress, (b) standard deviation values of equivalent stress, (c) mean values of maximum stress, (d) standard deviation values of maximum stress.

5.4.1.1 Observations

From Figure 5.10-a it is observed that fluctuation in the mean value of equivalent stress persists till 250 simulations and attains a steady value of 0.847 GPa at 300 simulations. The final value achieved is almost close to the initial value experienced. The maximum stress (σ_{max}) curve in Figure 5.10-c gains a steady state after 150 simulations though a slight variation is observed at 200 simulations and correspondingly the mean maximum stress value is 1.385 GPa. But the curve in Figure 5.10-c traces a reverse path when compared with the curve in Figure 5.10-a. It is to be noted that in addition to the stochastic variation of material properties, variations in the value of characteristic length and geometry of the hole also exist. Apparently these unpredictable parameters contribute to a prolonged and non-uniform variation in the pattern. But the trend remains the same when a comparison is made between the standard deviation of equivalent stress curve and standard deviation of maximum stress curve as depicted in Figures 5.10-b and 5.10-d.

5.4.2 Uniaxial load on $[0/90]_{4s}$ uncontrolled hole laminate

Figure 5.11 shows the Gaussian distribution curve for the value of characteristic length a_o for $[0/90]_{4s}$ laminate. Following distribution is achieved by supplying values from the Table 4.5. It can be noticed that the curve has a minimum value of 2.24 mm and maximum of 7.04 mm as can be made out from Table 4.5 also.

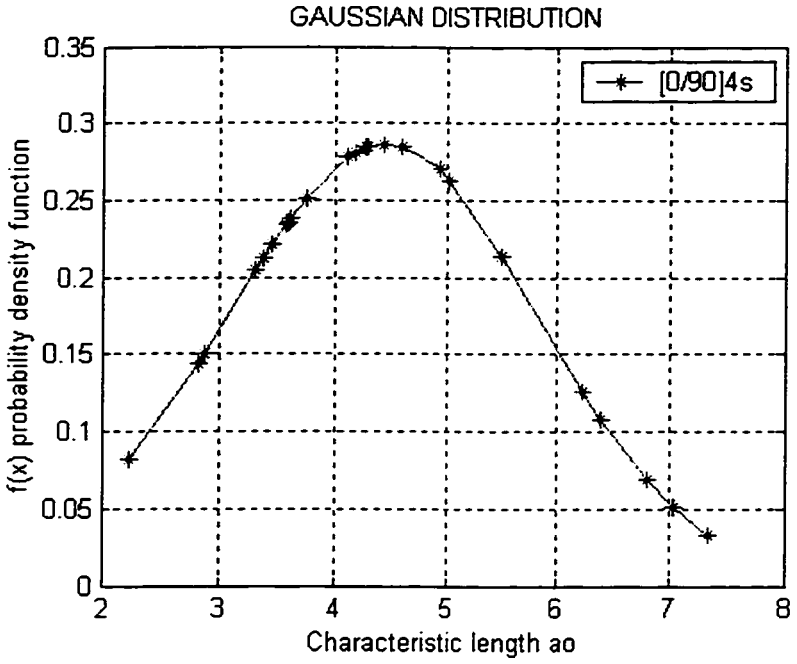

Figure 5.11 Gaussian distribution curve for the value of characteristic length a_o considering $[0/90]_{4s}$ configuration

Maintaining similar conditions as expressed for $[0/90]_{4s}$ controlled hole laminate, simulation is carried out to achieve mean equivalent and mean maximum stress values for the uncontrolled hole laminate. The corresponding plots are shown in Figure 5.12.

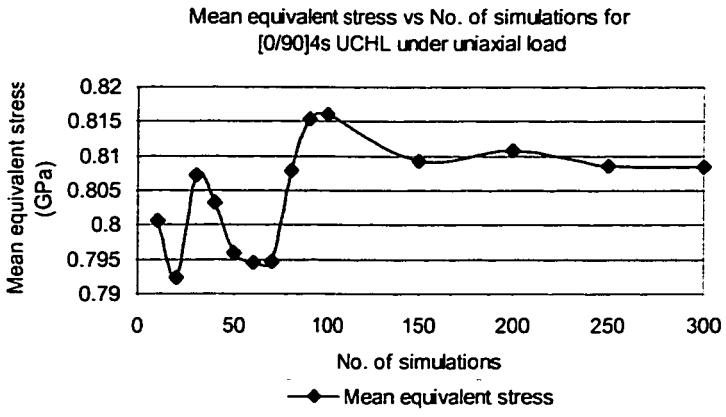

(a)

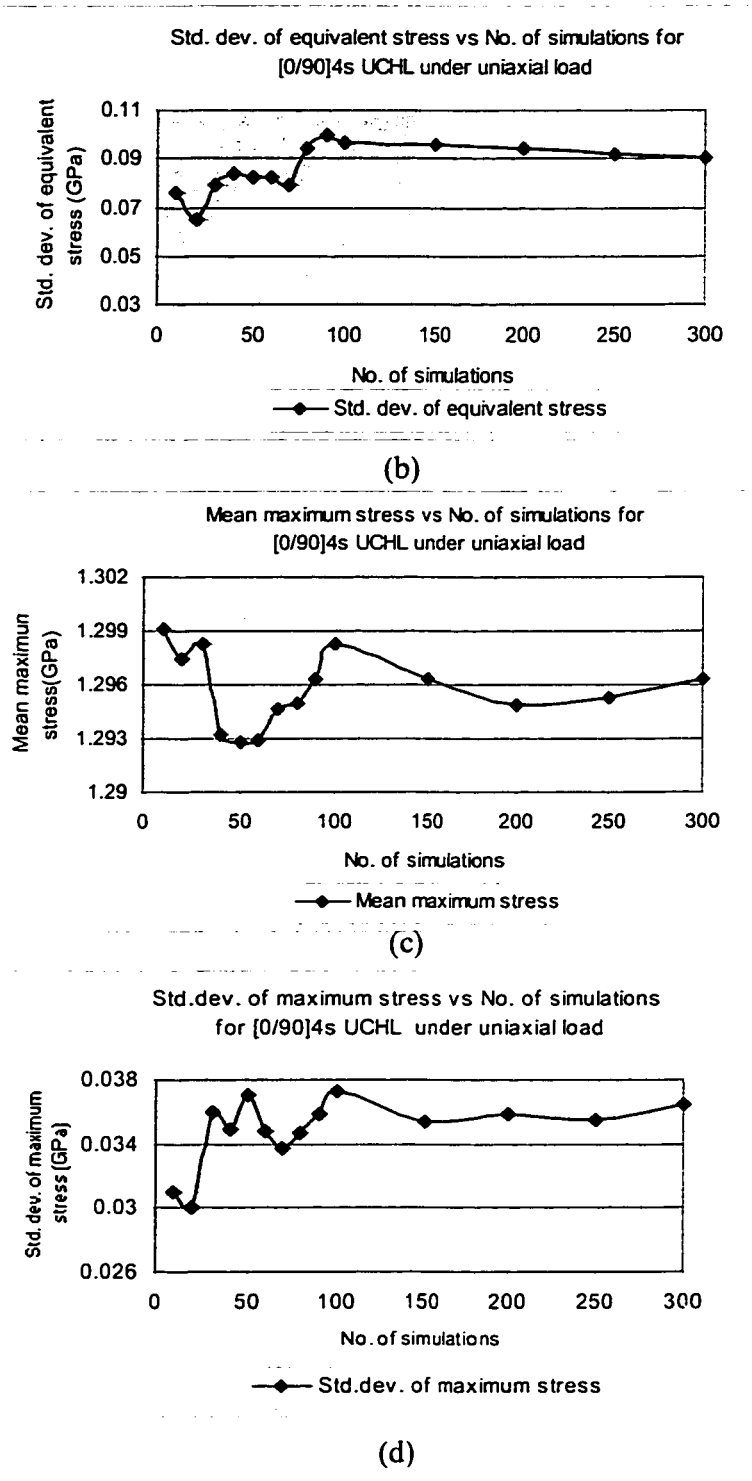

Figure 5.12 Stress analysis of $[0/90]_{4s}$ uncontrolled hole laminate subjected to uniaxial load: (a) mean values of equivalent stress, (b) standard deviation values of equivalent

stress, (c) mean values of maximum stress, (d) standard deviation values of maximum stress.

5.4.2.1 Observations

It is observed that the mean value of equivalent stress (σ_{equ}) converges at 300 simulations ending with a value of 0.808 GPa as shown in Figure 5.12-a. But observing Figure 5.12-c for mean maximum stress parameter even after 300 simulations a steady state is not achieved. Correspondingly the standard deviation value from Figure 5.12-d also fluctuates and never reaches a convergence. Due to time constraint, values attained at 300 simulations are considered for further discussion.

Table 5.4 distinguishes the mean values of stress parameters, their standard deviation values and values of coefficient of variation. As an observation, we can make out that the value of coefficient of variation obtained for $[0_2/\pm 45]_{2s}$ laminate considering the mean equivalent stress parameter is less as against $[0/90]_{4s}$ laminate. This means that the variation for $[0/90]_{4s}$ laminate is high and varies more than 100% when compared with $[0_2/\pm 45]_{2s}$ laminate. When mean maximum stress parameter is considered the variation is minimal and the value of $[0/90]_{4s}$ laminate exceeds that of $[0_2/\pm 45]_{2s}$ laminate by 0.72 %.

Laminate Type	UDL MN/m	No. of simulations	Mean value of max. stress (σ_{max}) (GPa)	Std. dev. of max. stress (GPa)	C.O.V of max. stress	Mean value of equ. stress (σ_{equ}) (GPa)	Std. dev. of equ. stress (GPa)	C.O.V of equ. stress
$[0_2/\pm 45]_{2s}$	1.35	300	1.385	0.0381	0.0275	0.847	0.0423	0.0499
$[0/90]_{4s}$	1.06	300	1.296	0.036	0.0277	0.808	0.0900	0.1113

Table 5.4 Mean values, standard deviation values and coefficient of variation values of the parameters calculated for both the laminate configurations for an uncontrolled hole laminate under uniaxial load condition

To study the amount of variation the uncontrolled hole laminate would generate on the stress parameters, Table 5.5 is prepared, highlighting the mean values of the stress parameters obtained for controlled hole and uncontrolled hole laminates.

Laminate type	Controlled Hole		Uncontrolled Hole	
	Mean max. stress value (σ_{max}) (GPa)	Mean equivalent stress value (σ_{equ}) (GPa)	Mean maximum stress value (σ_{max})(GPa)	Mean equivalent stress value (σ_{equ})(GPa)
$[0_2/\pm 45]_{2s}$	1.2411	0.6914	1.385	0.847
$[0/90]_{4s}$	1.0266	0.7877	1.296	0.808

Table 5.5 Comparison of mean maximum and equivalent stresses corresponding to controlled and uncontrolled hole laminates under uniaxial load

On comparing the mean value of maximum stress for controlled and uncontrolled hole laminates with $[0_2/\pm 45]_{2s}$ configuration, an increase of 143.9 MPa in the later case can be observed. This increase in the stress value is attributed to the irregularity of hole shape and eccentricity of the hole. The cause for the increase in the stress can be reasoned as

follows; when the circular opening moves closer to the laminate edge, in the process of maintaining a uniform stress distribution along the axis perpendicular to the loading direction, a higher stress value is attained near the hole edge. It is of utmost importance to consider this extra stress developed while designing the laminates.

The increase in the mean value of maximum stress achieved through simulation, accounts for only one hole driven in the laminate. But in practical applications, series of holes would be driven to have a good fixity of the parts in union. In such conditions, a multiplied effect of the severity in stress can be expected. Similar trend is observed

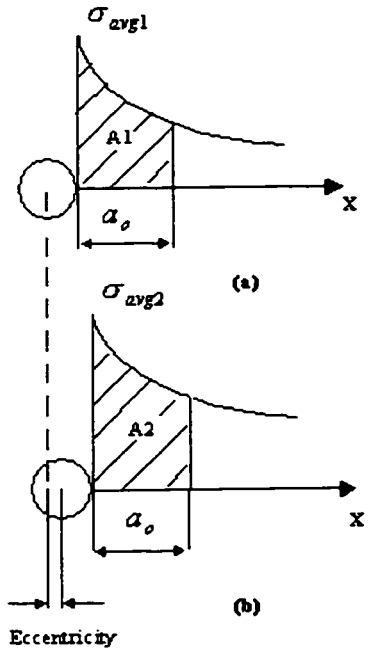

(a) Controlled hole laminate
(b) Uncontrolled hole laminate

Figure 5.13 Explanation for the increase in equivalent stress value

when comparing equivalent stress parameter. An increase of the order of 155.6 MPa in the uncontrolled hole laminate is sighted. A logical reason for the equivalent stress to be higher in case of uncontrolled hole laminate can be explained with Figure 5.13 given below.

As expressed in section 5.4, the value of characteristic length in uncontrolled hole laminate is changing as per the Gaussian distribution. When compared with a fixed value of characteristic length of the controlled hole laminate, a higher, lower or a similar value of the characteristic length is expected in uncontrolled hole laminate during the simulation. Considering, a similar value of characteristic length for the uncontrolled hole laminate, it is clear from the Figure 5.13, that, due to the eccentricity of the hole, area A2 under integration for the second laminate has increased when compared with the area A1 for controlled hole laminate. Thus the equivalent stress for uncontrolled laminate σ_{avg2} is more when compared with controlled hole laminate σ_{avg1}. This leads to a higher value of equivalent stress in case of uncontrolled hole laminate. Accordingly an increase of the order of 155.6 MPa in case of $[0_2/\pm 45]_{2s}$ laminate is observed.

A similar explanation can be given for $[0/90]_{4s}$ configuration also. An increase by an amount of 269 MPa for maximum stress and 20.7 MPa in equivalent stress is observed for the uncontrolled hole laminate. Magnitude of the change in mean value of equivalent stress for $[0/90]_{4s}$ configuration is not significant when compared with $[0_2/\pm 45]_{2s}$ laminate.

5.4.3 Biaxial load on $[0_2/\pm 45]_{2s}$ uncontrolled hole laminate

All the conditions expressed in section 5.3.3 are maintained in the present analysis also. But in addition to these conditions, the variation in the geometry around the hole, the hole eccentricity and Gaussian variation in the value of characteristic length are also imposed. Figure 5.14 depicts the mean stress parameters and their standard deviation values obtained based on these variations.

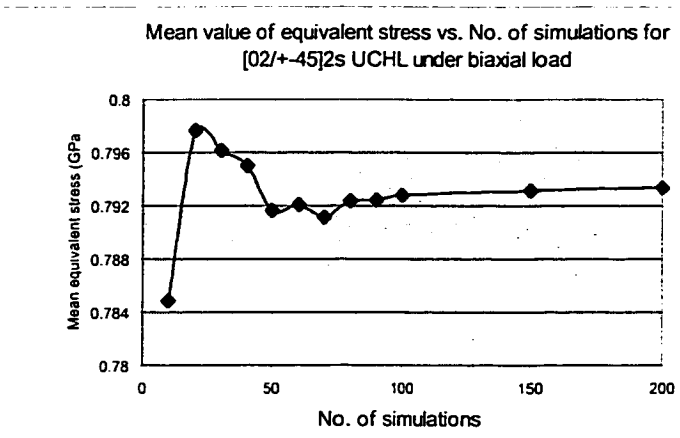

(a)

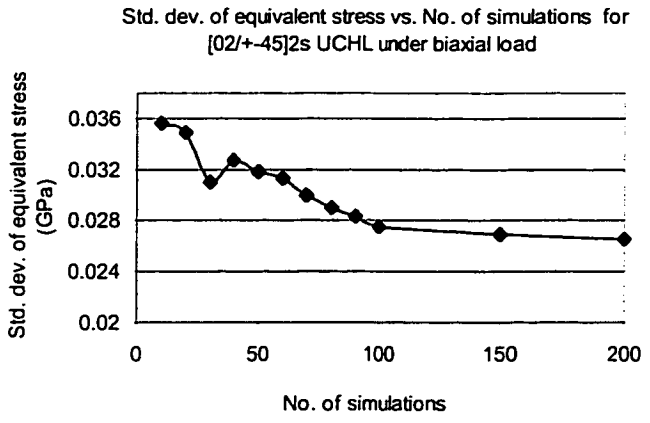

(b)

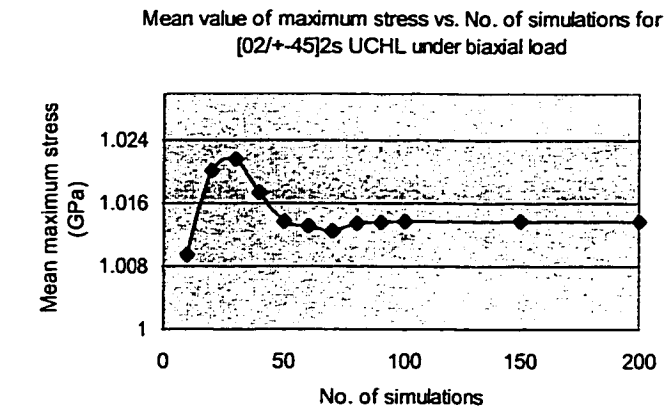

(c)

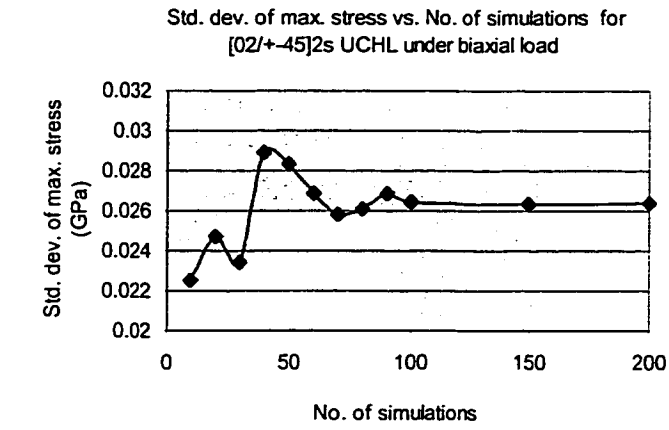

(d)

Figure 5.14 Stress analysis of $[0_2/\pm 45]_{2s}$ uncontrolled hole laminate subjected to biaxial load: (a) mean values of equivalent stress, (b) standard deviation values of equivalent stress, (c) mean values of maximum stress, (d) standard deviation values of maximum stress.

5.4.3.1 Observations

It is seen from Figure 5.14-a to 5.14-d that all the plots attain a constant value at 150 simulations itself. Commenting on the values of coefficient of variation corresponding to the mean equivalent stress and mean maximum stress parameters we see that the variation is slightly higher in the latter case, exceeding the former by 27.4%.

5.4.4 Biaxial load on $[0/90]_{4s}$ uncontrolled hole laminate

The variations in the mean values and standard deviation values with the number of simulations for the two stress parameters have been presented in Figures 5.15-a - 5.15-d.

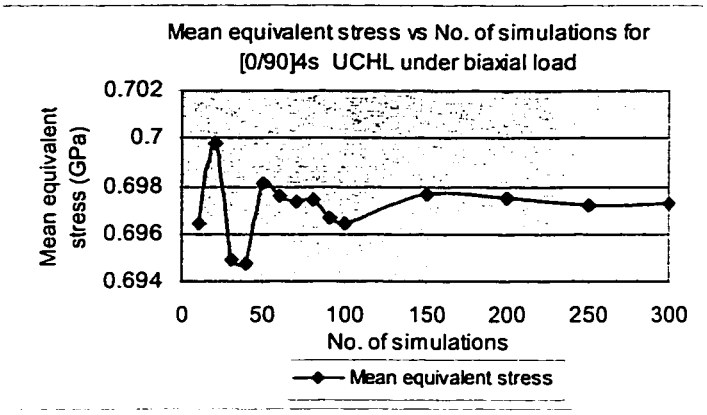

(a)

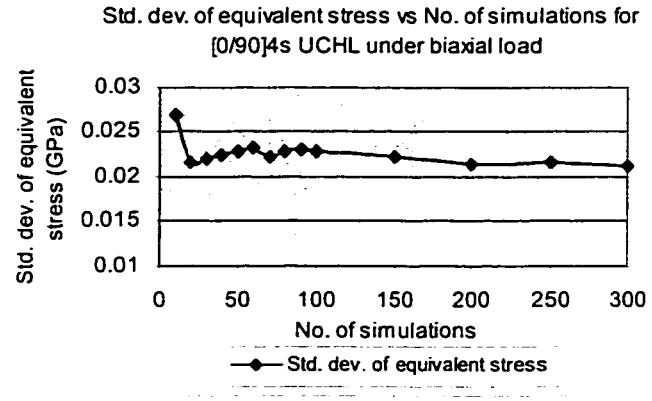

(b)

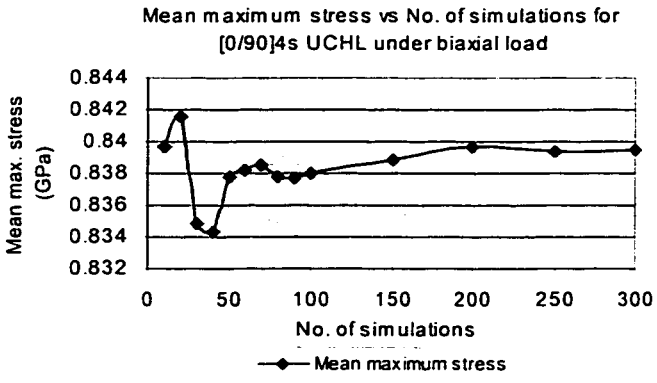

(c)

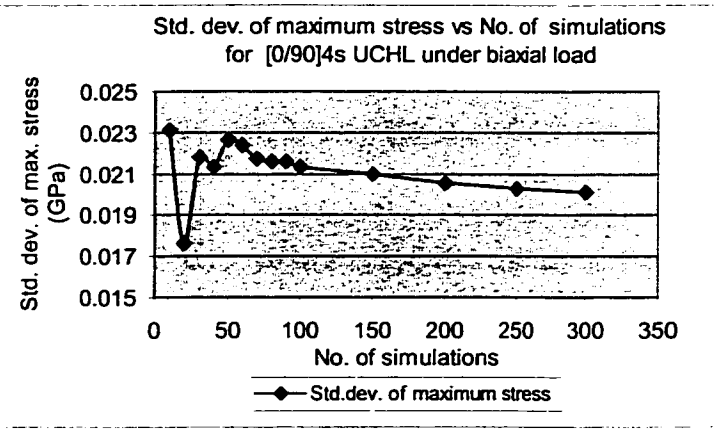

(d)

Figure 5.15 Stress analysis of $[0/90]_{4s}$ uncontrolled hole laminate subjected to biaxial load: (a) mean values of equivalent stress, (b) standard deviation values of equivalent stress, (c) mean values of maximum stress, (d) standard deviation values of maximum stress.

5.4.4.1 Observations

Convergence in the $[0/90]_{4s}$ laminate case is achieved at 300 simulations, which is nearly after 100 simulations more than the $[0_2/\pm 45]_{2s}$ laminate case. All the plots exhibit a high fluctuation in the first 150 simulations. Further increase in the number of simulations increases the correlation between the previous value and the current value and convergence occurs. Figure 5.15-a shows the variation of the mean equivalent stress parameter with the number of simulations. The fluctuation in the value can be attributed to the stochastic variation of material properties and the geometric variation in the laminate. Convergence of mean equivalent stress occurs at 0.6973 GPa and corresponding standard deviation at 0.0211 GPa. Similarly the mean maximum stress converges at 0.839 GPa and its standard deviation at 0.0201 GPa. Table 5.6 gives a detailed listing of values of the stress parameters under consideration. Observing the values of coefficient of variation corresponding to the mean equivalent stress and mean

maximum stress parameters, we see that there is an increase in the fluctuation in the former case by 25.5%.

Laminate Type	UDL MN/m	No. of simulations	Mean value of max. stress (σ_{max}) (GPa)	Std. dev. of max. stress (GPa)	C.O.V of max. stress	Mean value of equ. stress (σ_{equ}) (GPa)	Std. dev. of equ. stress (GPa)	C.O.V of equ. stress
$[0_2/\pm 45]_{2s}$	1.35	200	1.013	0.0263	0.0259	0.7933	0.0265	0.033
$[0/90]_{4s}$	1.06	300	0.839	0.0201	0.0239	0.6973	0.0211	0.030

Table 5.6 Mean values, standard deviation values and coefficient of variation values of the parameters calculated for both the laminate configurations for an uncontrolled hole laminate under biaxial load condition: stress ratio used $\sigma_x : \sigma_y = 1:1$

Difference in the values of stress parameters developed considering a controlled hole laminate and an uncontrolled hole laminate is well understood by observing Table 5.7.

Laminate Type	Stress ratio	Controlled Hole		Uncontrolled Hole	
		Maximum stress value (σ_{max}) (GPa)	Equivalent stress value (σ_{equ}) (GPa)	Maximum stress value (σ_{max}) (GPa)	Equivalent stress value (σ_{equ}) (GPa)
$[0_2/\pm 45]_{2s}$	$\sigma_x : \sigma_y = 1:1$	0.9066	0.7557	1.013	0.7933
$[0/90]_{4s}$	$\sigma_x : \sigma_y = 1:1$	0.8272	0.6936	0.8391	0.6973

Table 5.7 Comparison of mean maximum and equivalent stresses corresponding to controlled and uncontrolled hole laminates under biaxial load

Following discussions can be put forth from Table 5.7:

1) On observing the results for $[0_2/\pm 45]_{2s}$ laminate, maximum stress value for an uncontrolled hole laminate exceeds that of controlled hole laminate by an appreciable amount of 106.4 MPa.

2) The trend of increase in the mean value of maximum stress for uncontrolled hole laminate from that of controlled hole laminate by 11.9 MPa is observed for $[0/90]_{4s}$ configuration also.

3) The mean value of equivalent stress in uncontrolled hole case increases by 3.7 MPa for $[0/90]_{4s}$ laminate, while it is 37.6 MPa for $[0_2/\pm 45]_{2s}$ configuration.

In the next section, a controlled hole laminate subjected to uniformly distributed shear load is analyzed.

5.5 Shear analysis of notched composite laminates

The lack of understanding, concerning the response of composite laminates containing discontinuities under shear loading is obvious. It has been shown [1] that a better result can be achieved in determining the stress distribution for a composite laminate subjected to a shear load based on the minimum strength model (MSM). As explained in section 5.3.3, the MSM analyzes the strength distribution over the laminate, point-by-point along the characteristic curve, which is at a distance of the value of characteristic length. The value of characteristic length (along x-axis) is considered to be independent of the loading condition for the laminate configuration and thus it is the same as in the case of uniaxial loading [1].

Due to the unavailability of the experimental test data concerning the ultimate shear load-bearing capacity of the notched laminate and un-notched laminate, it is not viable to adopt the average stress criterion to predict the failure of laminates. Thus, maximum

stress failure criterion is used which assumes that failure occurs when any one of the stress components in the local co-ordinate system reaches, or is greater than, its corresponding strength value.

A study has been conducted in the present work to determine the maximum shear stress developed in the laminate near the hole edge due to the application of the shear load. This value can be used in the maximum stress criterion.

In the present analysis of composite laminates subjected to a shear load, one must calculate the stresses developed in each and every layer individually. Accordingly, the nodal values through the thickness are functions of the in-plane coordinates (x, y) as shown in Figure 5.16. Each layer of the laminate can be treated either as a mathematical or a physical layer, giving the flexibility to the analyst to treat several physical layers as a sub-laminate wherever necessary and model delaminations, ply terminations, ply splits and so on.

The in-plane displacements and strains $(\varepsilon_x, \varepsilon_y, \gamma_{xy})$ are continuous through the thickness of the laminate. Thus the mid-plane strains calculated, would be the strains for the entire laminate. But the in-plane stresses $(\sigma_x, \sigma_y, \tau_{xy})$ will be discontinuous through the thickness of the laminate. Thus the stresses are found out individually for each and every ply separately. To the existing MATALB® program files, two more sub-routines are added i.e. *EMODPS.m* and *STRESSH.m*. Sub-routine *EMODPS.m* generates an elasticity matrix for a ply angle in the laminate and *STRESSH.m* calculates the nodal stresses for each and every layer in the laminate.

5.5.1 Shear analysis of $[0/90]_{4s}$ controlled hole laminate

In the present analysis, a square $[0/90]_{4s}$ composite laminate of dimensions 151.6 x 151.6 mm^2 and material properties described in Table 2.5 is employed. A positive shear load of 0.886 x 10^5 N/m is applied on the laminate and the stochastic finite element analysis is carried out on a controlled hole laminate. It is to be noted that in all further cases, the above parameters are maintained the same. MATLAB® program is aimed at calculating the stresses acting in the fiber and transverse directions using the Gauss point stresses obtained over the entire laminate. Figure 5.16 represents the boundary conditions employed in the analysis.

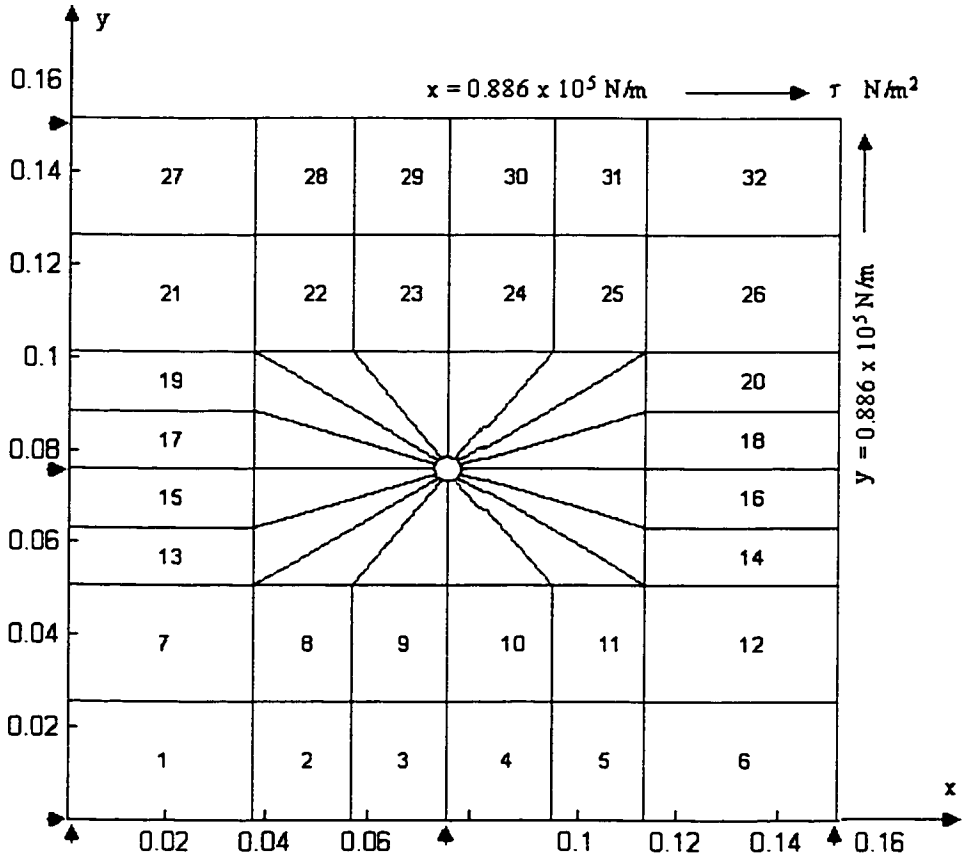

Figure 5.16 Boundary condition and shear load imposed on a square plate.

The ply numbering starts from the bottom layer as represented in Figure 2.5 and the first layer is 0° ply as numbered along the vertical axis. Since the analysis is based on the global co-ordinate system as shown in Figure 5.16, the first ply would actually be 90° ply. Stochastically simulated data are presented in Figure 5.17. The mean value of maximum shear stress and its standard deviation are shown in Table 5.8.

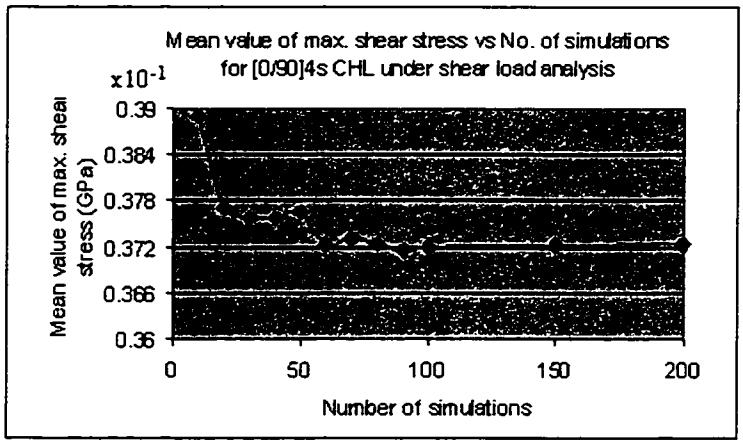

(a)

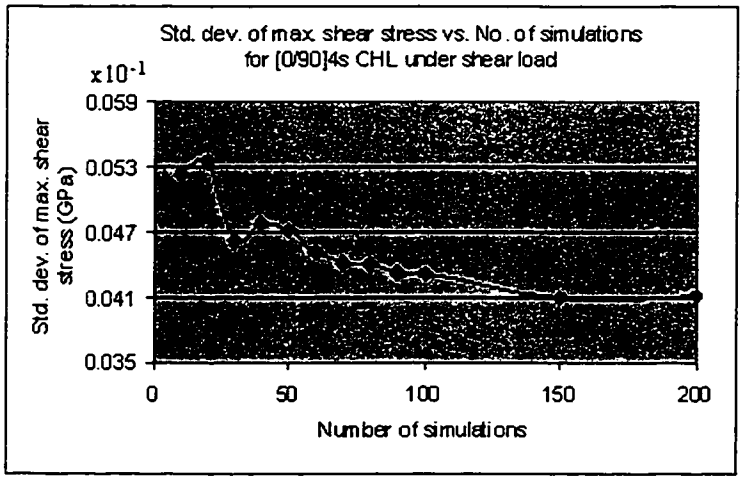

(b)

Figure 5.17 Stress analysis of $[0/90]_{4s}$ controlled hole laminate subjected to shear load: (a) mean value of maximum shear stress, (b) standard deviation value of maximum shear stress.

5.5.1.1 Observations

Convergence in mean value of maximum shear stress occurs at about 200 simulations. The mean value of maximum shear stress developed in the laminate is 0.0372 GPa as shown in Figure 5.17-a. As per the maximum stress criterion, this mean value of maximum shear stress should be less than the average shear strength value of the laminate determined experimentally and it is observed [51] to have a value of 0.0333 GPa. It is seen clearly that the mean value of maximum shear stress obtained from the MATLAB® simulation exceeds the experimentally determined average shear strength value by a greater margin. Thus the laminate is not in the safe design limits. This implies that in the shear load analysis a higher factor of safety has to be imposed on the application of load value.

Reducing the load value by 20 %, which gives a uniformly distributed load value of 0.7088×10^5 N/m, the simulation is carried out. Accordingly the mean value of maximum shear stress and the standard deviation value observed are 0.02954 GPa and 0.005 GPa respectively. Since the mean value of maximum shear stress is below the experimental average shear strength value of 0.0333 GPa, the design is now safe.

5.5.2 Shear analysis of $[0_2/\pm 45]_{2s}$ controlled hole laminate

Stochastic analysis is carried out on a $[0_2/\pm 45]_{2s}$ laminate. All the relevant parameters considered during the analysis of a $[0/90]_{4s}$ laminate are retained in the present analysis. Figure 5.18 shows the stochastic variation of mean and standard deviation values of the shear stress parameter.

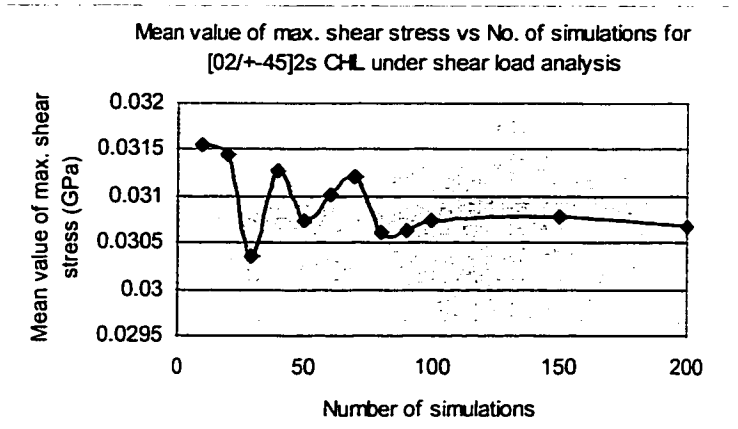

(a)

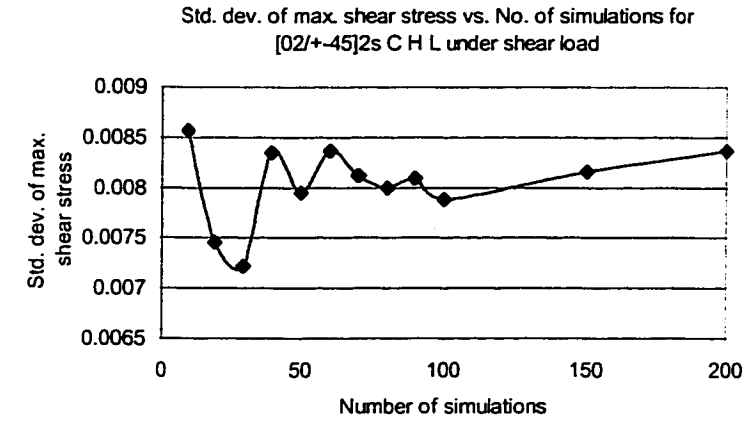

(b)

Figure 5.18 Stress analysis of $[0_2/\pm 45]_{2s}$ controlled hole laminate subjected to shear load: (a) mean value of maximum shear stress, (b) standard deviation value of maximum shear stress.

5.5.2.1 Observations

From Figure 5.18-a, comparing the mean value of maximum shear stress (0.0306 GPa), with the experimentally determined average shear strength value [51] of the laminate (0.0333 GPa), it is clear that, the mean value of maximum shear stress is barely within the limits. Figure 5.18-b shows the standard deviation curve for the shear stress parameter. Since the variation is small, the value corresponding to 200 simulations is taken as the final value, which is 0.0084 GPa.

5.6 Shear analysis of uncontrolled hole laminate

5.6.1 Shear analysis of $[0/90]_{4s}$ uncontrolled hole laminate

As in the previous cases, the effects of the stochastic variation of the material properties and geometric variation on the notched laminate are studied considering an uncontrolled hole laminate subjected to shear load. A layer-wise stress analysis is carried out and the mean value of maximum shear stress developed in the laminate is determined using the simulation process. Figure 5.19 shows the variation of the mean value of maximum shear stress and its standard deviation over the number of simulations under the application of a UDL value of 0.7088 x 10^5 N/m.

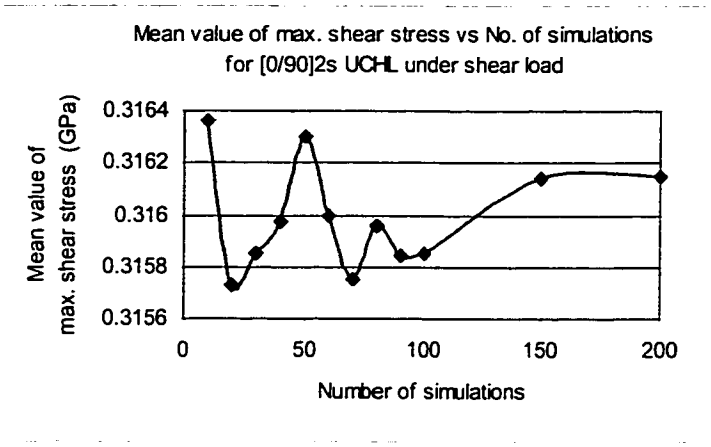

(a)

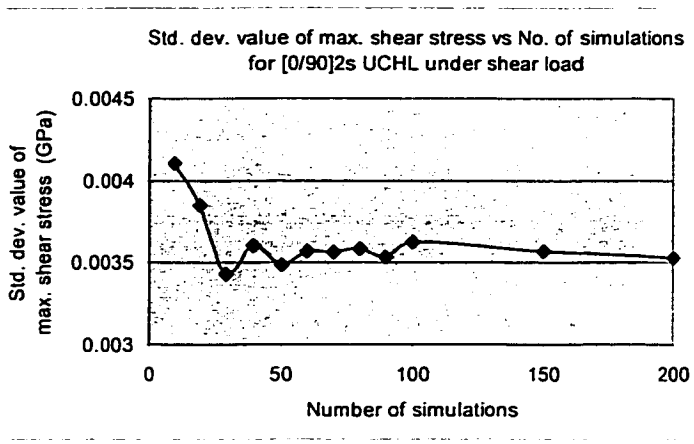

(b)

Figure 5.19 Stress analysis of $[0/90]_{4s}$ uncontrolled hole laminate subjected to shear load: (a) mean value of maximum shear stress, (b) standard deviation value of maximum shear stress.

5.6.1.1 Observations

From Figure 5.19-a, we notice that, after the initial non-linear trend, at about 150 simulations the mean value of maximum shear stress tries to gain a constant value and thus a slight linearity in the curve can be observed. Convergence is achieved at 200 simulations thus attaining a value of 0.0316 GPa and corresponding standard deviation value is 0.0035 GPa. Since the experimentally determined average shear strength value [51] (0.0333 GPa) is high compared to the mean value of maximum shear stress, the laminate is in the safe design limits.

5.6.2 Shear analysis of $[0_2/\pm 45]_{2s}$ uncontrolled hole laminate

In the following section, the variations of the mean values and standard deviations of the shear stress parameter with the number of simulations are discussed. Accordingly Figure 5.20 shows the variation of the parameter for a $[0_2/\pm 45]_{2s}$ laminate.

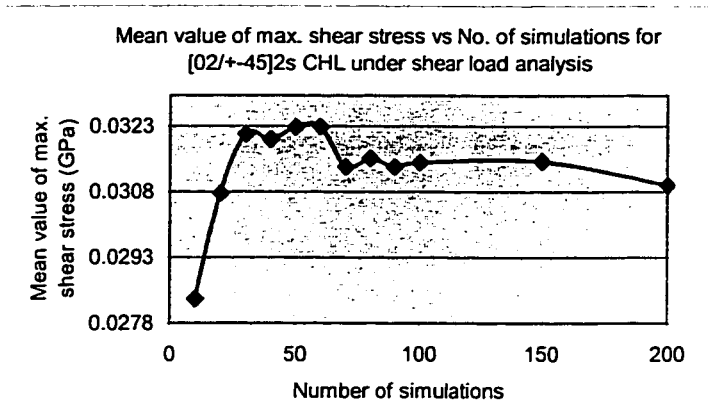

(a)

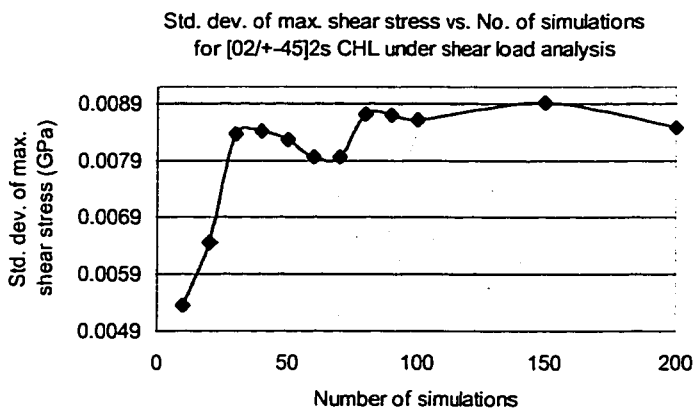

(b)

Figure 5.20 Stress analysis of $[0_2/\pm 45]_{2s}$ uncontrolled hole laminate subjected to shear load: (a) mean value of maximum shear stress, (b) standard deviation value of shear stress.

5.6.2.1 Observations

It is clear from Figure 5.20-a that the convergence of mean value of maximum shear stress occurs at 0.0309 GPa and correspondingly the standard deviation assumes a value of 0.0084 GPa. It can be observed from Table 5.8, that the uncontrolled hole symmetric angle-ply $[0_2/\pm 45]_{2s}$ laminate has a higher value for both the mean and standard

deviation of the shear stress parameter. The mean value of shear stress is within the limits of experimentally determined shear strength value [51] of the laminate.

Laminate Type	Controlled hole laminate		Uncontrolled hole laminate	
	Mean max. shear stress value $(\sigma_{max})\,(GPa)$	Std. dev. of max. shear stress value (GPa)	Mean max. shear stress value $(\sigma_{max})\,(GPa)$	Std. dev. of max. shear stress value (GPa)
$[0/90]_{4s}$	0.02954	0.005	0.0316	0.0035
$[0_2/\pm 45]_{2s}$	0.030	0.008	0.030	0.008

Table 5.8 Comparison of mean and standard deviation values of maximum shear stress corresponding to the controlled and uncontrolled hole laminates.

5.7 Bending analysis of composite laminates

The characterization of deformation of composite laminates is not a trivial task and it calls for a simulation process. For the deformation of laminated structures, the layerwise distribution of mechanical properties in the thickness direction leads to the fact that displacement and transverse-stress fields are continuous, but their derivatives with respect to the thickness co-ordinate at layer interfaces are discontinuous. Modeling of this phenomenon remains a challenging problem. Failure to capture these characteristics will result in unreasonable predictions of stress and strain fields in the analysis of multi-layered composite structures. The evaluations of stress and strain predictions through the laminate thickness, which are critical in the analysis of structural integrity, demand more accurate analysis methods.

The MATLAB® program developed for the bending analysis of a composite laminate is used in the following work for the purpose of simulation. In section 3.2.4.2 an application problem involving the 4-point bending analysis of a composite laminate without a notch

is discussed. But in the following sections, simulation is carried out on notched composite laminates. Thus the existing program has been modified to analyze the stress distribution over the laminate due to the presence of a notch. Since we lack experimental results, pertaining to the maximum bending load a laminate can assume, it is not possible to extend the work based on the average stress criterion. As mentioned in section 5.5, we adopt the maximum stress criterion and determine the in-plane stresses developed in the local axes of the laminate due to the application of an out-of-plane load. Simulation is carried out on symmetric cross-ply $[0/90]_{4s}$ and angle-ply $[0_2/\pm 45]_{2s}$ laminate configurations. It is to be noted that the formulation employs 5 d.o.f. at each and every node.

5.7.1 4-point bending analysis of $[0/90]_{4s}$ controlled hole laminate

In the present analysis, a square cross-ply $[0/90]_{4s}$ notched laminate of dimensions 151.6 x 151.6 mm^2 is subjected to 4-point bending. Two edges of the laminate are completely fixed, thus all the d.o.f. associated with the nodes lying on the two edges of the laminate assume a zero value. Application of the 4-point load (two uniformly distributed line loads) is symmetric about the notch boundary. Since the ultimate load bearing capacity of the laminate is not known, on an arbitrary basis, a uniformly distributed load of 2 MN/m is applied. All the in-plane stress component values are calculated and the stress parameter that is found critical on comparing with the experimentally determined strength value [51] is further analyzed. Thus the probabilistic quantities are calculated concerning the stress in the transverse direction (in 1-2 plane), as the chance of failure of the laminate is more in this direction. Figure 5.21 gives the variation of the mean and

standard deviation values of the in-plane stress along the transverse direction (in 1-2 plane) at the critical location.

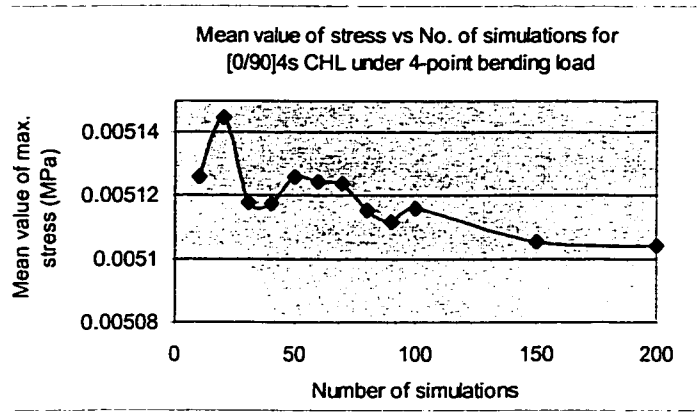

(a)

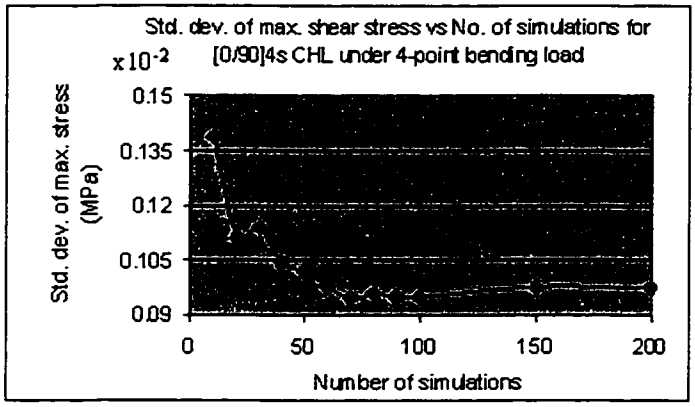

(b)

Figure 5.21 Stress analysis of $[0/90]_{4s}$ controlled hole laminate subjected to 4-point bending: (a) mean values of maximum stress in transverse direction, (b) standard deviation values of maximum stress in transverse direction.

5.7.1.1 Observations

It is observed that the stress in the transverse direction near the hole edge is high in the first ply of the $[0/90]_{4s}$ laminate. It is clear that the top most layer experiences a compressive stress and bottom most layer a tensile stress. The mean value of maximum stress in transverse direction converges at about 200 simulations and the value is 0.0051 MPa. Accordingly the standard deviation value is 0.00097 MPa. It is clear that,

the values attained are extremely low in comparison with the experimentally determined strength in the transverse direction, which is 48.28 MPa. This means to say that, a higher amount of load in the transverse direction can be imposed over the laminate.

5.7.2 4-point bending analysis of $[0_2/\pm 45]_{2s}$ controlled hole laminate

In the present analysis, the uniformly distributed load is assumed to have a value of 2 MN/m. It is the same value as set for the case of $[0/90]_{4s}$ controlled hole laminate. The probabilistic quantities are calculated and their variation is depicted in Figure 5.22.

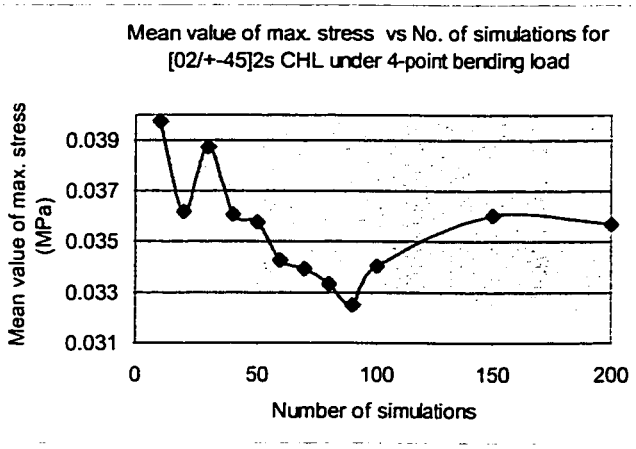

(a)

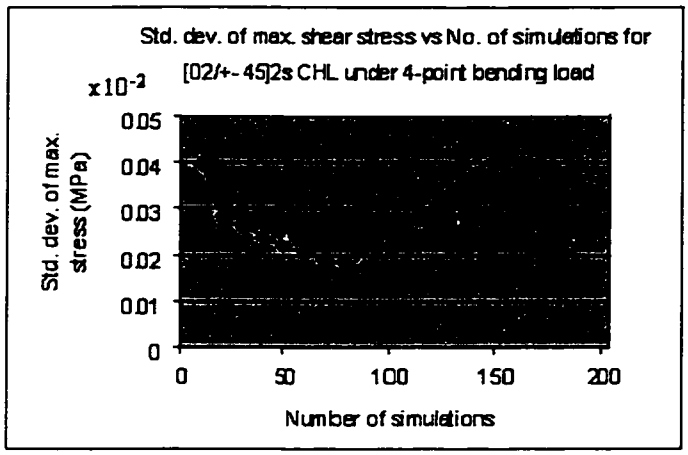

(b)

Figure 5.22 Stress analysis of $[0_2/\pm 45]_{2s}$ controlled hole laminate subjected to 4-point bending: (a) mean values of maximum stress in transverse direction (b) standard deviation values of maximum stress in transverse direction.

5.7.2.1 Observations

It is observed in the $[0_2/\pm 45]_{2s}$ laminate also, that the maximum stress occurs near the hole edge and in the first ply of the laminate. From Figure 5.22-a it is clear that the maximum stress value in the transverse direction for the $[0_2/\pm 45]_{2s}$ laminate converges at about 200 simulations attaining a value of 0.0356 MPa. It is observed that the maximum stress value in the case of $[0_2/\pm 45]_{2s}$ laminate exceeds that of the $[0/90]_{4s}$ laminate for the same amount of load by nearly 7 times. It is evident that, in the bending mode, a cross-ply $[0/90]_{4s}$ laminate can resist more amount of transverse load when compared with an angle-ply $[0_2/\pm 45]_{2s}$ laminate. The standard deviation for the maximum stress in transverse direction as shown in Figure 5.22-b is found to be 0.00036 MPa.

5.7.3 4-point bending analysis of $[0/90]_{4s}$ uncontrolled hole laminate

Simulation is performed on uncontrolled hole laminate to check the influence of the geometric variations on the stress values in the plies. Figure 5.23 gives the variation of the stress values in the transverse direction.

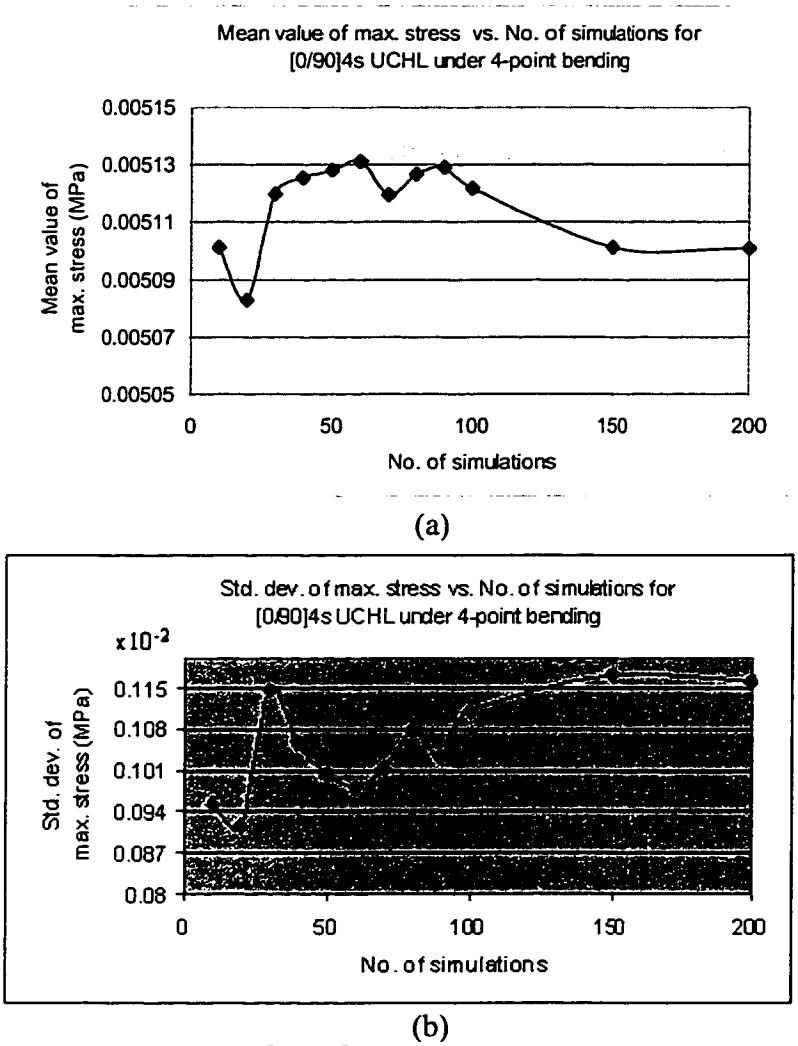

Figure 5.23 Stress analysis of $[0/90]_{4s}$ uncontrolled hole laminate subjected to 4-point bending: (a) mean values of maximum stress in the transverse direction, (b) standard deviation values of stress in the transverse direction.

5.7.3.1 Observations

It is clear that the mean value of maximum stress in transverse direction converges at 200 simulations assuming a value of 0.0051 MPa. It can be seen from Table 5.9 that the achieved mean and standard deviation of maximum stress value in transverse direction for an uncontrolled hole laminate is same as in the case of controlled hole laminate. Thus it is evident that the geometric variations of the hole in a $[0/90]_{4s}$ laminate will not affect the stress distribution over the laminate due to the application of a 4-point bending load.

5.7.4 4-point bending analysis of $[0_2/\pm 45]_{2s}$ uncontrolled hole laminate

The influence of the number of simulations on the probabilistic moments of stress in transverse direction has been studied for an uncontrolled hole $[0_2/\pm 45]_{2s}$ laminate and is shown in Figure 5.24.

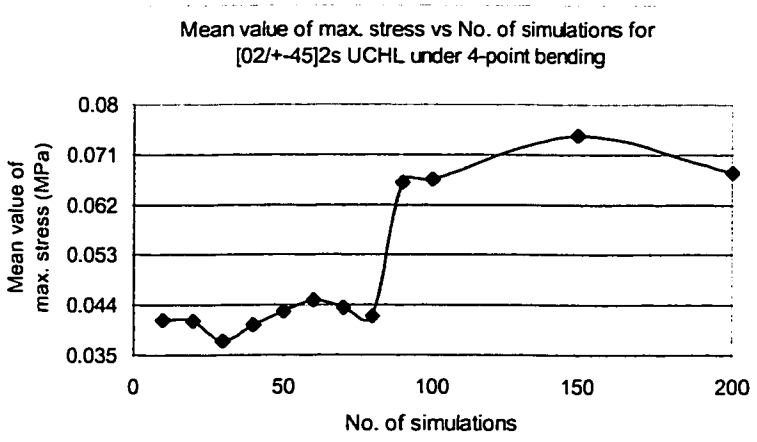

(a)

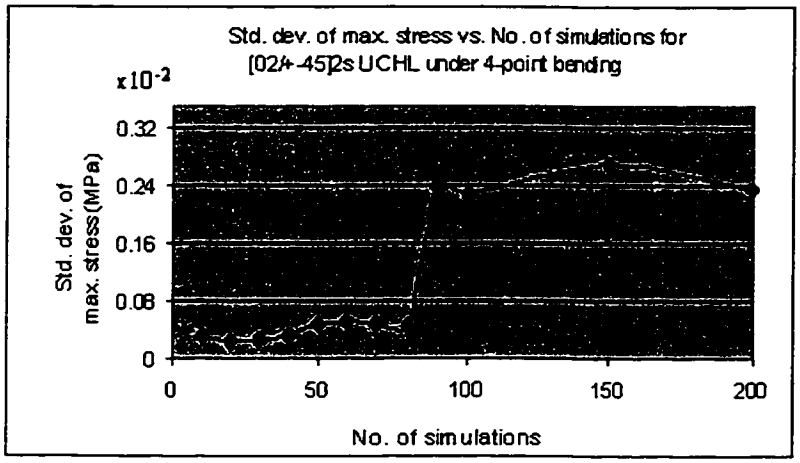

(b)

Figure 5.24 Stress analysis of $[0_2/\pm 45]_{2s}$ uncontrolled hole laminate subjected to 4-point bending: (a) mean values of maximum stress in transverse direction, (b) standard deviation values of maximum stress in transverse direction.

5.7.4.1 Observations

Simulation is carried out on an uncontrolled hole $[0_2/\pm 45]_{2s}$ laminate subjected to 4-point bending load. From Figures 5.24-a and 5.24-b it is observed that both the curves follow a similar trend. The fluctuations persist even after 200 simulations for both the quantities. A drastic increase in the mean value of the maximum stress is noticed at about 200 simulations. This is true for the standard deviation value also. But for further discussions, values corresponding to 200 simulations are taken as the convergence value. Thus the mean value of maximum stress in transverse direction is 0.0677 MPa and standard deviation value is 0.00234 MPa.

Laminate Type	Controlled hole laminate		Uncontrolled hole laminate	
	Mean value of max. stress in transverse direction (σ_{max}) (MPa)	Std. dev. value of max. stress in transverse direction (MPa)	Mean value of max. stress in transverse direction (σ_{max}) (MPa)	Std. dev. value of max. stress in transverse direction (MPa)
$[0/90]_{4s}$	0.0051	0.00097	0.0051	0.00115
$[0_2/\pm 45]_{2s}$	0.0356	0.0035	0.0677	0.00234

Table 5.9 Comparison of mean value of maximum stress in transverse direction corresponding to the controlled and uncontrolled hole laminates under 4-point bending

Comparing the values from Table 5.9, the difference in the maximum stress values corresponding to controlled and uncontrolled hole $[0/90]_{4s}$ laminate is not significant. But an uncontrolled hole $[0_2/\pm 45]_{2s}$ laminate exhibits a higher stress value as opposed to a controlled hole $[0_2/\pm 45]_{2s}$ laminate.

5.8 Conclusions and discussions

In this chapter a thorough numerical investigation is performed on notched composite laminates to study their behavior using random fields for different material and physical properties to determine the probabilistic quantities of the stress parameters. Analysis is made for two laminate configurations: a symmetric cross-ply $[0/90]_{4s}$ and an angle-ply $[0_2/\pm 45]_{2s}$ laminate respectively.

In each of the laminate configurations, two separate cases of notched laminates are dealt with: controlled hole and uncontrolled hole laminate cases. Controlled hole laminates exhibit only the stochastic variation of material properties over the laminate, but

uncontrolled hole laminate contains both stochastic variation of material properties as well as geometric variation of the hole. In addition to these variations, an eccentricity of the hole is also assumed. Accordingly the value of characteristic length for the laminate follows a stochastic variation, which is brought about using Gaussian distribution method.

Simulation results showed that, as the number of iterations is increased, a better convergence of the probabilistic quantities is achieved. It is also shown that the mean and standard deviation values converge in between 200 to 300 simulations for both the configurations.

Different load conditions are imposed on the laminates i.e. uniaxial tensile load, biaxial load, shear load, and bending load. The probabilistic quantities for the stress parameters are calculated. Equivalent stress value is found out by averaging the stresses over the value of characteristic length obtained through a number of tests conducted on both the laminate configurations in the uniaxial load case.

Since the ultimate tensile load value for un-notched laminate is known for both the laminate configurations $[0/90]_{4s}$ and $[0_2/\pm 45]_{2s}$, average stress criterion is employed to find out the equivalent stress values for both the uniaxial and biaxial load cases. But the above-mentioned criterion is not viable for shear and bending analyses. Thus, maximum stress criterion is used in shear and bending analyses and accordingly the stress parameters are calculated and compared with the experimentally determined strength values of the laminate.

Considering the cross-ply $[0/90]_{4s}$ laminate configuration, the equivalent stress and maximum stress values of the uncontrolled hole laminate under uniaxial and biaxial load conditions exceed the corresponding values of the controlled hole laminate. Observations indicate that, the mean value of maximum shear stress determined under shear load and mean value of maximum stress in the transverse direction determined under bending load also show a similar trend. Similar conclusions can be derived for $[0_2/\pm 45]_{2s}$ laminate configuration also. The increase in the stress value is attributed to the geometric variation of the hole, eccentricity of the hole and variation in the value of characteristic length, which are the additional features that an uncontrolled hole laminate exhibits in addition to stochastic variation of material properties. Further the reliability indices for both the laminate configurations are found out and are presented in chapter 6.

Chapter 6

Reliability Analysis of Notched Composite Laminates

6.1 Introduction

Composite structures can develop local failures or exhibit local damage such as matrix cracks, fiber breakage, fiber-matrix debonds, and delaminations under fundamental loading conditions such as tensile, compressive, shear, bending and twisting which may contribute to their failure. It is shown in the previous chapter that the performance of a composite laminate with an opening differs from one laminate to another laminate configuration under various loading circumstances. Thus it becomes necessary to choose the best laminate configuration for a specific loading condition. At the same time decision has to be taken on reliability of the laminate for worthiness of intended application. *"Reliability is defined [66] as the probability that a component or device or system will achieve a specified life without failure under a given loading".*

It is to be noted that in order to evaluate the reliability of any structure, two parameters are required, for instance, one representing the strength and the other representing the stress developed due to the external loading. In the present case, equivalent stress (σ_{equ}) and maximum stress (σ_{max}) of a notched laminate are used as parameters for evaluating

the probabilistic reliability of anisotropic laminates with respect to stress applied (σ_o) over an un-notched laminate.

6.2 Strength distribution of composite laminates

The analysis and design of composite structures require the input of reliable experimental data. One of the major objectives of testing composite materials is the determination of the un-notched and notched laminate strength values and hence the exact distribution of characteristic length data for individual laminates.

Probability distribution arises from experiments where the outcome is subject to chance. The nature of the experiment, dictates which probability distribution may be appropriate for modeling the resulting random outcomes. In the present work, the Gaussian distribution method is used to generate probability density function (PDF) for the stress parameters and hence to calculate the reliability. Probability density function is the basic tool for codifying and communicating uncertainty about the value of a continuously varying variable. This information together with the distribution of the (σ_{ave}) obtained using the stochastic finite element analysis can then be used to determine the reliability of the laminate.

6.3 Stress distribution in notched laminates

The main purpose of stochastic analysis when both the parameters i.e. equivalent stress (σ_{equ}) and applied stress on un-notched laminate (σ_o) are involved, is to determine the reliability considering both the distributions which are known at a critical location in the

component. The distributions followed by each of these two representatives might be quite different from each other and they can be represented as

$$F_1 = A\left(\mu_{\sigma_{equ}}, s_{\sigma_{equ}}\right) \quad \text{and} \quad F_2 = B\left(\mu_{\sigma_0}, s_{\sigma_o}\right) \tag{6.1}$$

in which A and B represent the two different distributions followed by (σ_{equ}) and the (σ_o) respectively.

6.4 Gaussian distribution

The Gaussian distribution is a very important statistical distribution. It is an approximation to the distribution of values of a characteristic. The exact shape of the normal distribution depends on the mean and the standard deviation of the distribution. The standard deviation is a measure of spread and indicates the amount of departure of the values from the mean. All normal distributions are symmetric and have bell-shaped density curves with a single peak and tails go to infinity at both ends. The probability density function of the normal distribution is given by [67].

$$f(x) = \frac{1}{\sigma\sqrt{2\pi}} \exp^{\left(-(x-\mu)^2/2\sigma^2\right)} \quad , -\infty < x < \infty \tag{6.2}$$

where

μ is the mean value

σ is the standard deviation

We have here two populations, a population of strengths and a population of stresses. If we assume that both are normally distributed, there is a possibility that the forward tail of the stress distribution may overlap the rearward tail of the strength distribution and the

result is some failures. To determine the reliability, we combine both populations, and compute the standardized variable z_R. Corresponding standardized variable z_R is,

$$z_R = \frac{\mu}{\sigma} = \frac{\mu_{\sigma_o} - \mu_{\sigma_{equ/\max}}}{\sqrt{\sigma_{\sigma_o}^2 + \sigma_{\sigma_{equ/\max}}^2}} \tag{6.3}$$

where

μ_{σ_o} is the mean value of stress applied over the un-notched laminate, $\mu_{\sigma_{equ/\max}}$ is the mean value of equivalent stress or the mean value of maximum stress of a notched laminate, σ_{σ_o} is the standard deviation value of the applied stress over the un-notched laminate and $\sigma_{equ/\max}$ is the standard deviation value of the equivalent stress or maximum stress of a notched laminate.

Entering the value z_R in Table A-10 [67] the area under the normal distribution curve corresponding to the combined population is found out. Equation (6.3) enables us to determine the standardized variable z_R corresponding to any desired reliability. Life of the laminate is recognized as a random variable, and the reliability function is related to the standardized variable by,

$$R = 1 - z_R \tag{6.4}$$

6.5 Reliability calculation

In this chapter two laminate configurations i.e. $[0/90]_{4s}$ and $[0_2/\pm 45]_{2s}$ are analyzed by subjecting them to uniaxial load condition. To have a better understanding on the load bearing capacity of the laminates, how reliable and safe the design is, laminates are loaded with different values of factor of safety on the ultimate load and stochastic simulation is performed.

6.5.1 Reliability of $[0/90]_{4s}$ laminate under uniaxial load

As an example, a $[0/90]_{4s}$ laminate configuration is considered for the stochastic simulation. Both the controlled and uncontrolled hole laminate cases are analyzed by subjecting them to uniaxial tensile load. Probabilistic quantities such as mean and standard deviation values of equivalent stress (σ_{equ}) parameter considered for the judgment of failure of laminate are calculated. Section 6.4 provides a detailed description of the calculation of reliability based on the Gaussian distribution method. Proceeding in a similar manner, reliability is calculated for both controlled and uncontrolled hole laminates and is presented in the last column of Tables 6.1 to 6.4.

The effect of decreasing the factor of safety on the area of interference, obtained by superposition of distribution curves of equivalent stress and un-notched laminate strength is shown pictorially in Figures 6.2 and 6.3. Figure 6.2 shows the distribution curves developed for the two stress parameters at a factor of safety value of 1.2 for an uncontrolled hole $[0/90]_{4s}$ laminate subjected to uniaxial tensile load. Figure 6.3 shows

the distribution curves developed for the two stress parameters at a factor of safety value of 1.1 for an uncontrolled hole $[0/90]_{4s}$ laminate.

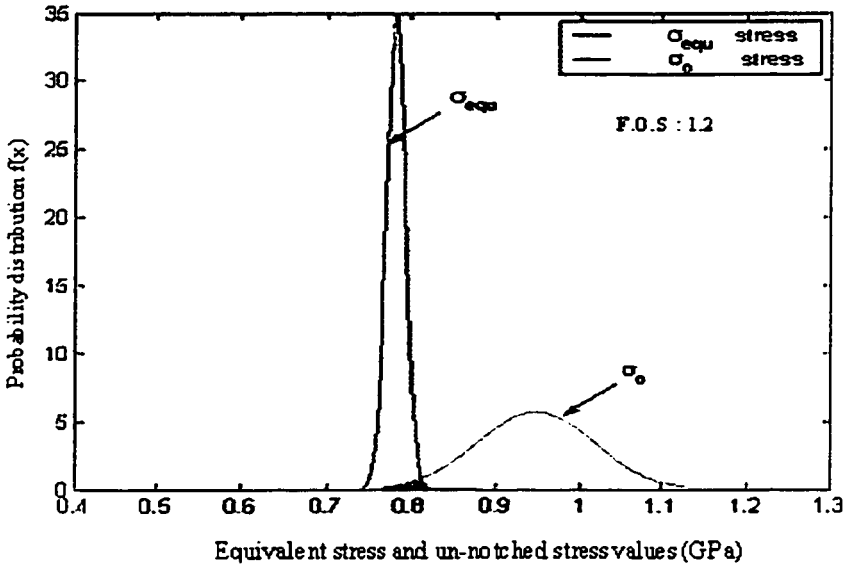

Figure 6.1 Area of interference at a factor of safety (F.O.S) of 1.2

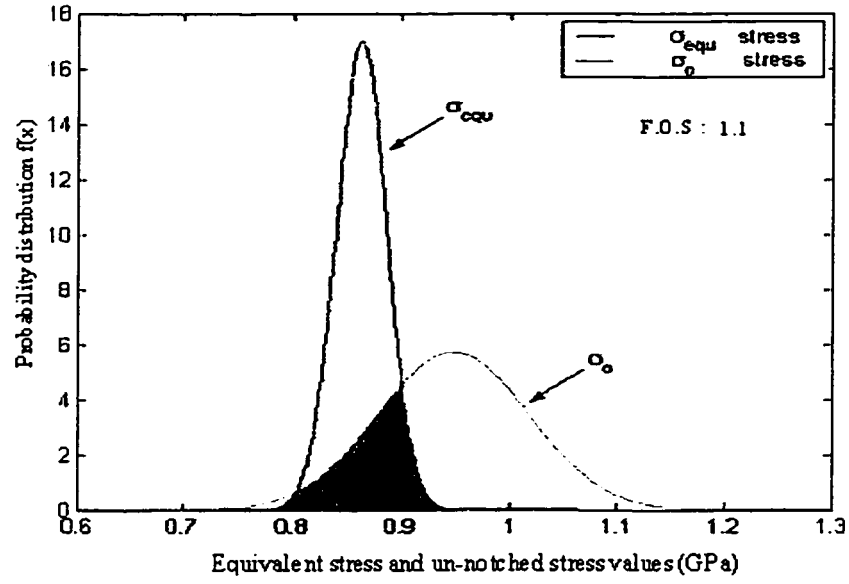

Figure 6.2 Area of interference at a factor of safety (F.O.S) of 1.1

From Figures 6.1 and 6.2, it is seen that for a factor of safety of 1.2, the area of interference between the two stress parameters is less than the area of interference when factor of safety is 1.10. Thus by increasing the factor of safety, it is possible to make the area of interference to be close to zero, thus preventing the failure that might be caused while in use.

Table 6.1 lists the values associated with a controlled hole laminate and Table 6.2 contains the values pertaining to uncontrolled hole laminate. In these tables R_{equ} refers to the reliability calculated using the equivalent stress parameter.

Factor of safety (F.O.S)	Load (MN/m)	$\mu_{equ}\ (GPa)$	$\sigma_{equ}\ (GPa)$	R_{equ}
1.45	0.886	0.6910	0.0323	99.99
1.20	1.060	0.7821	0.0114	99.08
1.15	1.113	0.8265	0.0189	95.45
1.10	1.160	0.8633	0.0235	87.70
1.05	1.219	0.9091	0.0249	70.19
1.00	1.280	0.9381	0.0393	55.17

Table 6.1 Reliability of $[0/90]_{4s}$ controlled hole laminate under uniaxial load condition

Factor of safety (F.O.S)	Load (MN/m)	μ_{equ} (GPa)	$\sigma_{equ}\ (GPa)$	R_{equ}
1.45	0.886	0.7310	0.0405	99.65
1.20	1.060	0.8111	0.0931	88.11
1.15	1.113	0.8450	0.0885	81.86
1.10	1.160	0.8884	0.0948	69.50
1.05	1.219	0.9222	0.0725	60.26
1.00	1.280	0.9411	0.0362	53.59

Table 6.2 Reliability of $[0/90]_{4s}$ uncontrolled hole laminate under uniaxial load condition

Using the values from Tables 6.1 and 6.2, a plot of tensile load along x-axis and reliability along y-axis is prepared and this is shown in Figure 6.3.

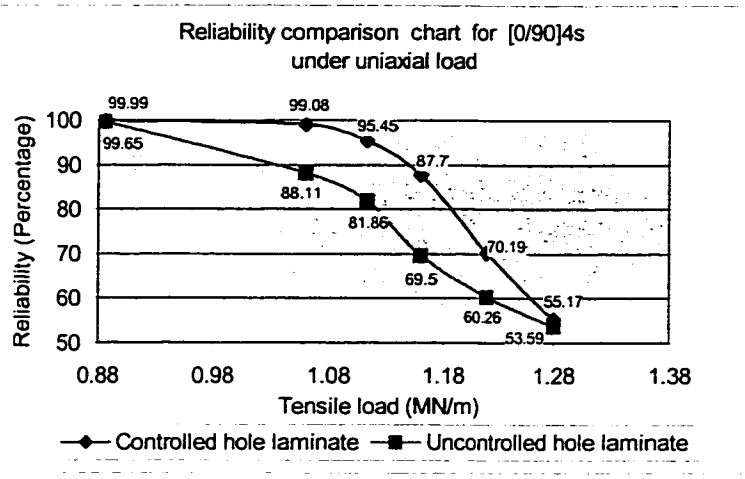

Figure 6.3 Plot of reliability curves for controlled and uncontrolled hole laminates for $[0/90]_{4s}$ laminate configuration

From Figure 6.3, it is evident that the reliability of the uncontrolled hole laminate has reduced drastically from the controlled hole laminate case and is predominantly seen between the factor of safety values of 1.45 and 1.05. Thus it is not advisable to consider the ideal controlled hole laminate condition in practical applications subjected to uniaxial tensile load. The geometry perturbation around the circumference of the hole, eccentricity of the hole and stochastic variation in the material properties together enhance the stresses around the hole region of the laminate. This in turn increases the probability of failure of the laminate. Thus, proper precautions are to be taken while designing a symmetric $[0/90]_{4s}$ laminate in tensile mode, as it fails much earlier than expected.

6.5.2 Reliability of $[0_2/\pm 45]_{2s}$ laminate under uniaxial load

The stochastic simulation is carried out on a laminate of $[0_2/\pm 45]_{2s}$ configuration. Reliability is calculated by slowly increasing the uniaxial distributed tensile load acting on the laminate. Analysis is carried out on both controlled and uncontrolled hole laminates. Once again the mean and standard deviation values of equivalent stress (σ_{equ}) parameter are found out. Table 6.3 lists the probabilistic parameter values associated with a controlled hole laminate and Table 6.4 contains the values obtained for uncontrolled hole laminate.

Factor of safety (FOS)	Load (MN/m)	$\mu_{equ}\ (GPa)$	$\sigma_{equ}\ (GPa)$	R_{equ}
1.45	1.131	0.6726	0.0211	100.0
1.20	1.366	0.6914	0.0169	100.0
1.15	1.426	0.8500	0.0084	99.9
1.10	1.490	0.9217	0.0125	92.2
1.05	1.561	0.9667	0.0011	62.9
1.00	1.640	1.0287	0.0266	14.9

Table 6.3 Reliability of $[0_2/\pm 45]_{2s}$ controlled hole laminate under uniaxial load condition

Factor of safety (FOS)	Load (MN/m)	$\mu_{equ}\ (GPa)$	$\sigma_{equ}\ (GPa)$	R_{equ}
1.45	1.131	0.6930	0.0314	100.0
1.20	1.366	0.8470	0.0423	99.7
1.15	1.426	0.8943	0.0253	96.7
1.10	1.490	0.9763	0.0469	51.9
1.05	1.561	0.9914	0.0038	38.2
1.00	1.640	1.0297	0.0236	15.6

Table 6.4 Reliability of $[0_2/\pm 45]_{2s}$ uncontrolled hole laminate under uniaxial load condition

Figure 6.4 depicts a plot of tensile load shown along the x-axis and reliability along the y-axis. The values listed in Tables 6.3 and 6.4 are used in achieving the following plot.

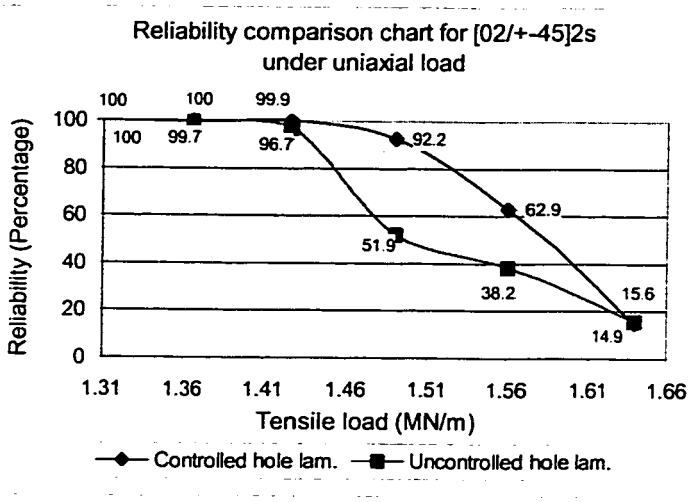

Figure 6.4 Plot of reliability curves for controlled and uncontrolled hole laminates for $[0_2/\pm 45]_{2s}$ laminate configuration

Observing Figure 6.4, it is clear that the reliability of the controlled hole laminate and the reliability of the uncontrolled hole laminate assume a similar path till a uniformly distributed load of 1.426 MN/m is reached. Later on, with the increase in load value, the two curves diverge and this trend is observed till a load value of 1.561 MN/m is imposed on the laminate. Increasing the load value further, both the curves indicate nearly the same reliability. Also, it can be observed that the gradient of the reliability curve for controlled hole laminate stabilizes after 1.426 MN/m load value and the variation follows an almost linear trend. Contrarily the reliability curve for uncontrolled hole laminate assumes a downward slope and with the increase in load attains a better reliability value. Thus in the design of $[0_2/\pm 45]_{2s}$ laminate the region between 1.426 MN/m and 1.64

MN/m load value is considered to be sensitive and care must be taken to include the reduction in the reliability.

6.6 Conclusion and discussions

In the present chapter a reliability study is conducted on $[0/90]_{4s}$ and $[0_2/\pm 45]_{2s}$ laminate configurations. A stochastic simulation is carried out on both the laminates subjected to uniaxial and biaxial load conditions. A safety factor value is assumed on the ultimate load bearing capacity of the laminate and stochastic finite element analysis is carried out. The standardized variable calculation is made using Gaussian distribution method and hence the reliability is found out. A series of reliability values are obtained by varying the safety factor value. Following observation is made on both controlled hole laminate and uncontrolled hole laminate cases.

From the Figures 6.3 and 6.4, we can see that for $[0/90]_{4s}$ and $[0_2/\pm 45]_{2s}$ laminates under uniaxial load mode, the uncontrolled hole laminate provides a lesser reliability as against controlled hole laminate. The effect is more predominantly seen in $[0_2/\pm 45]_{2s}$ laminate with a maximum reduction in the reliability by 40.3% over the load range. Thus while designing the laminates precautions must be taken to consider this reduction in reliability, which can be solely attributed to the geometric variation around the hole region and to the eccentricity of the hole from the center. Further, the reliability calculations can be extended to other load conditions employed in the present thesis.

Chapter 7

Conclusions and Recommendations

In the present thesis work, stress distributions in notched isotropic plate and notched composite laminate are determined using the stochastic finite element methodology. A MATLAB® code is developed, which reflects the stochastic variation of the material properties and imposes the geometric variation on the laminates. The program is capable of handling both the in-plane and out-of-plane load analyses. First order shear deformation theory is adopted to take care of the transverse shear deformation in the laminates.

The flowchart of the program is shown in Chapter 2, which performs the in-plane analysis for a number of simulated laminates and returns the mean and standard deviation values of the stress parameter. Program validation is demonstrated using suitable example problems on different laminates at appropriate stages. Similarly, the program validation is performed for an out-of-plane load analysis in Chapter 3.

The present work considers two laminate configurations to study the stress concentration effects on the notched laminates: Symmetric cross-ply laminate $[0/90]_{4S}$ and angle-ply laminate $[0_2/\pm 45]_{2S}$. The value of characteristic length is calculated based on the average stress criterion. An extensive experimental investigation is performed on notched

and un-notched coupons subjected to uniaxial tensile test. Coupons are prepared using NCT-301 graphite-epoxy and corresponding ultimate tensile load values are recorded. It is observed that, the ultimate tensile load bearing capacity for an angle-ply laminate $[0_2/\pm 45]_{2s}$ is more in both notched and un-notched laminate categories when compared with a cross-ply laminate $[0/90]_{4s}$.

Stochastic simulation is performed on the laminates subjected to various loading conditions viz. uniaxial load, biaxial load, shear load and bending load. The mean and standard deviation of equivalent and maximum stress parameters are calculated for uniaxial and biaxial load cases. It is found that, the uncontrolled hole laminate develops higher stress values due to the presence of the geometric variation in the radius of the hole and eccentricity of the hole from hole center in addition to the stochastic variation of material properties. A layer-wise analysis is performed in shear and bending load cases, as average stress criterion is not applicable. Thus maximum stress criterion is employed. Shear stress and stress in the transverse direction are calculated for shear load and bending load analysis respectively. It is observed that an uncontrolled hole laminate possesses higher stress value as against controlled hole laminate in shear and bending load analysis also. Observations indicate that, a $[0/90]_{4s}$ laminate can resist higher bending load when compared with $[0_2/\pm 45]_{2s}$ laminate.

Finally in Chapter 6, reliability study is conducted. The Gaussian distribution is used to model the distribution of a set of randomly distributed values. The distributions thus obtained are used to compute the reliability of the orthotropic laminates under uniformly distributed tensile load. The reliability graph depicting the variation in the reliability of

the laminate with the change in the applied load is obtained for both controlled and uncontrolled hole laminates. It is observed that the uncontrolled hole $[0_2/\pm 45]_{2s}$ laminate experiences a sudden reduction in the reliability value, when a factor of safety of 1.15 on the ultimate load is imposed under uniaxial tensile load. But the reliability curve for an uncontrolled hole $[0/90]_{4s}$ laminate runs almost parallel to the controlled hole laminate but with a considerable reduction in the reliability value.

The thesis can be further extended on the following topics, which will constitute the future research work:

* A three-dimensional model can be developed which offers better features in the analysis and thus helps in arriving at a more accurate result.

* Analysis can be extended to different types of notch opening shapes in the laminate such as elliptical and triangular shapes.

* Further, testing can be conducted on a laminate having a configuration of $[0/90/\pm 45]_{2s}$ which brings in a combination of $0^o, 90^o$, *and* $\pm 45^o$ ply orientations.

* Reliability charts for the cases involving biaxial, shear and bending loads can be developed.

References

[1] Tan, S.C., *Stress Concentrations in Laminated Composites*, 1994, Technomic Publishing Company, Lancaster.

[2] Muskhelishvili, N.I, *Some Basic Problems of Mathematical Theory of Elasticity*, 1954, Published by Academy of Sciences of the USSR.

[3] Lekhnitskii, S.G, *Anisotropic Plates*, Translated from the Second Russian Edition by Tsai., S.W. and Cheron, T., 1968, Gordon and Breach, New York.

[4] Savin, G.N., *Stress Concentration Around Holes*, Translated by Eugene Gros for the Department of Scientific and Industrial Research and made available by the Department for publication in book form. Translation Editor: W. Johnson, 1961, Pergamon Press, New York.

[5] Green, A.E., "Stress systems in isotropic and aelotropic plates V ", Proceedings of Royal Society of London, Series A, Vol. 184, 1945, pp. 231-288.

[6] Greszczuk, L.B., "Stress concentrations and failure criteria for orthotropic and anisotropic plates with circular openings", Composite Materials: Testing and Design (Second Conference), ASTM STP 497, ASTM, 1972, pp. 363-381.

[7] Fischer, L., "How to predict structural behavior of RP laminates", Modern Plastics, 1960, pp. 122-209.

[8] Hayashi, T., "Stress analysis of the anisotropic plate with a hole under the uniaxial loading". Composites'86: Recent Advances in Japan and the US, U.S.C.C.M -III, Editors: Kawata, K., Umekawa, S. and Kobayashi, A., Tokyo 1986, pp. 197-204.

[9] Jong, T.D., "Stresses around rectangular holes in orthotropic plates", Journal of Composite Materials, Vol. 15, 1981, pp. 311-328.

[10] Hwu, C., "Anisotropic plates with various openings under uniform loading or pure bending", Journal of Applied Mechanics, Trans. ASME, Vol. 57, 1990, pp. 700-706.

[11] Hufenbach, W., Schafer, M. and Herrmann, A.S., "Calculation of the stress and displacement field of anisotropic plates with elliptical hole", Ingenieur-Archiv, Vol. 60, 1990, pp. 507-517.

[12] Daoust, J. and Hoa, S.V., "An analytical solution for anisotropic plates containing triangular holes", Computers and Structures, Vol. 19, 1991, pp. 107-130.

[13] Ukadgaonker, V.G. and Rao, D.K.N., "Stress distribution around triangular holes in anisotropic plates", Computers and Structures, Vol. 45(3), pp. 171-183.

[14] Theocaris, P.S. and Petrou, J., "Stress distributions and intensities at corners of equilateral triangular holes", International Journal of Fracture, Vol. 31, 1986, pp. 271-289.

[15] Theocaris, P.S. and Petrou, L., "From the rectangular hole to the ideal crack", International Journal of Solids and Structures, Vol. 25(3), 1989, pp. 213-233.

[16] Ukadgaonker, V.G. and Awasare, P.J., "A novel method of stress analysis of an infinite anisotropic plate with elliptical hole or crack with uniform tensile stress", Journal of Institution of Engineers (India), Vol. 75, 1994, pp. 53-55.

[17] Ukadgaonker, V.G. and Awasare, P.J., "A novel method of stress analysis of an infinite plate with small radius equilateral triangular hole", Journal of Institution of Engineers (India), Vol. 73, 1993, pp. 312-317.

[18] Ukadgaonker V.G, Awasare P.J., "A novel method of stress analysis of an infinite plate with rounded corners of a rectangular hole under uniform edge loading", Indian Journal of Engineering and Material Science, Vol. 1, 1994, pp. 17-25.

[19] Simha, K.R.Y. and Mahapatra, S.S., "Stress concentration around irregular holes using complex variable method", Sadhana (India), Vol. 23(4), 1998, pp. 393-412.

[20] Cheng, Y.F., "Elastic properties and stress concentrations at a hole in some composite laminates", Fibre Science and Technology, Vol. 8, 1975, pp. 145-163.

[21] Shastry, B.P and Rao, G.V., "Effect of fiber orientation on stress concentration in a unidirectional tensile laminate of finite width with a central circular hole", Fibre Science and Technology, Vol. 10, 1977, pp. 151-154.

[22] Tan, S.C., "Notched strength prediction and design of laminated composites under in-plane loadings", Journal of Composite Materials, Vol. 21, 1987, pp. 750-780.

[23] Tan, S.C., "Laminated composites containing an elliptical opening. II. Experiment and model verification", Journal of Composite Materials, Vol. 21, 1987, pp. 949-968.

[24] Lin, J. and Ueng, C.E.S., "Stresses in laminated composites containing two elliptical holes", Composite Structures, Vol. 7, Elsevier Applied Science, London, Chapter 2, 1987, pp. 1-20.

[25] Fan, W. and Wu, J., "Stress concentration of a laminate weakened by multiple holes", Composite Structures, Vol. 10, 1988, pp. 303-319.

[26] Tan, S.C., "Finite-width correction factor for anisotropic plate containing a central opening", Journal of Composite Materials, Vol. 23(11), 1988, pp. 1088-1097.

[27] Rowlands, R.E., Daniel, I.M. and Whiteside, J.B., "Geometric and loading effects on strength of composite plates with cutouts", Composite Materials: Testing and Design, ASTM STP 546, American Society for Testing and Materials, 1974, pp. 361-375.

[28] Awerbuch, J. and Madhukar, M.S., "Notched strength of composite laminates: Predictions and experiments – A review", Journal of Reinforced Plastics and Composites, Vol. 4, 1985, pp. 3-59.

[29] Greszczuk, L.B., "Shear-modulus determination of isotropic and composite materials", Composite Materials: Testing and Design, ASTM STP 460, 1969, pp. 140-149.

[30] Petit, P.H., "A simplified method of determining the in-plane shear stress-strain response of unidirectional composites", Composite Materials: Testing and Design, ASTM STP 460, 1969, pp. 83-93.

[31] Whitney, J.M, Stansbarger, D.L. and Howell, H.B., "Analysis of the rail shear test - applications and limitations", Journal of Composite Materials, Vol.5, 1971, pp. 24-34.

[32] Herakovich, C.T, Bergner, H.W. and Bowles, D.E., "A comparative study of composite shear specimens using the finite-element method", Test Methods and Design Allowables for Fibrous Composites, ASTM STP 734, 1981, pp. 129-151.

[33] Goodier, J.N., "The influence of circular and elliptical holes on the transverse flexure of elastic plates", Philosophical Magazine, Series 7, Vol. 22, 1936, pp. 69-80. (Referred in [34])

[34] Reissner, E., "The effect of transverse shear deformation on the bending of elastic plates", Journal of Applied Mechanics, Trans. ASME, Vol. 12, 1945, pp. A69-77.

[35] Naghdi, P.M., "Effect of elliptic holes on the bending of thick plates", Journal of Applied Mechanics, Trans. ASME, Vol. 22, 1955, pp. 89-94.

[36] Lee, C.W. and Conlee, G.D., "Bending and twisting of thick plates with a circular hole", Journal of Franklin Institute, Vol. 285(5), 1968, pp. 377-385.

[37] Chen, P.S and Archer, R.R., "Stress concentration factors due to bending of a thick plate with a circular hole", Ingenieur-Archiv, Vol. 59, 1989, pp. 401-411.

[38] Hoffman, O., "The brittle strength of orthotropic materials", Journal of Composite Materials, Vol. 1, 1967, pp. 200-206.

[39] Cowin, S.C., "On the Strength Anisotropy of Bone and Wood", Journal of Applied Mechanics, Vol. 46, 1979, pp. 832-838.

[40] Contreras, N., "The stochastic finite element method," Computers and Structures, Vol.12, 1980, pp. 541-548.

[41] Vanmarcke, E. and Grigoriu, M., "Stochastic finite element analysis of simple beams," ASCE, Journal of Engineering Mechanics, Vol. 109, 1983, pp.1203 – 1214.

[42] Yamazaki, F., Shinozuka, M. and Dasgupta, G., "Neumann expansion for stochastic finite element analysis," ASCE Journal of Engineering Mechanics, Vol.111, 1985, pp. 1335-1357.

[43] Ganesan, R. and Haque, Z., " Stochastic characteristics of fracture in laminated composites", Proceedings of the Third Joint Canada-Japan Workshop on

Composites, Edited by Hoa, S.V., Hamada, H., Lo, J. and Yokoyama, A., 2000, Technomic Publishing Company, Lancaster.

[44] Ganesan, R. and Pondugala, L.V.P., "Stochastic J-integral of laminated composites based on an efficient finite element analysis methodology", Advances in Composite Materials and Structures VII, 2000, WIT Press, Southampton.

[45] Waddoups, M.E., Eisenmann, J.R. and Kaminski, B.E., "Macroscopic fracture mechanics of advanced composite materials", Journal of Composite Materials, Vol. 5, 1971, pp. 446-454.

[46] Whitney, J.M. and Nuismer, R.J., "Stress fracture criteria for laminated composites containing stress concentrations", Journal of Composite Materials, Vol.8, 1974, pp. 253-265.

[47] Cook, R.D., Malkus, D.S. and Plesha, M.E., *Concepts and Applications of Finite Element Analysis*, 1989, John Wiley & Sons, N.Y.

[48] Timoshenko, S., *Strength of Materials*, Third Edition, 1956, D.Van Nostrand Company, N.Y.

[49] Boresi, A.P. and Sidebottom, O.M., *Advanced Mechanics of Materials*, Fourth Edition, 1985, John Wiley & Sons, N.Y.

[50] Tan, S.C, "Mixed-Mode fracture of notched composite laminates under uniaxial and multiaxial loading", Engineering Fracture Mechanics, Vol.31, 1988, pp. 733-746.

[51] Lakshmi Vara Prasad Pondugala, "Stochastic J-integral and reliability of composite laminates based on a computational methodology combining

experimental investigation, stochastic finite element analysis and maximum entropy method", June 2000, M.A.Sc Thesis, Concordia University.

[52] Md. Zakiul Haque, "A combined experimental and stochastic finite element analysis methodology for the probabilistic fracture behavior of composite laminates", December 1999, M.A.Sc Thesis, Concordia University.

[53] William, W.F., "A failure criterion for composite materials", Journal of Composite Materials, Vol. 25, 1991, pp. 88-100.

[54] Vanmarcke, E., Shinozuka, M., Nakagiri, S., Schueller, G.I. and Grigoriu, M., "Random fields and stochastic finite elements", Structural Safety, Vol. 3, 1986, pp. 143-166

[55] Konish, J.H. and Whitney, J.M., "Approximate stresses in an orthotropic plate containing a circular hole", Journal of Composite Materials, Vol. 9, 1975, pp. 157-166.

[56] Timoshenko, S. and Woinowsky-Krieger, S., *Theory of Plates and Shells*, Second Edition, 1959, McGraw-Hill, New York.

[57] Ambartsumyan, S.A., *Theory of Anisotropic Plates*, Translated from Russian by Cheron, T., Edited by Ashton, J.E., 1969, Technomic Publishing Company, Lancaster.

[58] Ashton, J.E. and Whitney, J.M., *Theory of Laminated Plates*, 1970, Technomic Publishing Company, Lancaster.

[59] Reddy, J.N., *An Introduction to the Finite Element Method*, 1984, McGraw-Hill, New York.

[60] Timoshenko, S. and Woinowsky-Krieger, S., *Theory of Plates and Shells*, First Edition, 1952, McGraw-Hill, New York.

[61] Whitney, J.M., *Structural Analysis of Laminated Anisotropic Plates*, 1987, Technomic Publishing Company, Lancaster.

[62] Reddy, J.N. and Miravete, A., *Practical Analysis of Composite Laminates*, 1995, CRC Press, Boca Raton, Florida.

[63] Tan, S.C., "Laminated composites containing an elliptical opening. I. Approximate stress analyses and fracture models", Journal of Composite Materials, Vol. 21, 1987, pp. 925-948.

[64] Nuismer, R.J. and Whitney, J.M., "Uniaxial failure of composite laminates containing stress concentrations", Fracture Mechanics of composites, ASTM STP 593, pp. 117-142.

[65] Givoli, D. and Elishakoff, I., "Stress concentration at a nearly circular hole with uncertain irregularities", Journal of Applied Mechanics, Vol. 59, 1992, pp. S65-S71.

[66] Siddall, J.N., *Probabilistic Engineering Design: Principles and Applications*, 1983, Marcel Dekker, New York.

[67] Shigley, J.E. and Mischke, C.R., *Mechanical Engineering Design*, 1989, McGraw-Hill, New York.

APPENDIX –A

A1. Finite element formulation for isotropic plates

The strain matrix for 2-D finite element formulation can be expressed as

$$\{\varepsilon\}^{(e)} = \left\{ \frac{\partial u}{\partial x} \quad \frac{\partial v}{\partial y} \quad \left(\frac{\partial u}{\partial y} + \frac{\partial v}{\partial x} \right) \right\}^{T(e)} = [B]^{(e)} \{d\}^{(e)} \tag{A1.1}$$

in which the $[B]^{(e)}$ matrix relates the element nodal displacements to the element strains and is given by

$$[B]^{(e)} = \begin{bmatrix} \frac{\partial}{\partial x} & 0 \\ 0 & \frac{\partial}{\partial y} \\ \frac{\partial}{\partial y} & \frac{\partial}{\partial x} \end{bmatrix} [N]^{(e)} \tag{A1.2}$$

The derivatives of the shape functions are expressed in terms of the local co-ordinates and they can be obtained by using the chain rule of partial differentiation as

$$\begin{aligned} \frac{\partial N_i}{\partial \xi} &= \frac{\partial N_i}{\partial x}\frac{\partial x}{\partial \xi} + \frac{\partial N_i}{\partial y}\frac{\partial y}{\partial \xi} \\ \frac{\partial N_i}{\partial \eta} &= \frac{\partial N_i}{\partial x}\frac{\partial x}{\partial \eta} + \frac{\partial N_i}{\partial y}\frac{\partial y}{\partial \eta} \end{aligned} \tag{A1.3}$$

The above expressions can be expressed in the matrix form as

$$\begin{Bmatrix} \frac{\partial N_i^{(e)}}{\partial \xi} \\ \frac{\partial N_i^{(e)}}{\partial \eta} \end{Bmatrix} = \begin{bmatrix} \frac{\partial x}{\partial \xi} & \frac{\partial y}{\partial \xi} \\ \frac{\partial x}{\partial \eta} & \frac{\partial y}{\partial \eta} \end{bmatrix}^{(e)} \begin{Bmatrix} \frac{\partial N_i^{(e)}}{\partial x} \\ \frac{\partial N_i^{(e)}}{\partial y} \end{Bmatrix} \tag{A1.4}$$

In the above, the matrix relating the derivatives of the shape functions with respect to the local co-ordinates to the derivatives of the shape functions with respect to the global co-ordinates is called as the *Jacobian* matrix of transformation and is denoted by $[J]$. Thus the Jacobian of transformation is given as,

$$[J] = \begin{bmatrix} J_{11} & J_{12} \\ J_{21} & J_{22} \end{bmatrix} = \begin{bmatrix} \frac{\partial x}{\partial \xi} & \frac{\partial y}{\partial \xi} \\ \frac{\partial x}{\partial \eta} & \frac{\partial y}{\partial \eta} \end{bmatrix}^{(e)} \tag{A1.5}$$

The components of the Jacobian matrix are calculated using the shape functions and the nodal co-ordinates. For instance,

$$J_{11} = \frac{\partial x}{\partial \xi} = \sum_{i=1}^{Num.ofNodes} \frac{\partial N_i}{\partial \xi} x_i \tag{A1.6}$$

APPENDIX –B

MAIN PROGRAM FOR ISOTROPIC PLATES

```
clear all;
format long;

dummy=0;          % To pass a dummy variable to GETDAT & GETARR
nelem=0;  ndofn=0; node=0; ngaus=0; ntype=0; mmats=0; numnp=0; nstre=0; nstr1=0; props =0;
lnods = 0; coord = 0;

%%%%%%%%%%%      GETDAT -  Get are relevant scalar variables

[nelem,ndofn,nnode,ngaus,ntype,mmats,numnp,nstre,nstr1]=GETDAT(dummy);

%%%%%%%%%%%      GETARR - Get all relevant data in Array from

[props,lnods,coord]=GETARR(dummy);

%%%%%%%%%%%%%%%%%%%%%    ESTABLISH THE NODAL CONNECTIVITY

nevab=ndofn*nnode;

[lm,id] = ELCON(ndofn,nnode,nelem,numnp,lnods);

%%%%%%%%%%%%%    START COMPUTING THE STIFFNESS MATRICES
for ielem = 1 : nelem
 matno(ielem) = 1;
end

globK = zeros(numnp*ndofn);  % Initialize the Global "K" matrix.

for ielem = 1 : nelem              %  Loop over NELEM

 lprop = matno(ielem);     %  Initialize properties for that element.

%%%%%%%%%%%     Get the coordinates of each node in the element

 for inode = 1 : nnode
  lnode = round(abs(lnods(ielem,inode)));
  for idime = 1 : ndofn
   elcod(idime,inode) = coord(lnode,idime);
  end
 end

 shape = zeros(8,1);
 deriv = zeros(2,8);
 xjacm = zeros(2,2);
 cartd = zeros(2,8);
 estif = zeros(nevab,nevab);

%%%%%%%%%%%%%%%%%%%%%%%  Evaluate Elasticity Matrix for PLANE SITUATIONS
```

```
 [dmatx] = MODPS(ntype,mmats,lprop,props);

  thick = props(lprop,3);

%%%%%%%%%%%%%%%%%%%%%%%%%%    Start GAUSSIAN INTEGRATION

  kgasp = 0;

  [posgp,weigp] = GAUSSQ(ngaus);

  for igaus = 1 : ngaus                % Loop over each Gauss point along "XZI" axis
                                               % i.e., horizontally, starting from left.
    for jgaus = 1 : ngaus      % Loop over each Gauss point along "ETA" axis
                                               % i.e., vertically, starting from bottom.
      kgasp = kgasp+1;

%%%%%%%%%%   Evaluate the Shape functions,derivatives,dvolu.. etc.

      exisp = posgp(igaus);
      etasp = posgp(jgaus);

      [shape,deriv] = SFR2(exisp,etasp);

      [xjacm,djacb,gpcod,cartd]=JACOB2(ielem,kgasp,ndofn,nnode,shape,deriv,elcod);

      dvolu = djacb*weigp(igaus)*weigp(jgaus);

      if thick>0.0
        dvolu = dvolu*thick;
      end

%%%%%%%%%%%%%%%   Evaluate the 'B' matrix and 'DB' matrices

      [bmatx] = BMATPS(nnode,cartd);
      [dbmat] = DBE(dmatx,bmatx);

%%%%%%%%%%%%%%%   Calculate the element stiffness matrices
      estif = estif + transpose(bmatx)*dbmat*dvolu;
    end
  end

%%%%%    Endof GAUSSIAN INTEGRATION

%%%%%    Assemble the element stiffness matrices

 [globK] = ASMBLK(ielem,nevab,lm,estif,globK);

end

%%%%    END OF ASSEMBLY FOR "estif" OF "ielem"
          iRuns = 1;

%%%%    Read the nodal loads and assemble into
```

```
%%%%%      Global Force Vector

[eload]=LOADPS(nelem,numnp,nnode,nevab,ndofn,ngaus,posgp,weigp,coord,lnods,matno,props,iRun
s);

 [asmblF] = FORCE(nelem,nevab,lm,eload);

%%%%%%%%              Solve for Displacements
 [displ,eldis] = BCSOLVE(asmblF,globK,lm,nelem,nevab,numnp,nnode,iRuns);

%%%%%%%%            Solve for GAUSS POINT STRESSES

 strsp=zeros(nstre,ngaus*ngaus,nelem);
 sgtot=zeros(nstrl,ngaus*ngaus,nelem);

[sgtot,strsp]=STREPS(nelem,matno,props,ntype,mmats,nnode,ndofn,coord,ngaus,nstre,nevab,nstrl,eld
is,lnods,iRuns);

%%%%%%%%%%%%%%%%%%%%%%%%%%%%%%%%%%%%%%%%%%%%%%%%%%%%%%%%%%%%%%%%%%%%%%%%%%%%%%%%%%%%%%%%%%%%
```

APPENDIX-C

C1. Stress concentration effects in composite laminate

The solution for the σ_i^* component can be written in the following form

$$\sigma_i^* = 2\,\mathrm{Re}[\mu_1^2\phi_1'(z_1)+\mu_2^2\phi_2'(z_2)]$$

$$\sigma_2^* = 2\,\mathrm{Re}[\phi_1'(z_1)+\phi_2'(z_2)] \qquad \text{(C1.1)}$$

$$\tau_{12}^* = -2\,\mathrm{Re}[\mu_1\phi_1'(z_1)+\mu_2\phi_2'(z_2)]$$

where

μ_1 and μ_2 are the principal complex roots of a characteristic equation, and ϕ_1 and ϕ_2 are the corresponding complex potentials; the prime symbol denotes differentiation with respect to z_1 and z_2 respectively.

The componenets of displacements due to the circular opening field can be expressed as:

$$u^* = 2\,\mathrm{Re}[p_1\phi_1(z_1)+p_2\phi_2(z_2)]$$

$$v^* = 2\,\mathrm{Re}[q_1\phi_1(z_1)+q_2\phi_2(z_2)] \qquad \text{(C1.2)}$$

where

u^* *and* v^* are local displacements in the 1 and 2-axes, respectively and,

$$p_k = a_{11}\mu_k^2 + a_{12} - a_{16}\mu_k \qquad k = 1,2$$

$$q_k = a_{12}\mu_k + \frac{a_{22}}{\mu_k} - a_{26} \qquad k = 1,2 \qquad \text{(C1.3)}$$

where

$a_{ij}, i, j = 1,2,6$ designate the laminate compliance with 1 and 2 axes being parallel to the 1 and 2-axes of the opening respectively.

In equation (C1.2) ϕ_1' and ϕ_2' denote the derivatives of ϕ_1 and ϕ_2 with respect to z_1 and z_2 respectively, and

$$\phi_1(z_1) = \frac{\beta_1 - \mu_2\alpha_1}{\mu_1 - \mu_2}\frac{1}{\zeta_1} \tag{C1.4}$$

$$\phi_2(z_2) = \frac{\beta_1 - \mu_1\alpha_1}{\mu_1 - \mu_2}\frac{1}{\zeta_2} \tag{C1.5}$$

where

$$\alpha_1 = -\frac{\bar{\sigma}_y \sin\varphi}{2}(a\sin\varphi - ib\cos\varphi) \tag{C1.6}$$

$$\beta_1 = \frac{\bar{\sigma}_y \cos\varphi}{2}(a\sin\varphi - ib\cos\varphi) \tag{C1.7}$$

and

$$\zeta_k = \frac{z_k + \sqrt{z_k^2 - a^2 - \mu_k^2 b^2}}{a - i\mu_k b} \qquad k = 1,2 \tag{C1.8}$$

where

$$z_k = x + \mu_k y \qquad k = 1,2 \tag{C1.9}$$

Substituting equations (C1.4-C1.9) into equation (C1.1) yields

$$\sigma_1^* = \bar{\sigma}_y \,\mathrm{Re}\{\delta_1[-\mu_1^2\delta_2\zeta_1^{-1} + \mu_2^2\delta_3\zeta_2^{-1}]\}$$

$$\sigma_2^* = \bar{\sigma}_y \,\mathrm{Re}\{\delta_1[-\delta_2\zeta_1^{-1} + \delta_3\zeta_2^{-1}]\}$$

$$\tau_{12}^* = -\bar{\sigma}_y \,\mathrm{Re}\{\delta_1[-\mu_1\delta_2\zeta_1^{-1} + \mu_2\delta_3\zeta_2^{-1}]\} \qquad \text{(C1.10)}$$

$$u^* = \bar{\sigma}_y \,\mathrm{Re}\{\delta_1[p_1\delta_4\zeta_1^{-1} - p_2\delta_5\zeta_2^{-1}]\}$$

$$v^* = \bar{\sigma}_y \,\mathrm{Re}\{\delta_1[q_1\delta_4\zeta_1^{-1} - q_2\delta_5\zeta_2^{-1}]\}$$

where

$$\delta_1 = \frac{a\sin\varphi - ib\cos\varphi}{\mu_1 - \mu_2}$$

$$\delta_2 = \frac{\cos\varphi + \mu_2\sin\varphi}{\sqrt{z_1^2 - a^2 - \mu_1^2 b^2}}$$

$$\delta_3 = \frac{\cos\varphi + \mu_1\sin\varphi}{\sqrt{z_2^2 - a^2 - \mu_2^2 b^2}} \qquad \text{(C1.11)}$$

$$\delta_4 = \cos\varphi + \mu_2\sin\varphi$$

$$\delta_5 = \cos\varphi + \mu_1\sin\varphi$$

APPENDIX-D

SUB-ROUTINE: A0CAL.m

```
%%%%%%%%%%%%%%%%%%%%%%%%%%%%%%%%%
% Sub-routine to calculate the value of characteristic length %
%%%%%%%%%%%%%%%%%%%%%%%%%%%%%%%%%

ChLen = zeros(25,1);

% [02/+-45]4S EXPERIMENTAL OUTPUT RESULT

sigmaN = 1e9*[0.8536
0.8084
0.8461
0.7988
0.7688
0.8660
0.7751
0.8549
0.7863
0.8325
0.7993
0.8082
0.8453
0.8463
0.8399
0.8544
0.8419
0.8039
0.7855
0.8608
0.6919
0.8679
0.7540
0.8213
0.7755]; % Ultimate tensile stress of the notched laminate

sigO = 1e9*[0.9774

0.9766
1.0699
0.9775
0.9785
1.0519
0.9863
1.0482
1.0069
0.9989
0.9499
0.9675
0.9598
0.9699
```

```
0.9726
1.0218
0.9862
0.9840
1.0008
0.9854
1.0094
0.9636
0.9567
1.0156
0.9618];  % Ultimate tensile stress of the un-notched laminate

for i =1:25
  ratio = (sigN(i)/sigO(i));

  dmatx = 1.0e+010 *[ 2.4120   1.7159  -1.5281
                      1.7159   8.5267  -1.5281
                     -1.5281  -1.5281   1.8767];  % Equivalent elasticity matrices.

 t = 0.002;  % Laminate thickness
 A= dmatx*t ; % Axial stiffness matrix
 a=inv(A);
 Ktinf = 1+ sqrt((2/A(2,2))*( sqrt(A(1,1)*A(2,2)) - A(1,2) + ( A(1,1)*A(2,2) - A(1,2)^2)/(2*A(3,3)))) ;
%  Equation 3.70 SCTan

  R = 0.00254;   %    Radius of the hole in meters
  right=0;
  for ao = 0.001 : 0.00001 : 0.1
    if (right ~= ratio)
      xzi= R/(R+ao);
      Nu = (2*(1-xzi));
      den = (2 - xzi^2 - xzi^4 + (Ktinf-3)*(xzi^6 - xzi^8));
      right = Nu/den;
       if (right > ratio)
       ChLen(i) = ao ;
       break,end
    end
  end
end

ChLen                          % Display all the values of characteristic length
mean(ChLen)                    % Mean of characteristic length value
std(ChLen)                     % Standard deviation of characteristic length value
```

APPENDIX-E

MAIN PROGRAM FOR COMPOSITE LAMINATES

```
%%%%%%%%%%%%%%%%%%%%%%%%%%%%%%%%%%%%%%%%%%%%%%%%%%%%%%
%%%%%%%%%        MODIFYSTIFPS TO CALCULATE THE          %%%%%%%
% %%%%%%%%  DISPALCEMENT AND STRESSES FOR IN-PLANE AND  %%%%%%%
%%%%%%%%%            OUT-OF-PLANE ANALYSIS          %%%%%%%%%%%
%%%%%%%%%%%%%%%%%%%%%%%%%%%%%%%%%%%%%%%%%%%%%%%%%%%%%%

clear all;
tic;
format long;

dummy=0; nelem=0;

ndofn=0; nnode=0; ngaus=0; ntype=0; nmats=0; numnp=0; nstre=0; nstr1=0; props = 0; lnods = 0;
coord = 0;

%********************************%
% SELECT THE TYPE OF ANALYSIS: %
%********************************%

k = menu ('CHOOSE THE TYPE OF ANALYSIS','IN-PLANE ANALYSIS','OUT-OF-PLANE
ANALYSIS ');

if k==1
fprintf('\n WORKING ON OUT-OF-PLANE ANALYSIS \n');
m = menu('OPENING TYPE','CIRCULAR ');
plyconfig = menu('PLY CONFIGURATION','[02/+-45]2S','[0/90]4S','[0/90/+-45]2S');

%%%%%%%%%%%%    bendGETDAT -  Get all relevant scalar variables    %%%%%%%%

nlami = 200;
for ilami = 1 : nlami
  kgaus = 0;
[nelem,ndofn,nnode,ngaus,ntype,nmats,numnp,nstre,nstr1,ntotg,aW_Ratio,WL_Ratio,ctnode]=
bendGETDAT(plyconfig);

fa = fopen('propgbend.m','w');
fprintf(fa,'\n\n\t\t\t-----------------------------------\n');
fprintf(fa,' \t   properties at each and every gauss point for bending');
fprintf(fa,'\n\t\t\t-----------------------------------\n\n');

[props,tetag,plytk,matno,propgbend,lnods,coord,EThetaPly,distriao] =
bendGETARR(nelem,ngaus,ndofn,nnode,ntotg,aW_Ratio,WL_Ratio,ctnode,nlami,ilami,m,plyconfig);
 save all;
fclose('all');
nevab = ndofn*nnode;
globK = zeros(numnp*ndofn); % Initialize the Global "K" matrix for each element
B=zeros(nstre,numnp*ndofn);
b=zeros(nstre,ndofn*nnode);
```

```
[lm,id] = bendELCON(ndofn,nnode,nelem,numnp,lnods);


%%%%   START COMPUTING THE STIFFNESS MATRICES  %%%%%

for ielem = 1 : nelem            %  Loop over NELEM

%%%%%%%   Get the coordinates of each node in the element   %%%%%%%%

 for inode = 1 : nnode
  lnode = round(abs(lnods(ielem,inode)));
  for idime = 1 : (ndofn-3)
   elcod(idime,inode) = coord(lnode,idime);
  end
 end

 shape = zeros(8,1);
 deriv = zeros(2,8);
 xjacm = zeros(2,2);
 cartd = zeros(2,8);
 estif = zeros(nevab,nevab);

%%%%%%%%   Start GAUSSIAN INTEGRATION    %%%%%%%%%

 kgasp = 0;   % Keep track over the gauss points in each element.

 [posgp,weigp] = GAUSSQ(ngaus);

 for igaus = 1 : ngaus                % Loop over each Gauss point along "ZETA" axis
                                      % i.e., horizontally, starting from left.
  for jgaus = 1 : ngaus               % Loop over each Gauss point along "ETA" axis
                                      % i.e., vertically, starting from bottom.
    kgasp = kgasp + 1;
    kgaus = kgaus + 1;
    lprop = matno(kgaus);
    ThetaPly = tetag(kgaus,:);
    thick = sum(plytk(kgaus,:));

    exisp = posgp(igaus);
    etasp = posgp(jgaus);

    [w1bar,wbar,W,matxA,matxB,matxD,matxF,Dmatx,bendEx] =
bendMODPS(ntype,nstre,nmats,lprop,propgbend,ThetaPly,kgaus);

%%%%%%%  Evaluate the Shape functions,derivatives,dvolu  %%%%%%%

    [shape,deriv] = SFR2(exisp,etasp);
    [xjacm,djacb,gpcod,cartd]=bendJACOB2(ielem,kgasp,ndofn,nnode,shape,deriv,elcod);
    dvolu = djacb*weigp(igaus)*weigp(jgaus);
    if thick > 0.0
     dvolu = dvolu*thick;
    end
```

```
%%%%   Evaluate the 'B' matrix and 'DB' matrices   %%%%%

    [bmatx] = bendBMATPS(nnode,cartd,shape);
    [dbmat] = bendDBE(bendEx,bmatx);

%%%%%%   Calculate the element stiffness matrices          %%%%%%%%%

    estif = estif + transpose(bmatx)*dbmat*dvolu;

%%%%%%   End of GAUSSIAN INTEGRATION    %%%%%%%%
    end
 end
     if ielem > 1
        [B]=[B bmatx];
     end

     if ielem==1
        [B]= [bmatx];
     end

%%%   Assemble the element stiffness matrices   %%%%

     [globK] = ASMBLK(ielem,nevab,lm,estif,globK);
end

%%%%%   END OF ASSEMBLY FOR "estif" OF "ielem"  %%%%%%%%%

for iRuns = 1 : 3

%%%%%%          Read the nodal loads and assemble into       %%%%%%
%%%%%%                    Global Force Vector                %%%%%%

[eload] =
bendLOADPS(nelem,numnp,nnode,nevab,ndofn,ngaus,posgp,weigp,coord,lnods,matno,props,iRuns,pl
yconfig);

[asmblF] = FORCE(nelem,nevab,lm,eload);

%%%%%   Solve for Displacements     %%%%%

[globK,FxdofData,Fxdof,temp1,displ,eldis] =
bendBCSOLVE(ndofn,coord,asmblF,globK,lm,nelem,nevab,numnp,nnode,iRuns,plyconfig);

%%%%%  Solve for GAUSS POINT STRESSES     %%%%%

strsp=zeros(nstre,ngaus*ngaus,nelem);
sgtot=zeros(nstre,ngaus*ngaus,nelem);

sgtot,strsp]=bendSTREPS(nelem,matno,props,propgbend,tetag,ntype,nmats,nnode,ndofn,coord,ngaus,
nstre,nevab,nstr1,eldis,lnods,iRuns);

end
```

```
%*****************************************************************************%
%   CALCULATION OF STRESSES IN INDIVISUAL LAYER UNDER BENDING LOAD   %
%*****************************************************************************%

% The displacement and strains are continuous through the thickness of the laminate.
% Thus the mid plane strains and displacements are the same for entire laminate.
% But the stresses vary through the thickness of the laminate. Thus the stresses are
% found out individually for each and every ply in the configuration. Files related
% to shear analysis :EMODPS,STRESSH :Maximum stress criterion is used for the analysis.

elestress = zeros(nstre,numnp*ndofn);

gsig = zeros(8,40);          % gsig : Gaussian stress for an element
eldistrans = (eldis');       % to store the transformed matrix of elemental displacement values
strain=zeros(8,1);           % to store the strain values obtained by [B] [d]
sigma126 = zeros(8,1);

if (plyconfig == 1)
 fprintf('\n WORKING ON [02/+-45]2S \n');

 ThetaPly = [ 0 0 45 -45 0 0 45 -45 0 0 45 -45 0 0 45 -45 0 0 45 -45 0 0 45 -45 0 0 45 -45 ...
         0 0 45 -45 0 0 45 -45 0 0 45 -45 0 0 45 -45 0 0 45 -45 -45 45 0 0 -45 45 0 0 -45 45 0 ...
         0 -45 45 0 0 -45 45 0 0 -45 45 0 0 -45 45 0 0 -45 45 0 0 -45 45 0 0 -45 45 0 0 -45 45 0 0 -45
        45 0 0];
end

if (plyconfig == 2)
 fprintf('\n WORKING ON [0/90]16S \n');
 ThetaPly = [ 0 90 0 90 0 90 0 90 0 90 0 90 0 90 0 90 0 90 0 90 0 90 0 90 0 90 0 90 0 90 0 ...
         90 0 90 0 90 0 90 0 90 0 90 0 90 0 90 90 0 90 0 90 0 90 0 90 0 90 0 90 ...
         0 90 0 90 0 90 0 90 0 90 0 90 0 90 0 90 0 90 0 90 0 90 0 90 0 90 0 90 0 90 0 90 0 90 0];
 end

 if (plyconfig == 3)
  fprintf('\n WORKING ON [0/90/+-45]2S \n');
  ThetaPly = [ 0 90 45 -45 0 90 45 -45 0 90 45 -45 0 90 45 -45 0 90 45 -45 0 90 45 -45 0 ...
    90 45 -45 0 90 45 -45 0 90 45 -45 0 90 45 -45 0 90 45 -45 0 90 45 -45 -45 45 90 0 ...
    -45 45 90 0 -45 45 90 0 -45 45 90 0 -45 45 90 0 -45 45 90 0 -45 45 90 0 -45 45 90 0 ...
    -45 45 90 0 -45 45 90 0 -45 45 90 0 -45 45 90 0];
 end

  EThetaPly = [ThetaPly]*pi/180;

ilami;
for nplies = 1: max(size(ThetaPly))
 % stresses and its orientation with respect to vertical axis are calculated in each and every layer

   [bendEx] = EMODPS(nstre,EThetaPly,nplies);

   [gsig,strain]= STRESSH(B,eldistrans,bendEx,nelem);
```

```
% sub routine to find the gaussian stress for the elements in the mid plane.
  gsig;

% this portion of the program calculates the stresses, layer wise using the gauss point stresses over the
entire lmainate

   for ielements = 1: nelem
     j=4;

     m = cos(EThetaPly(nplies));
     n = sin(EThetaPly(nplies)) ;

fstrsply(1,ielements) = m^2 * gsig(j,ielements) + n^2 * gsig(j+1,ielements) + 2*m*n *
gsig(j+2,ielements) ;  % sigma 1 : stress in the fiber direction
 fstrsply(2,ielements) = n^2 * gsig(j,ielements) + m^2 * gsig(j+1,ielements) - 2*m*n *
gsig(j+2,ielements);  % sigma 2 : stress in the matrix direction
fstrsply(3,ielements) = -m*n * gsig(j,ielements) + m*n * gsig(j+1,ielements) + (m^2 - n^2) *
gsig(j+2,ielements);  % sigma 1 : shear stress in the ply

    end
   nplies;
   maxstress = max(max(max(fstrsply(:,:))))

% represents the maximum stress in each and every layer of the laminate

     if nplies > 1
       [elestress]=[elestress fstrsply];
     end

     if nplies==1
       [elestress] = [fstrsply];
     end

 stress1(ilami,1) = max(elestress(1,:))        % Maximum stress in fiber direction for a laminate
 stress2(ilami,1) = max(elestress(2,:))        % Maximum stress in transverse direction for a laminate
 shearstress12(ilami,1) = max(elestress(3,:))   % Maximum shear stress for a laminate

  end
end

%****************************************
%   OUTPUT FOR BENDING LOAD ANALYSIS
%****************************************

if (plyconfig == 1)
 fprintf('\n print [02/+-45]2S \n');

fm = fopen('BPLYSTRESS0245.m','w');
fprintf(fm,' \t local co-ordinate stresses for nlaminates');

 fprintf(fm,'\n \t          STRESS 1          STRESS 2          SHEAR STRESS 12 \n');
 fprintf(fm,'\n \t          ----------        ----------        ---------- \n');
```

```
 for i = 1: nlami
   fprintf(fm,'\n NLAMI : %d  %13.5f MN/m2     %13.5f MN/m2     %13.5f MN/m2 ', ...
      i,stress1(i)/1e6,stress2(i)/1e6,shearstress12(i)/1e6);
 end
save all;
fclose('all');
end
%*****************************

if (plyconfig == 2)
 fprintf('\n print [0/90]2S \n');

fm = fopen('BPLYSTRESS090.m','w');
fprintf(fm,' \t local co-ordinate stresses for nlaminates');

 fprintf(fm,'\n \t          STRESS 1          STRESS 2          SHEAR STRESS 12 \n');
 fprintf(fm,'\n \t          ----------        ----------        ---------- \n');

 for i = 1: nlami
   fprintf(fm,'\n NLAMI : %d  %13.5f MN/m2     %13.5f MN/m2  %13.5f MN/m2', ...
      i,stress1(i)/1e6,stress2(i)/1e6,shearstress12(i)/1e6);
 end

save all;
fclose('all');

end
%*****************************

if (plyconfig == 3)
 fprintf('\n print [0/90/+-45]2S \n');
fm = fopen('BPLYSTRESS09045.m','w');
fprintf(fm,' \t local co-ordinate stresses for nlaminates');
 fprintf(fm,'\n \t          STRESS 1          STRESS 2          SHEAR STRESS 12 \n');
 fprintf(fm,'\n \t          ----------        ----------        ---------- \n');

 for i = 1: nlami
   fprintf(fm,'\n NLAMI : %d  %13.5f GN/m2     %13.5f GN/m2  %13.5f GN/m2', ...
      i,stress1(i)/1e9,stress2(i)/1e9,shearstress12(i)/1e9);
 end
save all;
fclose('all');
end
%%%%%%%%%%%%%%%%%%%%%%%%%%%%%%%%%%%%
          % END OF BENDING ANALYSIS %
%%%%%%%%%%%%%%%%%%%%%%%%%%%%%%%%%%%%

 if k==2

fprintf('\n WORKING ON IN-PLANE ANALYSIS \n');
m = menu ('OPENING TYPE','CIRCULAR ');
plyconfig = menu('PLY CONFIGURATION','[02/+-45]2S','[0/90]4S','[0/90/+-45]2S');
seload = menu('LOAD TYPE','AXIAL ','BIAXIAL','SHEAR' );
```

```
fprintf('\n Spatial values of the Material are stored in "propg.m" FILE \n ');
nlami = 300;

for ilami = 1 : nlami
  kgaus = 0;   % Keep track over the gauss points in the entire structure.

%%%%%%%     GETDAT - Get are relevant scalar variables     %%%%%%%

[nelem,ndofn,nnode,ngaus,ntype,nmats,numnp,nstre,nstr1,ntotg,aW_Ratio,WL_Ratio,ctnode]=
GETDAT(plyconfig);

fg = fopen('propg.m','w');
fprintf(fg,'\n\n\t\t\t----------\n');
fprintf(fg,' \t       properties at each and every gauss point');
fprintf(fg,'\n\t\t\t----------\n\n');
[props,tetag,plytk,matno,propg,lnods,coord,EThetaPly,distriao] =
GETARR(nelem,ngaus,ndofn,nnode,ntotg,aW_Ratio,WL_Ratio,ctnode,nlami,ilami,m,plyconfig,
seload);
 save all;
fclose('all');

%%%%%%    ESTABLISH THE NODAL CONNECTIVITY    %%%%%%%

nevab = ndofn*nnode;
globK = zeros(numnp*ndofn);  % Initialize the Global "K" matrix for each element
[lm,id] = ELCON(ndofn,nnode,nelem,numnp,lnods);

%%%%%%    START COMPUTING THE STIFFNESS MATRICES    %%%%%%%

for ielem = 1 : nelem            % Loop over NELEM

%%%%%%%    Get the coordinates of each node in the element    %%%%%%
 for inode = 1 : nnode
  lnode = round(abs(lnods(ielem,inode)));
  for idime = 1 : ndofn
   elcod(idime,inode) = coord(lnode,idime);
  end
 end
 shape = zeros(8,1);
 deriv = zeros(2,8);
 xjacm = zeros(2,2);
 cartd = zeros(2,8);
 estif = zeros(nevab,nevab);

%%%%%%%%%    Start GAUSSIAN INTEGRATION    %%%%%%%%%%%
 kgasp = 0;   % Keep track over the gauss points in each element.
 [posgp,weigp] = GAUSSQ(ngaus);
 for igaus = 1 : ngaus                % Loop over each Gauss point along "ZETA" axis
                                      % i.e., horizontally, starting from left.
  for jgaus = 1 : ngaus               % Loop over each Gauss point along "ETA" axis
                                      % i.e., vertically, starting from bottom.
   kgasp = kgasp + 1;
   kgaus = kgaus + 1;
```

```
    lprop = matno(kgaus);
    ThetaPly = tetag(kgaus,:);
    thick = sum(plytk(kgaus,:));

%%%%%%%  Evaluate the Shape functions,derivatives,dvolu.. etc.  %%%%%%%%

   exisp = posgp(igaus);
   etasp = posgp(jgaus);
   [dmatx] = MODPS(ntype,nstre,nmats,lprop,propg,ThetaPly,kgaus);
   [shape,deriv] = SFR2(exisp,etasp);
   [xjacm,djacb,gpcod,cartd]=JACOB2(ielem,kgasp,ndofn,nnode,shape,deriv,elcod);
   dvolu = djacb*weigp(igaus)*weigp(jgaus);  % volume calculation :  t*j*ds*dt

    if thick>0.0
     dvolu = dvolu*thick;
    end
%%%%%%%  Evaluate the 'B' matrix and 'DB' matrices          %%%%%%%%%

[bmatx] = BMATPS(nnode,cartd);
[dbmat] = DBE(dmatx,bmatx);
%%%%%%   Calculate the element stiffness matrices  %%%%%%
   estif = estif + transpose(bmatx)*dbmat*dvolu;
%%%%%   End of GAUSSIAN INTEGRATION    %%%%%%%
  end
end

%%%   Elemental B matrix i.e [bmatx] is stored in [B]. This matrix is appeneded by all the elements

    if ielem > 1
       [B]=[B bmatx];
    end

    if ielem==1
       [B]= [bmatx];
    end
%%%   Assemble the element stiffness matrices   %%%

 [globK] = ASMBLK(ielem,nevab,lm,estif,globK);
 end
%%%%%%   END OF ASSEMBLY FOR "estif" OF "ielem"  %%%%%%%%

for iRuns = 1 : 3

%%%        Read the nodal loads and assemble : Global Force Vector  %%%

 [eload] =
LOADPS(nelem,numnp,nnode,nevab,ndofn,ngaus,posgp,weigp,coord,lnods,matno,props,iRuns,seload,
plyconfig);

 [asmblF] = FORCE(nelem,nevab,lm,eload);

%%%%%%%%%      Solve for Displacements          %%%%%%%%%
```

```
[displ,eldis] =
BCSOLVE(ndofn,coord,asmblF,globK,lm,nelem,nevab,numnp,nnode,iRuns,seload,plyconfig);

%%%%          Solve for GAUSS POINT STRESSES        %%%%

strsp=zeros(nstre,ngaus*ngaus,nelem);
sgtot=zeros(nstr1,ngaus*ngaus,nelem);
[sgtot,strsp]=STREPS(nelem,matno,props,propg,tetag,ntype,nmats,nnode,ndofn,coord,ngaus,nstre,nev
ab,nstr1,eldis,lnods,iRuns,plyconfig);
end

B;
eldis';

%*************************************************************************
%    CALCULATION OF STRESSES IN INDIVISUAL LAYER UNDER SHEAR LOAD    %
%*************************************************************************

% The displacement and strains are continous through the thickness of the laminate.
% Thus the mid plane strains and displacements are the same for entire lamiante.
% But the stresses vary through the thickness of the laminate.Thus the stresses are
% found out indivisually for each and every ply in the configuration. Files related
% to shear analysis :EMODPS,STRESSH :Maximum stress criterion is used for the analysis.

elestress = zeros(nstre,numnp*ndofn);

gsig = zeros(3,16);              % gsig = gaussian stress for an element
eldistrans = (eldis');           % to store the transformed matrix of elemental displacement values
strain=zeros(3,1);               % to store the strain values obtained by [B] [d]
sigma126 = zeros(3,1);

if (plyconfig == 1)
 fprintf('\n WORKING ON [02/+-45]2S \n');
 ThetaPly = [ 0 0 45 -45 0 0 45 -45 -45 45 0 0 -45 45 0 0 ];  % w.r.t  Y-axis
end

if (plyconfig == 2)
 fprintf('\n WORKING ON [0/90]4S \n');
 ThetaPly = [ 0 90 0 90 0 90 0 90 90 0 90 0 90 0 90 0 ];  % w.r.t  Y-axis
end

 if (plyconfig == 3)
  fprintf('\n WORKING ON [0/90/+-45]2S \n');
  ThetaPly = [ 0 90 45 -45 0 90 45 -45 -45 45 90 0 -45 45 90 0 ];  % w.r.t  Y-axis
 end

  EThetaPly = [ThetaPly+90]*pi/180;
ilami;

for nplies = 1: max(size(EThetaPly))  % stresses and its orientation with respect to vertical axis
                                      % are calculated in each and every layer

   [Edmatx] = EMODPS(nstre,EThetaPly,nplies);
```

```
% Sub routine to find the Gaussian stresses for the elements in the mid plane.

   [gsig,strain]= STRESSH(B,eldistrans,Edmatx,nelem);

   % this portion of the program calculates the stresses in fiber and transverse direction,
   % layer wise using the gauss point stresses over the entire lmainate

    for ielements = 1: nelem
      j=1;

       m = cos(EThetaPly(nplies));
       n = sin(EThetaPly(nplies)) ;

fstrsply(1,ielements) = m^2 * gsig(j,ielements) + n^2 * gsig(j+1,ielements) + 2*m*n *
gsig(j+2,ielements) ;        % sigma 1 : stress in the fiber direction
fstrsply(2,ielements) = n^2 * gsig(j,ielements) + m^2 * gsig(j+1,ielements) - 2*m*n *
gsig(j+2,ielements);         % sigma 2 : stress in the tmasverse direction
fstrsply(3,ielements) = -m*n * gsig(j,ielements) + m*n * gsig(j+1,ielements) + (m^2 - n^2) *
gsig(j+2,ielements);        % sigma 12 : shear stress in the ply

end
nplies;
maxstress = max(max(max(fstrsply(:,:))))  % represents the maximum stress in each and every layer of
the laminate

      if nplies > 1
         [elestress]=[elestress fstrsply];
      end

      if nplies==1
         [elestress] = [fstrsply];
      end

   stress1(ilami,1) = max(elestress(1,:))        % Maximum stress in fiber direction for a laminate
   stress2(ilami,1) = max(elestress(2,:))        % Maximum stress in transverse direction for a laminate
   shearstress12(ilami,1) = max(elestress(3,:))    % Maximum shear stress for a laminate

end
%*********************************************************************
%  AVERAGE STRESS CALCULATION FOR UNIAXIAL AND BIAXIAL LOAD
%*********************************************************************

[sigavg] = AVGSTR(sgtot,coord,ngaus,nlami,ilami,distriao,plyconfig);
sigmavg(ilami,1) = sigavg;
maxstress(ilami,1) = max(max(max(sgtot)));
end

%*************************************
%  OUTPUT FOR SHEAR LOAD ANALYSIS %
%*************************************

if (plyconfig == 1)
```

```
 fprintf('\n print [02/+-45]2S \n');
fm = fopen('PLYSTRESS0245.m','w');
fprintf(fm,' \t local co-ordinate stresses for nlaminates');
 fprintf(fm,'\n \t          STRESS 1          STRESS 2          SHEAR STRESS 12 \n');
 fprintf(fm,'\n \t          ----------        ----------        ---------- \n');

 for i = 1: nlami
   fprintf(fm,'\n NLAMI : %d  %13.5f GN/m2    %13.5f GN/m2   %13.5f GN/m2 '...
     ,i,stress1(i)/1e9,stress2(i)/1e9,shearstress12(i)/1e9);
 end
save all;
fclose('all');
end

%*********************
if (plyconfig == 2)
 fprintf('\n print [0/90]2S \n');

fm = fopen('PLYSTRESS090.m','w');
fprintf(fm,' \t local co-ordinate stresses for nlaminates');

 fprintf(fm,'\n \t          STRESS 1          STRESS 2          SHEAR STRESS 12 \n');
 fprintf(fm,'\n \t          ----------        ----------        ---------- \n');

 for i = 1: nlami
   fprintf(fm,'\n NLAMI : %d  %13.5f GN/m2    %13.5f GN/m2  %13.5f GN/m2'...
     ,i,stress1(i)/1e9,stress2(i)/1e9,shearstress12(i)/1e9);
 end

save all;
fclose('all');
end
%*********************
if (plyconfig == 3)
 fprintf('\n print [0/90/+-45]2S \n');

fm = fopen('PLYSTRESS09045.m','w');
fprintf(fm,' \t local co-ordinate stresses for nlaminates');

 fprintf(fm,'\n \t          STRESS 1          STRESS 2          SHEAR STRESS 12 \n');
 fprintf(fm,'\n \t          ----------        ----------        ---------- \n');

 for i = 1: nlami
   fprintf(fm,'\n NLAMI : %d  %13.5f GN/m2    %13.5f GN/m2  %13.5f GN/m2'...
     ,i,stress1(i)/1e9,stress2(i)/1e9,shearstress12(i)/1e9);
 end
save all;
fclose('all');
end

%*****************************************
%  OUTPUT FOR AXIAL AND BIAXIAL LOAD  %
%*****************************************
```

```
if (plyconfig == 1)
 fprintf('\n print [02/+-45]2S \n');
fm = fopen('SIGMAVG0245.m','w');
fprintf(fm,' \t sigma average values for nlaminates');

 fprintf(fm,'\n \t          SIGAVG-"sigavg"    "maxstress"   \n');
 fprintf(fm,'\n \t          ------------       ------------ \n');

 for i = 1: nlami
   fprintf(fm,'\n NLAMI : %d   %13.5f GN/m2     %13.5f GN/m2',i,sigmavg(i)/1e9,maxstress(i)/1e9);
 end
save all;
fclose('all');
end
%**********************
if (plyconfig == 2)
 fprintf('\n print [0/90]4S \n');

fm = fopen('SIGMAVG090.m','w');
fprintf(fm,' \t sigma average values for nlaminates');

 fprintf(fm,'\n \t          SIGAVG-"sigavg"    "maxstress"   \n');
 fprintf(fm,'\n \t          ------------       ------------ \n');

 for i = 1: nlami
   fprintf(fm,'\n NLAMI : %d   %13.5f GN/m2     %13.5f GN/m2',i,sigmavg(i)/1e9,maxstress(i)/1e9);
 end
save all;
fclose('all');
end
%*******************************
if (plyconfig == 3)
 fprintf('\n print [0/90/+-45]2S \n');

fm = fopen('SIGMAVG09045.m','w');
fprintf(fm,' \t sigma average values for nlaminates');

 fprintf(fm,'\n \t          SIGAVG-"sigavg"    "maxstress"   \n');
 fprintf(fm,'\n \t          ------------       ------------ \n');

 for i = 1: nlami
   fprintf(fm,'\n NLAMI : %d   %13.5f GN/m2     %13.5f GN/m2',i,sigmavg(i)/1e9,maxstress(i)/1e9);
 end
save all;
fclose('all');

%*******************************
 end
end
RunTime = toc
```

```
%%%%%%%%%%%%%%%%%%%%%%%%%%%%%%%%%%%%%%%%%%%%%%%%%
%            Program to calculate the equivalent stress over the characteristic length           %
%%%%%%%%%%%%%%%%%%%%%%%%%%%%%%%%%%%%%%%%%%%%%%%%%

 function [sigavg] = AVGSTR(sgtot,coord,ngaus,nlami,ilami,distriao,plyconfig)

if (plyconfig == 1)
  ao= 0.01063;        % AS OBTAINED FROM THE EXPERIMENT : FOR [02/+-45]2S
end

if (plyconfig == 2)
 ao = 0.00444;        % AS OBTAINED FROM THE EXPERIMENT : FOR [0/90]4S
end

if (plyconfig == 3)
 ao = 0.00385;        % AS OBTAINED FROM THE EXPERIMENT : FOR [0/90/+-45]2S
end

width=0.0379;  radius =0.00255; sigavg=zeros(1,1); sigadd1=0; sigadd2=0; sigadd3=0; sigadd4=0;
sigadd11=0; sigadd22=0; sigadd33=0; sigadd44=0; s=zeros(5,1);

%-----------------------------------------------------------
% Two cases of Gauss order i.e 3 and 4 are considered
%-----------------------------------------------------------
 if (ngaus==3)
   n=1;

 for k = 1 : 5

   if (k==1)
   sigadd1 =  sgtot(2,9*k,41);
   sigadd2 =  sgtot(2,7*k,40);
   s(k) = (sigadd1 + sigadd2)/2;
   end

   if (k==2)
   sigadd1 =  sgtot(2,3*k,41);
   sigadd2 =  sgtot(2,k^2,40);
   s(k) = (sigadd1 + sigadd2)/2;
   end

   if (k==3)
   sigadd11 =  sgtot(2,k,41);
   sigadd22 =  sgtot(2,n,40);
   sigadd33 =  sgtot(2,n,18);
   sigadd44 =  sgtot(2,k,16);
   s(k) = (sigadd11 + sigadd22 +sigadd33 +sigadd44)/4;
   end

   if (k==4)
   sigadd1=  sgtot(2,k,18);
   sigadd2=  sgtot(2,(k+2),16);
   s(k) = (sigadd1 + sigadd2)/2;
```

```
    end

    if (k==5)
    sigadd1 =  sgtot(2,(k+2),18);
    sigadd2 =  sgtot(2,(k+4),16);
    s(k) = (sigadd1 + sigadd2)/2;
    end

 end


  x=[ s(1)
     s(2)
     s(3)
     s(4)
     s(5)];

  y= [ 1          0                          0                          0                  0
       1  (coord(149,1)- coord(157,1))  (coord(149,1)- coord(157,1))^2   (coord(149,1)-
coord(157,1))^3  (coord(149,1)- coord(157,1))^4

       1  (coord(106,1)- coord(157,1))  (coord(106,1)- coord(157,1))^2   (coord(106,1)-
coord(157,1))^3  (coord(106,1)- coord(157,1))^4

       1  (coord(119,1)- coord(157,1))  (coord(119,1)- coord(157,1))^2   (coord(119,1)-
coord(157,1))^3  (coord(119,1)- coord(157,1))^4

       1  (coord(132,1)- coord(157,1))  (coord(132,1)- coord(157,1))^2   (coord(132,1)-
coord(157,1))^3  (coord(132,1)- coord(157,1))^4 ];

  b = inv(y)*x ;       % constants sig1 = a0+a1*x+a2*x^2+a3*x^3+a4*x^4

  % Average stress criteria

  syms x

  f= b(1,1) + b(2,1)*x + b(3,1)*x^2 + b(4,1)*x^3 + b(5,1)*x^4;

  % To find the stress value at the characteristic length ao

  sigavg1 = (1/distriao(ilami))* int(f,x,0,distriao(ilami));

  sigavg=numeric(sigavg1);

end
%-------------------------------------------------

if (ngaus==4)
   n=1;
   for k = 1 : 5 %  Gauss order 4 ngaus

   if k == 1
      sigadd1 =  sgtot(2,16*k,41);
```

```
    sigadd2 =  sgtot(2,13*k,40);
    s(k) = (sigadd1 + sigadd2)/2;
  end

  if k == 2
    sigadd11 =  sgtot(2,6*k,41);
    sigadd22 =  sgtot(2,(k+7),40);
    sigadd33 =  sgtot(2,4*k,41);
    sigadd44 =  sgtot(2,(k+3),40);
    s(k) = (sigadd11 + sigadd22 +sigadd33 +sigadd44)/4;
  end
   if k == 3
    sigadd11 =  sgtot(2,(k+1),41);
    sigadd22 =  sgtot(2,n,40);
    sigadd33 =  sgtot(2,n,18);
    sigadd44 =  sgtot(2,(k+1),16);
    s(k) = (sigadd11 + sigadd22 +sigadd33 +sigadd44)/4;
   end

  if k == 4
    sigadd11 =  sgtot(2,(k+1),18);
    sigadd22 =  sgtot(2,(k+3),16);
    sigadd33 =  sgtot(2,(k+5),18);
    sigadd44 =  sgtot(2,(k*3),16);
    s(k) = (sigadd11 + sigadd22 +sigadd33 +sigadd44)/4;
  end

  if k == 5
    sigadd1 =  sgtot(2,(k+4),18);
    sigadd2 =  sgtot(2,(k+7),16);
    s(k) = (sigadd1 + sigadd2)/2;
    end
 end

x=[  s(1)
   s(2)
   s(3)
   s(4)
   s(5)];

 y= [ 1          0                    0                    0                    0

      1  (coord(149,1)- coord(157,1))  (coord(149,1)- coord(157,1))^2   (coord(149,1)-
coord(157,1))^3  (coord(149,1)- coord(157,1))^4

      1  (coord(106,1)- coord(157,1))  (coord(106,1)- coord(157,1))^2   (coord(106,1)-
coord(157,1))^3  (coord(106,1)- coord(157,1))^4

      1  (coord(119,1)- coord(157,1))  (coord(119,1)- coord(157,1))^2   (coord(119,1)-
coord(157,1))^3  (coord(119,1)- coord(157,1))^4

      1  (coord(132,1)- coord(157,1))  (coord(132,1)- coord(157,1))^2   (coord(132,1)-
coord(157,1))^3  (coord(132,1)- coord(157,1))^4 ];
```

```
 b = inv(y)*x ;
 % Average stress criteria
   syms x
     f= b(1,1) + b(2,1)*x + b(3,1)*x^2 + b(4,1)*x^3 + b(5,1)*x^4;
    sigavg1 = (1/distriao(ilami))* int(f,x,0,distriao(ilami));
    sigavg=numeric(sigavg1);

end

%%%%%%%%%%%%%%%%%%%%%%%%%%%%%%%%%%%%%%%%%
%    Program to determine the distribution of the value of characteristic length    %
%%%%%%%%%%%%%%%%%%%%%%%%%%%%%%%%%%%%%%%%%

function [distriao] = DISAO(plyconfig,nlami);

m=nlami;                              % No. of  rows of characteristic length values
n=1;                                   % One column needs to be generated
distriao=zeros(nlami,1);

if (plyconfig == 1)
   fprintf('\n WORKING ON [02/+-45]2S \n');
   MU = 0.01063;                      % Mean value of the characteristic length
   SIGMA = 0.0022115;                 % Standard deviation value of the characteristic length
   a = 0.00488;                       % Minimum value of the characteristic length
   b = 0.01378;                       % Maximum value of the characteristic length
   distriao = a + (b-a) * rand(m,n);  % Distributed values of characteristic length
end

if (plyconfig == 2)
   fprintf('\n WORKING ON [0/90]4S DISA0 \n');
   MU = 0.00444;                      % Mean value of the characteristic length
   SIGMA = 0.001392;                  % Standard deviation value of the characteristic length
   a = 0.00224;                       % Minimum value of the characteristic length
   b = 0.00734;                        % Maximum value of the characteristic length
   distriao = a + (b-a) * rand(m,n);  % Distributed values of characteristic length
end
```